SYNTHESIS AND CHARACTERIZATION OF SUPRAMOLECULAR ARCHITECTURES FROM POLY CARBOXYLIC ACID BUILDING BLOCKS

LIU RONG

NATIONAL UNIVERISTY OF SINGAPORE

2001

SYNTHESIS AND CHARACTERIZATION OF SUPRAMOLECULAR ARCHITECTURES FROM POLY CARBOXYLIC ACID BUILDING BLOCKS

LIU RONG

(***B. Sc. Wuhan University, P. R. China***)

A THESIS SUBMITTED

FOR THE DEGREE OF MASTER OF SCIENCE

DEPARTMENT OF CHEMISTRY

NATIONAL UNIVERISTY OF SINGAPORE

2001

Acknowledgements

It is a great pleasure to express my gratitude to Assistant Professor Suresh Valiyaveettil for his support and understanding throughout the course of the research, and Associate Professor Kum-Fun Mok for his patience in solving the crystal structures and correcting the thesis.

Thanks are due to my laboratory mates Fan Ailong, Balasubramaniam Venkataramanan, Zu Ning, Feng Zheng, Chinnappan Baskar, Rajamani Lakshminarayanan, Ye Huanwen, Jin Jianyong, Shu Wenmiao, Liao Shaowen, Dr. Du Xingyu, Dr. Thomas Johnson, Dr. Zaher Judeh, and Assoc. Prof. Kum-Fun Mok's group students Li Zhaohui and Vetrichelvan for their warm friendship, assistance and encouragement as well as to Angelia Kar Min Hoong and Bob Teo Boon Siah.

I am grateful to Assoc. Prof. Dr. J. J. Vittal and Ms. Tan Geok Kheng for their analysis of some crystal structures and VT powder XRD analysis. I am also grateful to the National University of Singapore for a research scholarship to pursue my master degree.

My deepest gratitude goes to my mother and my wife for their moral support and encouragement, without which, the work cannot be finished.

Table of Content

Summary

The design of new architectures for the purpose of crystal engineering has generated great interest in recent years. In particular, organic compounds have been the focus of many studies due to the presence of functional groups that can form strong and stable intermolecular interactions. Therefore, recognizing geometry and functionality at the molecular level has relevant implications in the design of supramolecular patterns. These patterns in turn can be translated to physical or chemical properties in a solid. Carboxylic acid group is undoubtedly the most commonly used functional group to construct supramolecular architectures. In this project, a series of diacids and triacids were designed and synthesized. Both synthetic and some commercially available diacids and triacids (i.e. isophthalic acid, trimesic acid) were employed to construct supramolecular architectures with the hope of understanding the molecular self-assembly in the solid state and designing novel functional materials.

Here seven dicarboxylic acids and seven tricarboxylic acids have been synthesized and successfully characterised using various techniques.

In order to get single crystals with suitable quality for x-ray analysis, several methods (solvent diffusion, slow evaporation, liquid diffusion etc.) were employed during our research. Deprotonated diacids and triacids, together with transitional metal ion such as Cu, Co, Zn etc, were used with the hope of getting stable organo-metallic frameworks or polymers.

Chapter 1 gives a brief introduction of crystal engineering focusing in architectures from carboxylic acid groups and cyanuric acid compounds.

Chapter 2 describes the preparation and characterization of four dicarboxylic acid compounds and their complexes with bipyridine molecules. In the solid state, these compounds exhibits wave-like structures formed by ribbons, which were connected by centro symmetrical acid dimers. When the conformations of the diacid molecules change, the wave-like ribbons also slightly change in the dimension and direction, which demonstrate the diacids as potential building blocks.

In Chapter 3, the result of self-assembly from tricarboxylic acids is discussed and their preparations are given. When cocrystallized with 1,3,5-trihydroxybenzene (THB), 1,3,5-benzenetricarboxylic acid (TMA) forms a planar close packed structure with a much smaller cavity compared with normal honeycomb structure. When TMA cocrystallized with 3-dodecyloxyl pyridine (C_{12}Py), the observed solid-state structure was very similar as that found from 5-hexadecyl isophthalic acid and one acid group of TMA formed salt with ddpy. The structure from cyanuric acid (CA) and 4,4'-dithiodipyridine (ddpy) complex is composed of cyanuric acid ribbons, interconnected by ddpy bridge molecules.

Chapter 4 gave some results of our approaches for microporous structure with the help of coordination chemistry. One crystal structure from the complex formed between isophthalate, Cu (II), and 2,2'-bipyridine (bpy) was discussed. There are two kinds of subunits inside the structure, in which the Cu atom has different coordination environments.

Abbreviations and Symbols

2D	two dimmension
3D	three dimmension
AIBN	2,2’-azobisisobutyronitrile
bipy	4,4’-bipyridine
bpy	2,2’-bipyridine
BTC	1,3,5-benzenetricarboxylate
$C_{12}Py$	4-dodecyloxy-pyridine
CA	cyanuric acid
$CDCl_3$	deuterated chloroform
Conc	concentrated
CnISA	5-alkoxyl-isophthalic acids
ddpy	4,4’-dithiodipyridine
dipet	1,2-di(4-pyridyl) ethylene
DMF	N,N’-dimethylformamide
DMSO	dimethyl sulfoxide
DMSO-d_6	deuterated dimethyl sulfoxide
DSC	differential scanning calorimetry
ESI-MS	electron spray ionization mass spectrum
g	gram(s)
HB	hydrogen bonding
hr	hour(s)
Hz	Hertz
i.e.	that is (Latin *id est*)

IPA	isophthalate
J	coupling constant
m	multiplet
mg	milligrams(s)
ml	milliliter(s)
MS	mass spectrum
NBS	N-bromosuccinimide
NMR	nuclear magnetic resonance
q	quartet
s	singlet
STM	scanning tunneling microscopy
t	triplet
TGA	thermogravimetric analysis
THB	1,3,5-trihydroxy benzene
THF	tetrahydronfuran
TLC	thin layer chromatography
TMA	trimesic acid
VT	variable temperature
XRD	x-ray diffraction
Å	angstrom(s)
δ	Chemical shift (in NMR spectroscopy)

Chapter 1 Introduction

*"**Crystal engineering** is the understanding of intermolecular interactions in the context of crystal packing and in the utilization of such understanding in the design of new solids with desired physical and chemical properties."*

--------Gautam R. Desiraju, in
<<Crystal Engineering: the Design of Organic Solids>>, 1989, Elsevier

The design of new architectures for the purpose of crystal engineering has generated great interest in recent years. In particular, organic compounds have been the focus of many studies due to the presence of functional groups that can form strong and stable intermolecular interactions. Therefore, recognizing geometry and functionality at the molecular level has relevant implications in the design of supramolecular patterns. These patterns in turn can be translated to physical or chemical properties in a solid.

Traditional synthetic chemistry is based on the controlled formation and cleavage of covalent bonds. However, complicated nanoscale systems would be extremely difficult to synthesize using traditional covalent methods. As a result, the development of a field known as *synthetic supramolecular chemistry* has recently begun to emerge. Investigations on the assembly of small organic molecules in solution and in the solid state are important in expanding these new notions for the design of well-defined supramolecular architectures.

1.1 Crystal engineering and molecular recognition

The term crystal engineering was first coined by Schmidt in connection with his work on the topochemical reactions of crystalline cinnamic acids in 1971 [1]. However, recently this field has developed rapidly due to its important implications in materials science. Desiraju defined crystal engineering as "the understanding of intermolecular interactions in the context of crystal packing and the utilization of such understanding in the design of new solids with desired physical and chemical properties" [2]. In this way crystal engineering, first designed for solid-state reactions, has been applied to the creation of solids that exhibit properties such as nonlinear optical activity [3], ferroelectricity [4], piezoelectricity [5], triboluminescence [6], and porosity [7].

Crystal engineering is based on concepts that have been broadly used in supramolecular chemistry [8]. Crystals are not just collections of molecules and their structural properties are different from those of their molecular constituents. Crystals are a repetitive arrangement of molecules in three dimensions with an impressive level of precision in molecular arrangements and have been regarded by Dunitz as "supermolecules *par excellence*" [9].

A large amount of efforts has been invested in the study of crystal growth [10, 11] and crystal packing [12]. The potential energy of a crystal has been factored into component parts and has been attributed to various kinds of interactions including electrostatic, hydrogen bonding, donor-acceptor interactions, steric repulsions and van der Waals attractions. While intermolecular interactions have been classified in different ways, the most meaningful criteria are their distance dependence and their directionality. Desiraju has classified intermolecular interactions in organic solids into two types: medium-range

isotropic forces (close-packing) and long-range anisotropic forces (electrostatic interactions) [13]. Isotropic forces include CΛC, CΛH and HΛH interactions and anisotropic forces include ionic interactions, strong hydrogen bonds (O–HΛO, N–HΛO), weak hydrogen bonds (C–HΛO, C–HΛN, O–HΛ*π)* and other forces such as halogenΛhalogen interactions.

Non-covalent interactions have been extensively used in crystal engineering, since they are the fundamental cause of the formation of crystals [9]. Hydrogen bonding, π…π interactions, and πΛhydrogen interactions were employed for this purpose. Intermolecular interactions are considered as synthetic vectors or "glue" in designing new solids [14, 15]. Therefore if geometry, strength, and directionality can be recognized in the functional groups of a molecule, it is possible to rationalize its supramolecular solid-state structure. Such a view would have been difficult to defend as recently as 1988 when Maddox made the following statement: "One of the continuing scandals in the physical sciences is that it remains in general impossible to predict the structure of even the simplest crystalline solids from a knowledge of their chemical composition" [16].

1.2 Strategies for crystal engineering

There are several approaches to the design of functional solids. Different strategies have been applied by several groups in order to obtain the desired intermolecular recognition. In 1954, Wald proposed that each component molecule could spontaneously assemble into an intact cell and suggested that they should contain all the necessary information to recognize and interact with other appropriate molecules [17].

Lawrence has suggested that certain factors that promote formation of small complexes can also be applied to crystal engineering. The use of the appropriate solvent and conditions can enhance the directionality and geometry of non-covalent interactions that are responsible for maintaining the structural integrity of a complex. He also suggested ways in which a supramolecular complex can be selectively isolated from solution in order to prevent dissociation of the aggregate to its component parts [18].

Most recently, Desiraju has drawn a parallel between organic synthesis and crystal engineering in an attempt to identify molecular recognition patterns in solids [19]. Stoddart has also discussed approaches to synthetic supramolecular chemistry of nanosystems [20]. Traditionally structural chemists examined a large number of known crystal structures and attempted to eliminate certain possibilities on the basis of previous knowledge of crystal packing. However, it has been repeatedly observed that certain building blocks or "supramolecular synthons" display a clear pattern preference. Molecules that contain these building blocks tend to crystallize in specific energetically favourable arrangements that can coexist with efficient close packing. In this way, by identifying these synthons, and with the aid of the Cambridge Structural Database (CSD), it is possible to work backwards and "retrosynthetically" formulate empirical rules about the recognition patterns of various geometrical and functional groups [19]. Some examples of the synthons identified by Desiraju are depicted in Figure **1.1**.

The dimer and the catemer motifs are patterns commonly observed for carboxylic acids [21] as well as for amides (Figure **1.1a**) [22]. A dimer is formed whenever hetero-functional group recognition between a carboxylic acid and an amide is available (Figure **1.1b**). This finding has been well documented and used in connection with carboxylic acid receptors [23]. Desiraju has also identified synthons based on the same geometry but with

different hydrogen bonding directionality. For example, the top components in Figure **1.1c** have, in left to right order, acceptor-donor-acceptor, acceptor-acceptor-donor, and acceptor-acceptor-acceptor hydrogen bonding orientation [21]. Their bottom counterparts have complementary functionalities. Figure **1.1d** shows the formation of cyclic trimers based on strong hydrogen bonds or polarization interactions [22]. The synthons described by Desiraju have been observed repeatedly in solid-state structures and have been used in the design of crystals, as well as in other areas of supramolecular chemistry [2].

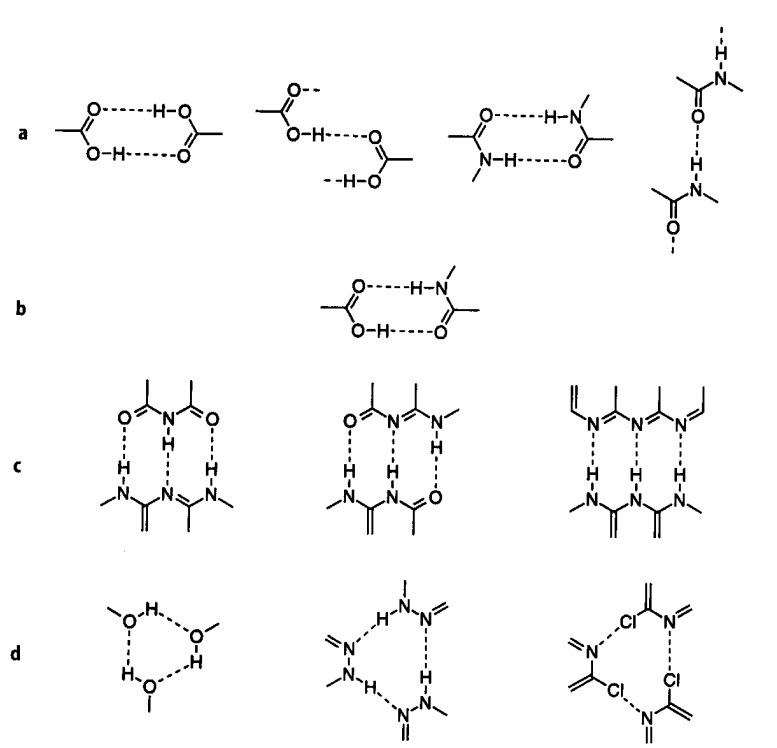

Figure 1.1 Representative supramolecular synthons.

1.3 Hydrogen bonding

Hydrogen bonding is without doubt the most studied intermolecular interaction, presumably due to its frequent presence in organic solids and biological molecules. Various attempts have been made to define the hydrogen bond [24, 25] and many detailed

investigations of its properties have been carried out [14, 26]. Pioneering scientists such as Etter [27, 28], Leiserowitz and Schmidt [21,22], Jeffrey and Saenger [29, 30], and Taylor and Kennard [31] have conducted extensive studies of the solid-state structures of organic compounds in a search for patterns, directionality, and strength in the occurrence of hydrogen bonding.

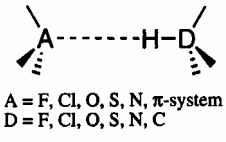

Figure 1.2 Hydrogen bonds formed between an acidic hydrogen atom (D-H) and an acceptor (A).

The selectivity and directional nature of hydrogen bonding has led to its extensive use in the construction and stabilization of large non-covalently bonded molecular and supramolecular structures. Hydrogen bonds are formed when a donor (D) with an available acidic hydrogen atom is brought into intimate contact with an acceptor (A) as shown in Figure **1.2** [32]. The strength of different hydrogen bonds can vary from 4 kJ/mol for C–HΛO [33] interactions to 170 kJ/mol for [F–H–F] [34, 35]. In terms of geometry, the hydrogen bond has been studied by statistical investigations [31] and by X-ray diffraction analysis [36].

One of the first detailed studies of hydrogen bonding patterns in the solid state was conducted by Etter [27]. Her studies showed that functional groups display a preference for certain recognition patterns, leading to the conclusion that hydrogen bonding is not random, but controlled by the directional strength of the intermolecular interactions. They illustrated that hydrogen bonding can be used as a synthetic tool to affect profoundly the

spatial arrangement of molecules and ions in the solid-state. Another important contribution by Etter was the development of graph sets in order to define the morphology of hydrogen-bonded arrays [27]. Recently, Bernstein et al. [37] have expanded the approach for those who wish to apply this method to their hydrogen bonding analysis.

1.4 Basic patterns in crystal engineering: tapes, ribbons, and sheets

In discussing tapes, ribbons, and sheets we should not ignore the competing formation of cyclic aggregates in many of the designed systems. There has been extensive discussion of the enthalpic and entropic influences on cyclic vs. linear aggregate formation. As a consequence, different approaches have been used to promote formation of cyclic aggregates rather than linear aggregates [38].

The terms tape and ribbon have not yet been defined in a way that allows them to be easily distinguished. In general, ribbons or tapes have been used to describe particular types of packing. For example, MacDonald and Whitesides [39] have distinguished tapes from ribbons formed by amides in the following manner: "a tape motif is generated when each molecule is hydrogen bonded to two neighbouring molecules, and when the hydrogen bonds between any two molecules form an eight membered ring; a ribbon motif is generated when each molecule is hydrogen bonded to three or more molecules, regardless of the connectivity of hydrogen bonds between the molecules".

Since our work is a compilation of structures that possess different functionalities and geometries, we will distinguish between tapes and ribbons in the following manner. A tape will form when the functional groups involved in intermolecular interactions on a molecule are antiparallel or at 120° to each other, thus the molecule can interact with only two adjacent molecules in a linear or zigzag fashion. In a ribbon pattern, the functional

groups may be oriented in different directions, giving some flexibility in the recognition to adjacent molecules. A sheet will involve the formation of two-dimensional arrays stabilized by intermolecular interactions. Most of the examples presented here will involve compounds with functional groups built around a cyclic template. A schematic representation of tapes, ribbons, cyclic and sheet aggregates is shown in Figure **1.3**. The triangle represents a template that may be the same or different components and the dashed lines represent intermolecular interactions.

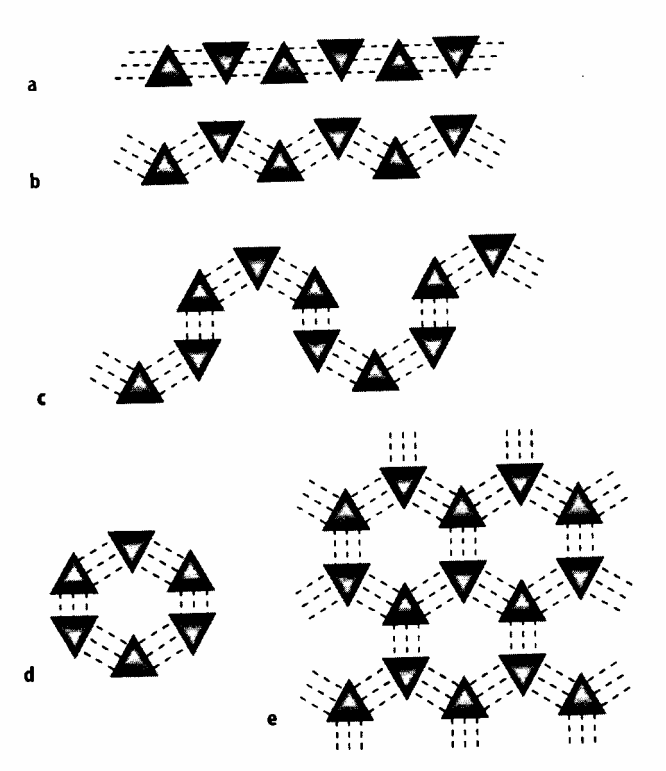

Figure 1.3a – e Schematic representation of: **a**, **b** tapes; **c** ribbons; **d** cyclic aggregates; **e** sheet aggregates.

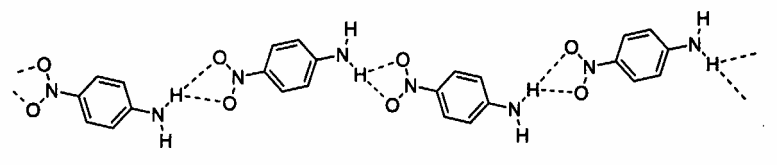

Figure 1.4 Tape structure formed by *p*-nitroaniline (**1**).

Tapes and ribbons have been of interest in crystal engineering due to various applications in materials science. Stabilization of the translation of molecules through intermolecular forces in a solid can generate polarity, which is a necessary condition for a number of physical properties. For example, small molecule nitroaniline compounds show preference for a motif that involves one amino proton associating with both oxygens of a nitro group, leading to the formation of a tape structure (Figure **1.5**). In particular, *p*-nitroaniline (**1**) has been studied for its non-linear optical properties [40].

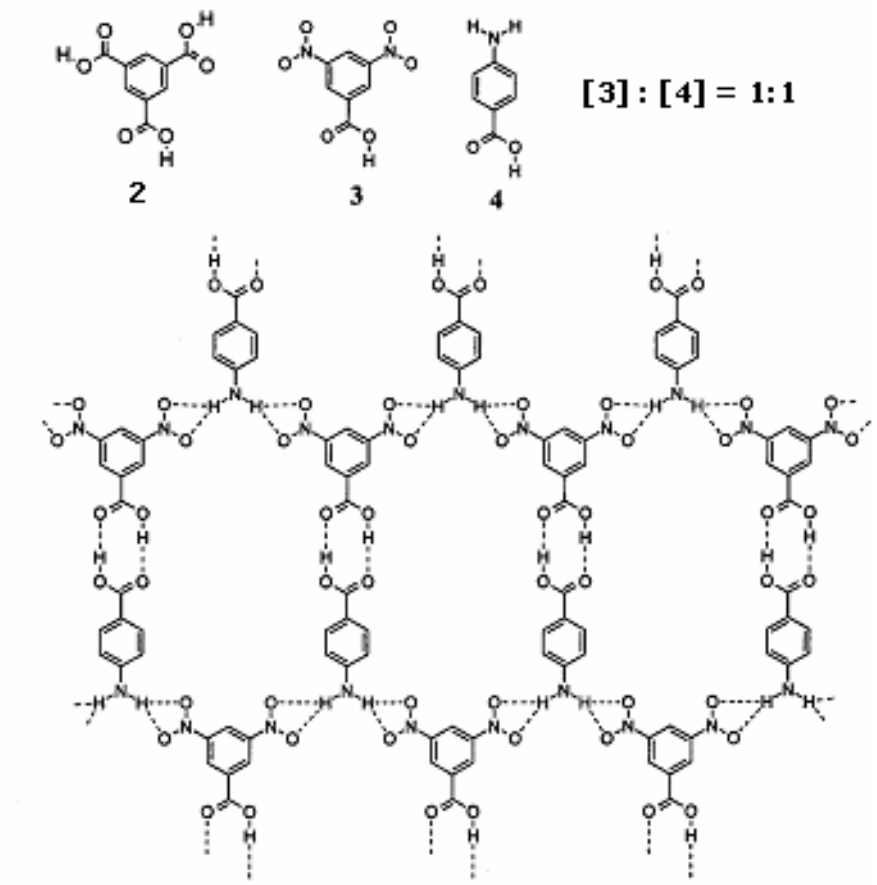

Figure **1.5**. Polar sheets formed by **3** and **4**.

The sheet type architecture has received much interest because of its potential to generate structural patterns that contain voids, which may in turn have applications in the area of zeolitic materials. Trimesic acid (**2**) (Figure **1.9**) has been extensively studied for this purpose [41]. However, Etter and Frankenbach have been able to form polar sheets when 2,5-dinitrobenzoic acid (**3**) and 4-aminobenzoic acid (**4**) were cocrystallized (Figure **1.5**) [42].

We will present some examples of tapes, ribbons, and sheets based on hydrogen bonding groups, especially strong hydrogen bonding from carboxylic acid groups.

1.5 Architectures from aromatic acids and cyanuric acid

Perhaps the best-known hydrogen-bonding pattern is formed by carboxylic acids. Carboxylic acids are divided into two sets based on the symmetry of their O–HΛO hydrogen bonding patterns. They can form hydrogen bonding patterns that contain a center of inversion (the dimer motif) and also aggregate in acentric one-dimensional chains (catemers) resulting from the formation of hydrogen bonds to two or more neighboring acids (Figure **1.6**).

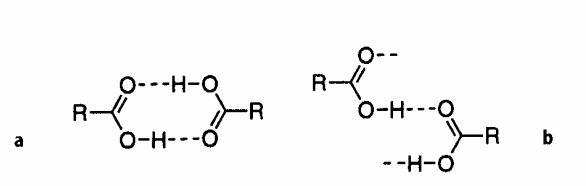

Figure **1.6 a, b** Hydrogen bonding patterns of carboxylic acids: **a** dimer; **b** catemer.

A set of 139 benzoic acids was analysed by Frankenbach and Etter, and a relationship between the presence of an inversion centre in the hydrogen-bonding pattern and inversion

symmetry in their crystal structure was observed [43]. Of the 118 crystals that contained the dimer motif, 98% crystallized in centrosymmetric space groups. On the other hand, of the 21 crystals that contained the chain motifs, 52% crystallized in acentric space groups. This study suggested that hydrogen-bonded aggregates bias the crystal growth processes [43]. Dicarboxylic acids with an antiparallel relationship between the hydrogen bonding groups can be expected to form one-dimensional (1-D) strands [21]. For example, terephthalic acid (1,4-benzene dicarboxylic acid) (**5**) self-assembles via the dimer motif to form 1-D tapes (Figure **1.7**) [44]. This packing is predictable because of the geometry and functionality of terephthalic acid. However, the arrangement of the chains with respect to their adjacent neighbours is less predictable, because there are no strong directional forces between them. Thus, terephthalic acid has at least two polymorphs [44].

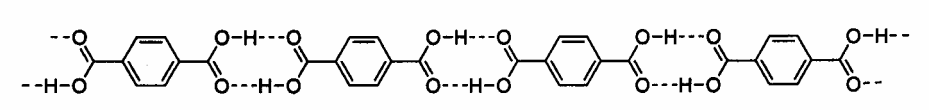

Figure 1.7 Hydrogen bonded tape formed by terephthalic acid (**5**).

1.5.1 Aromatic acids

The preference of pattern formation from carboxylic acid is based on the size of the R group in RCOOH. Acids containing small substituent groups (formic acid, acetic acid) form the catemer synthon, while most others (especially aromatic carboxylic acids) form dimers, although not exclusively [21]. Figure **1.8** shows the hydrogen bonding pattern of benzoic acid (**6**) and 3-(4-chlorophenyl)-prop-2-ynoic acid (**7**) [20].

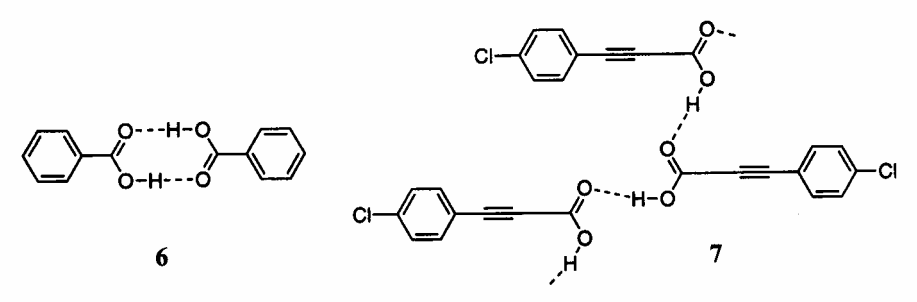

Figure 1.8 Carboxylic acid dimer formed by **6** and polymeric hydrogen bonds formed by **7**.

The dimer synthon formed by the carboxyl group has been used to assemble a variety of supermolecules due to its bidentate character which increases the strength of the interaction. For example, terephthalic acid (**8**) [44] and isophthalic acid (**9**) [45] form one dimensional tapes. Trimesic acid (**2**) with its threefold molecular symmetry forms a two dimensional hydrogen bonded sheet [46] and 1, 3, 5, 7-adamantanetetracarboxylic acid (**10**) with its tetrahedrally disposed carboxyl functionality forms a diamondoid network (Figure **1.9**) [47].

Yang et al. have induced the formation of a hexameric cyclic array by appropriately modifying isophthalic acid [48]. The reasoning behind this approach is that a bulky substituent at C-5 on isophthalic acid might disrupt the tape packing motif in the solid state. The structure of 5-decyloxyisophthalic acid (**11**) was successfully characterized by X-ray crystallography yielding the anticipated hydrogen bonding pattern (Figure **1.10**). Vapor pressure osmometry experiments indicated the presence of the cyclic hexamer in solution as well as in the solid state. The crystal structure of 5-octyloxyisophthalic acid (**12**) has also been determined and is observed to form the hydrogen bonding pattern in the same space group (R3) [49].

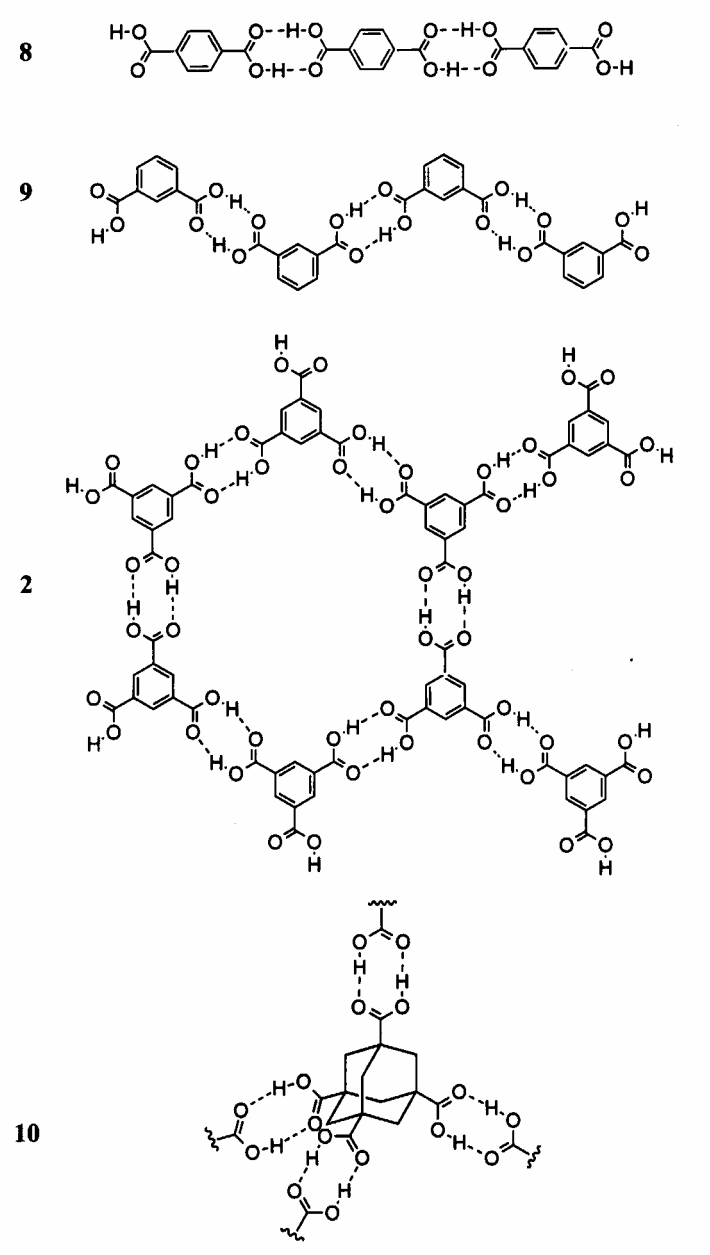

Figure 1.9 Examples of one-dimensional tapes (**8**) and (**9**), two-dimensional sheets (**2**) and three-dimensional structures (**10**) held together by the carboxylic acid dimer.

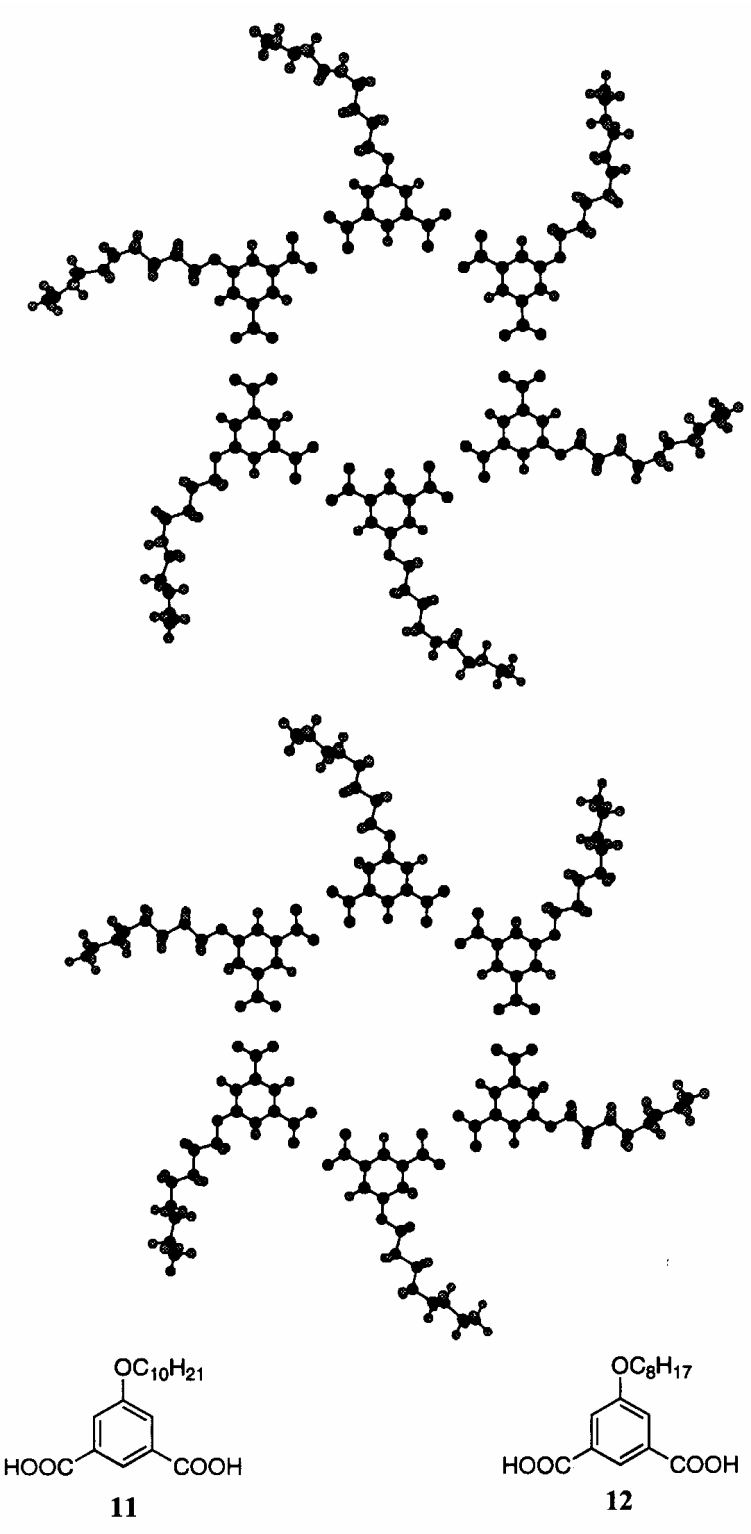

Figure 1.10 Cyclic hexameric aggregates formed by 5-alkoxyisophthalic acids **11** and **12** [48, 49].

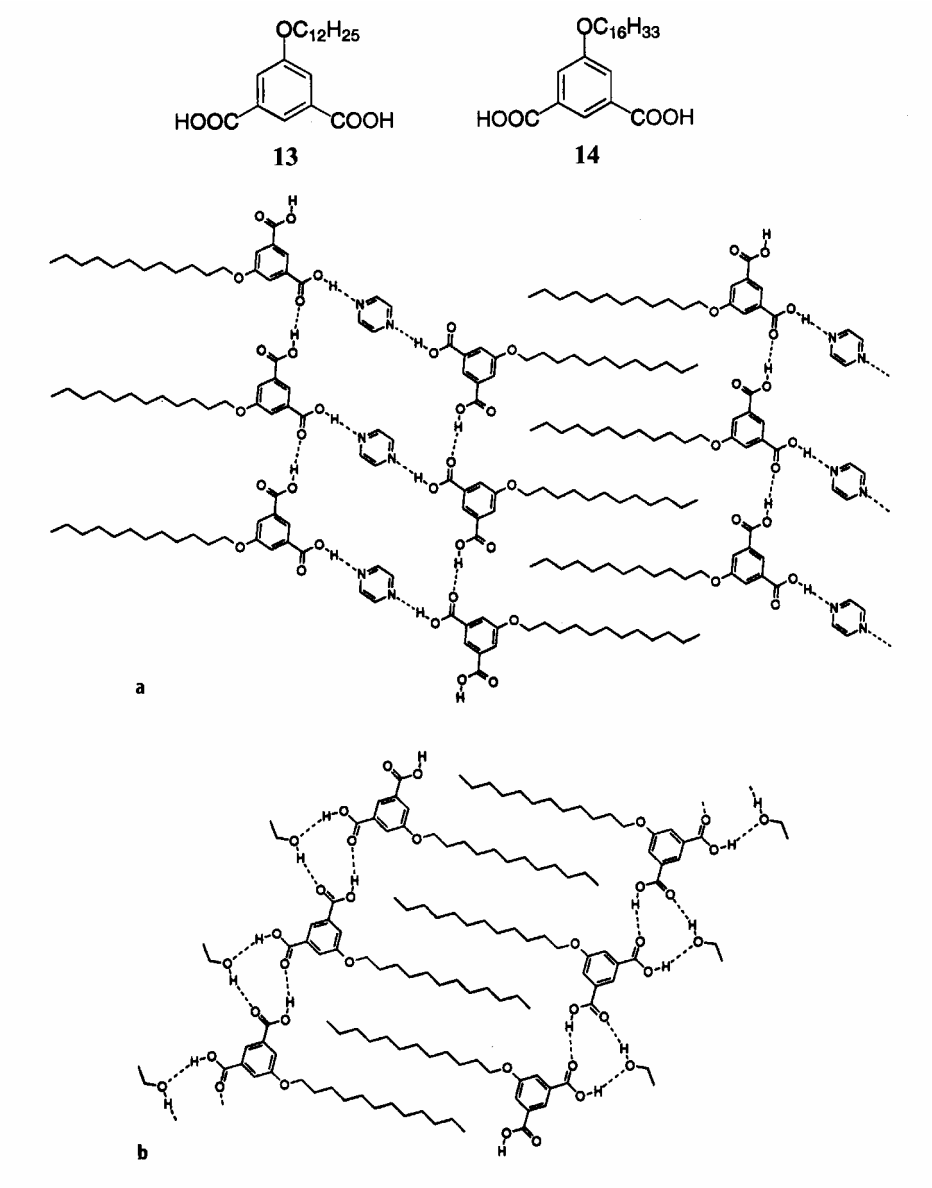

Figure 1.11 a, b Tapes and ribbons formed by **13** and **14**.

Several 5-alkoxyisophthalic acids, when cocrystallized with pyrazine, pyrimidine and ethanol, form tapes and ribbons in the crystal structure [50]. The carboxylic acid units of **13** engage in hydrogen bonding to other acids as well as to the bases and alcohol (Figure **1.11 a, b**). In Figure **1.11 c** the pyrimidine acts as a spacer between **14**, extending the tape formation.

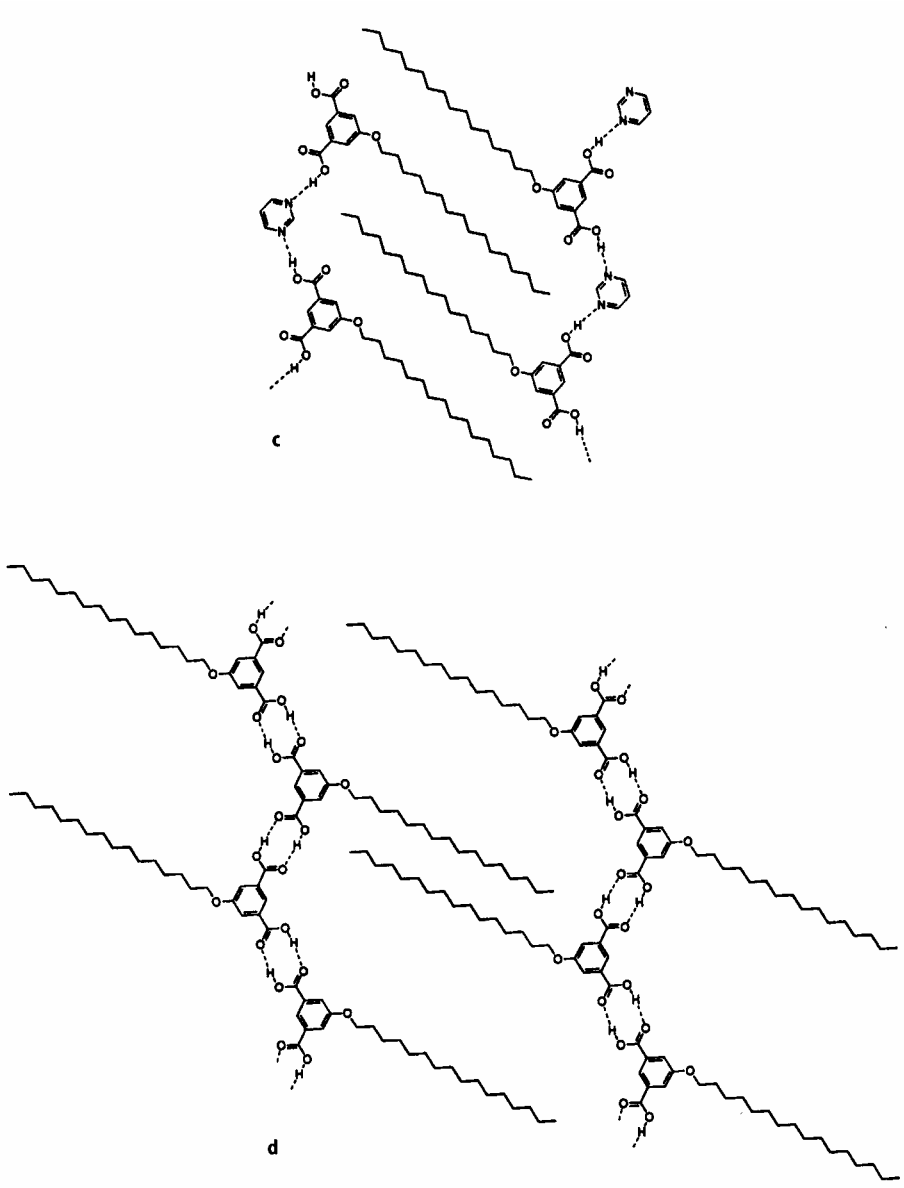

Figure 1.11 c, d.

However, when acid **14** is recrystallized in its pure form, the formation of the carboxylic acid dimer motif occurs between adjacent molecules. The aggregation of these molecules does not occur in a cyclic hexamer, but as tapes (Figure **1.11 d**) [51]. It is likely

that, despite the presence of a bulky substituent in the 5-position, formation of tapes optimizes van der Waals interactions between the longer hydrophobic chains.

The primary characteristic in the crystal packing of trimesic acid (**2**) (Figure **1.9**) that has caught the interest of chemists is the formation of cavities that are 14 Å in diameter [46]. These cavities have potential for the formation of inclusion compounds. However, in the room temperature crystal structure of **2**, the 14 Å cavities are filled by perpendicular sheet of equivalent trimesic acid molecules in a triple catenation arrangement. Herbstein has included a variety of guests in these pores unbranched and branched paraffins (n-tetradecane, isooctane), long-chain alcohols (heptanol, octanol, decanol, and oleyl alcohol), alkanes (l-octene, squalene), alicyclic (camphor) and other guests like methoxyethyl ether, propellane, and epichlorohydrin. Although in some cases catenation is prevented from occurring, at present only five hexagonal networks stacked on top of each other have been observed [41]. Sections of the crystal structures of **2** with n-tetradecane and oleyl alcohol included in the cavities are shown in Figure **1.12** [52].

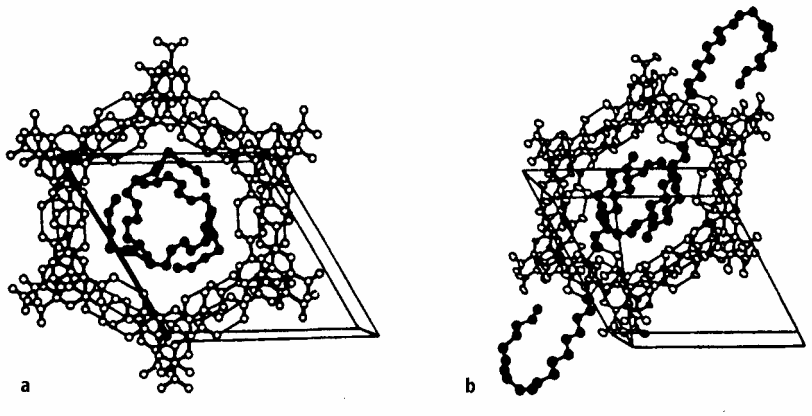

Figure 1.12 a, b. Structures of inclusion compounds of **2** with: **a** *n*-tetradecane; **b** oleyl alcohol.

Based on Herbstein's results using long chain guests, Zimmerman proposed to prevent interpenetration of the trimesic acid networks by including a large and relatively non-flexible guest molecule such as pyrene in the cavities. Indeed the pyrene is incorporated in the cavity as well as some ethanol solvent molecules (Figure **1.13**). The hydrogen-bonded dimer in **2** is actually expanded by the presence of ethanol molecules, although the formation of the hexamer prevails in the sheet structure [53].

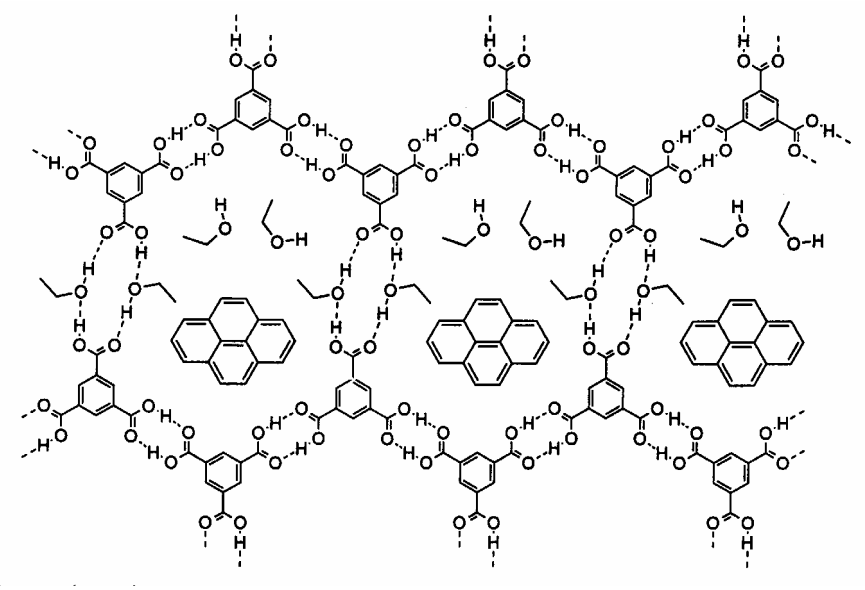

Figure 1.13 Sheets formed in the crystal structure of [**2** 2·pyrene·2EtOH].

In the context of generating porosity, Zaworotko's group has used a modular approach to propagate the symmetry of trimesic acid. This strategy involves the use of hydrogen bonding spacers between units of **2** to expand the size of the cavities. In this case secondary amines were reacted with **2** to form salts **15** and **16** (Figure **1.14**). The resulting solid lattices were observed in the crystal structure of **15** to have expanded their cavities from 11 Å (taking into account van der Waals radius) to 12.7 Å. In **16** the hexamer

cavities are distorted and therefore the diameter is reduced to 10.4 Å (see Figure **1.14**) [54].

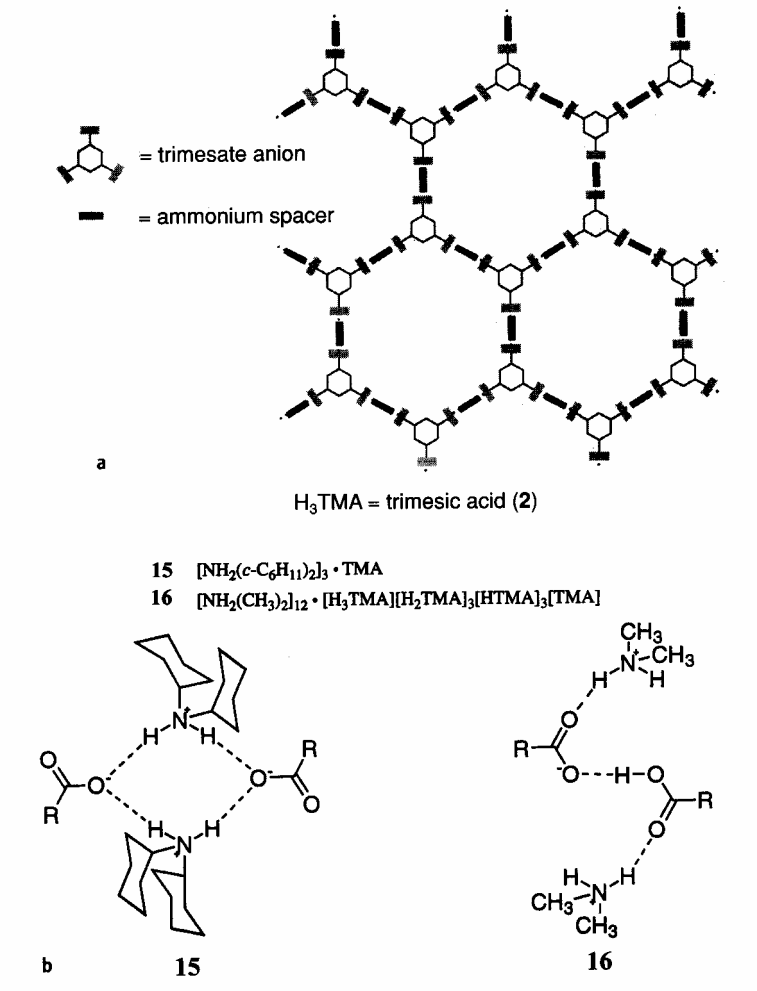

Figure 1.14a, b Schematic representation of the modular strategy for increasing cavity size in **2**. b Hydrogen bonding pattern in salts **15** and **16**.

The reason that many interesting structures were formed from trimesic acid is that the molecule has a rigid backbone and three acid groups, which can form strong hydrogen bonds and thus form extended network structure. Based on the same reason, cyanuric acid (CA, Scheme 1.1) absorbs our interest because of its similar rigid backbone and three hydroxy groups, which are also good donors to form hydrogen bonds.

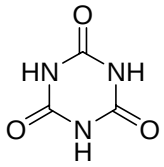

Scheme 3.1 Structure of cyanuric acid (CA).

1.5.2 Cyanuric acid (CA)

Recently, cyanuric acid absorbs much interest in crystal engineering. Lehn et al [55] used the CA to induce a strand to form helical structure. Whitesides et al [56] used CA to form an adduct with melamine which has the well-known rosette structure involving a hexagonal network

CA crystallized from methanol has a planar sheet structure wherein adjacent molecules are held together by symmetrical cyclic N–HΛO hydrogen bonds as shown in Figure **1.15a** [57]. This bonding gives rise to molecular tapes connected to each other by single N–HΛO hydrogen bonds. CA crystallized from water, however, incorporates the solvent of crystallization into the structure giving the composition $CA{\cdot}H_2O$. This has a chain structure where adjacent molecules are connected together by a single N–HΛO bond rather than by the cyclic hydrogen-bonded dimers [58] (Figure **1.15b**).

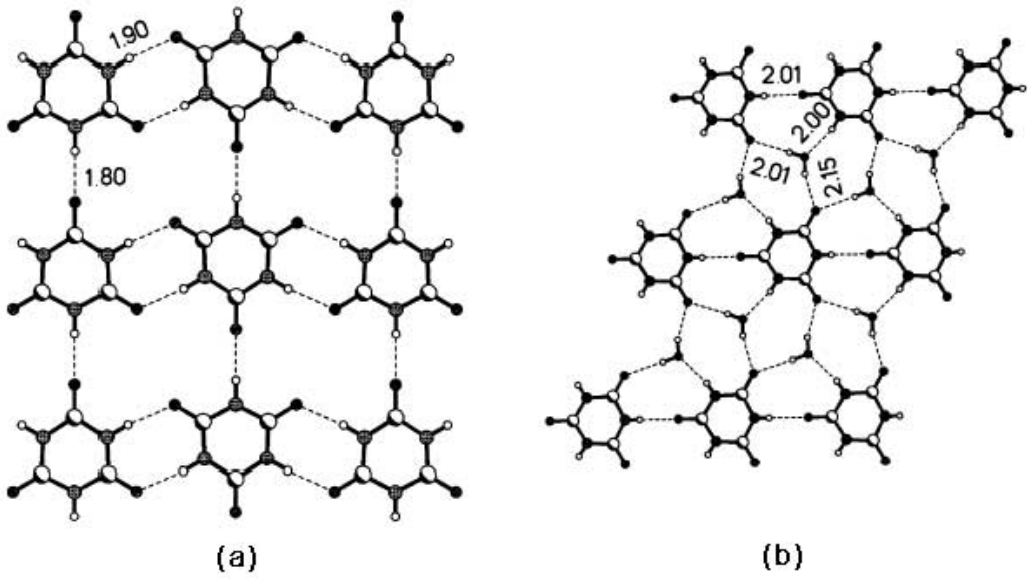

Figure 1.15 (a) Packing arrangement of CA molecules in the two-dimensional sheets[57], (b) Arrangement of CA and H_2O molecules in CA·H_2O forming two-dimensional sheets[58]. Notice single hydrogen bonds between CA molecules in (b) compared to the cyclic dimers in (a). Hydrogen bonds are shown as dashed lines. Unique HΛO distances are indicated.

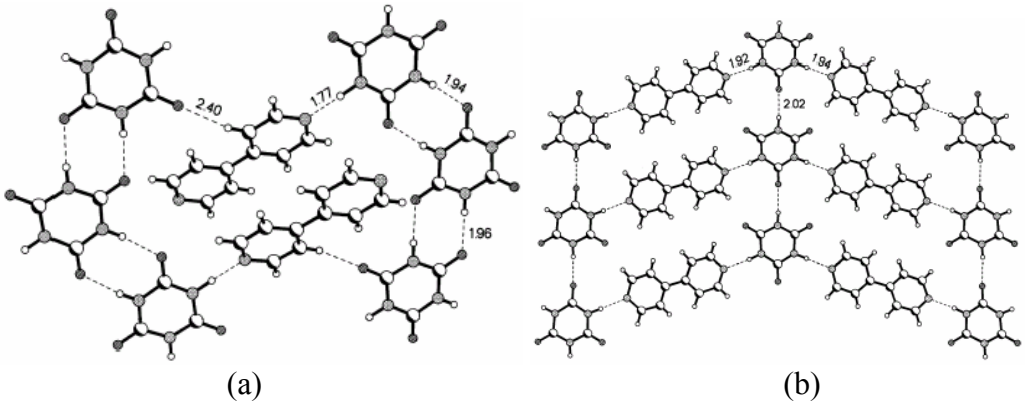

Figure 1.16 (a) Arrangement of CA and bipy in the 2:1 hydrogen-bonded adduct obtained from methanol. Notice the presence of cyclic hydrogen bonds. (b) Two-dimensional arrangement of CA and bipy in the 1:1 hydrogen-bonded adduct, obtained from water [59]. Notice the presence of only single hydrogen bonds (and the absence of cyclic hydrogen bonds).

Recently, Rao et al [59] revealed that when CA cocrystallize with 4,4'-bipyridine (bipy) using different solvents, the structures of hydrogen-bonded assemblies are entirely different. When crystallized from methanol, a sheet structure with cyclic dimeric hydrogen bonds between the adjacent CA molecules was observed (Figure **1.16a**). However, from water, a chain structure with single N–HΛO bonds was obtained (Figure **1.16b**).

1.6 Aim of the present project

Based on the introduction above, we were interested in creating new supramolecular architectures with compounds having multiple acid functional groups and cynauric acid.

The purposes of this work were to synthesize polyacid compounds (diacids and triacids), and use them (together with some commercially available diacids and triacids, i.e. isophthalic acid, trimesic acid) as potential building blocks to construct 2D or 3D, ribbon or sheet type of supramolecular architectures.

1) Synthesize a few structural analogues of benzene dicarboxylic acids;
2) Synthesize a few structural analogues of benzene tricarboxylic acids;
3) Investigate the self-assembly of diacids and triacids in the absence and presence of bipyridine bases;
4) Investigate the coordination structure formed from the deprotonated diacids and triacids using metal ion complexation.

1.7 Reference

[1] G. M. J. Schmidt, *Pure Appl. Chem.,* **1971**, 27, 647.

[2] G. R. Desiraju, *Crystal engineering, the design of organic solids*, **1989**, Elsevier, Amsterdam.

[3] S. H. Lee, S. Balasubramanian, D. Y. Kim, N. K. Viswanathan, S. Bian, J. Kumar, S. K. Tripathy, *Macromolecules*, **2000**, 33, 6534.

[4] T. KATO, J. M. J. FRECHET, *Macro. Symp*, **1995**, 98, 311.

[5] H. Xu, N. Kang, P. Xie, R. B. Zhang, D. F. Xu, *Liq. Cryst*., **2000**, 27, 169.

[6] L. M. Sweeting, A. L. Rheingold, J. M. Gingerich, A. W. Rutter, R. A. Spence, C. D. Cox, T. J. Kim, *Chem. Mater*. **1997**, 9, 1103.

[7] M. Eddaoudi, H. L. Li, O. M. Yaghi, *J. Am. Chem. Soc*. **2000**, 7, 1391.

[8] J. –M. Lehn, *Angew Chem., Int. Ed. Eng.,* **1988**, 27, 89.

[9] J. D. Dunitz, *Pure Appl. Chem*., **1991**, 63, 177.

[10] D. Braga, F. Grepioni, *Acc. Chem. Res*., **1994**, 27,51.

[11] J. Hulliger, *Angew Chem. Int. Ed. Engl.*, **1994**, 33, 143.

[12] B. K. Vainshtein, V. M. Fridkin, V. L. Indenbom, *Structure of Crystals*, 2nd Edn. **1994**, Springer, Berlin.

[13] G. R. Desiraju, *The Crystal As a Supramolecular Entity*, **1995**, Wiley, Chichester.

[14] C. B. Aakeroy, K. R. Seddon, *Chem. Soc. Rev*., **1993**, 22, 397.

[15] M. J. Zaworotko, *Chem. Soc. Rev*., **1994**, 283.

[16] J. Maddox, *Nature*, **1988**, 335, 201.

[17] G. Wald, *Sci. Am.*, **1954**, 191, 44.

[18] D. S. Lawrence, T. Jiang, M. Levett, *Chem. Rev*., **1995**, 95, 2229.

[19] G. R. Desiraju, *Angew Chem. Int. Ed. Engl*., **1995**, 34, 2311.

[20] M. C. T. Fyfe, J. F. Stoddart, *Acc. Chem. Res*., **1997**, 30, 393.

[21] L. Leiserowitz, *Acta Crystallogr., B*, **1976**, 32, 775.

[22] L. Leiserowitz, G. M. J. Schmidt, *J. Chem. Soc*., **1969**, 2372.

[23] F. Garcia-Tellado, S. J. Geib, S. Goswami, A. D. Hamilton, *J. Am. Chem. Soc*., **1991**, 113, 9265.

[24] T. Zeegers-Huyskens, P. Huyskens P, *Intermolecular forces -an introduction to modern methods and results*, **1991**, Springer- Verlag, Berlin Heidelberg New York.

[25] P. W. Atkins, *General Chemistry*, **1989**, Scientific American Books, New York.

[26] S. N. Vinogradov, R. H. Linnell, *Hydrogen Bonding*, **1971**, Van Nostrand Reinhold, New York.

[27] M. C. Etter, *Acc. Chem. Res*., **1990**, 23, 120.

[28] M. C. Etter, *J. Phys. Chem*., **1991**, 95, 4601.

[29] G. A. Jeffrey, W. Saenger, *Hydrogen bonding in biological structures*, **1991**, Springer, Berlin.

[30] G. A. Jeffrey, *An introduction to hydrogen bonding*, **1997**, Oxford University Press, New York.

[31] R. Taylor, O. Kennard, *Acc. Chem. Res*., **1984**, 17, 320.

[32] D. Philp, J. F. Stoddart, *Angew Chem. Int. Ed. Engl*., **1996**, 35, 1155.

[33] L. Turi, J. J. Dannenberg, *J. Phys. Chem*., **1993**, 97, 7899.

[34] J. Emsley, *Chem. Soc. Rev*., **1980**, 9, 91.

[35] T. B. McMahon, J. W. Larson, *J. Am. Chem. S*oc., **1982**, 104, 5848.

[36] R. Taylor, O. Kennard, *Acta Crystallogr., B*, **1983**, 39, 133.

[37] J. Bernstein, R. E. Davis, L. Shimoni, N. –L. Chang, *Angew Chem. Int. Ed. Engl*., **1995**, 34, 1555.

[38] J. H. Lady, K. B. Whetsel, *J. Phys. Chem*., **1964**, 68, 1001.

[39] J. C. MacDonald, G. M. Whitesides, *Chem. Rev*., **1994**, 94, 2383.

[40] T. W. Panunto, Z. Urbanczyk-Lipkowska, R. Johnson, M. C. Etter, *J. Am. Chem. Soc*., **1987**, 109, 7786.

[41] F. H. Herbstein, *1,3,5-Benzenetricarboxylic acid (trimesic acid) and some analogues*, **1996**, J. –M. Lehn, Atwood JL et al. (eds) In: *Solid state supramolecular chemistry: crystal enginee- ring*. Pergamon, New York, Chap. 3. See also: F. H. Herbstein In: Weber E (ed). *Molecular inclusion and molecular recognition -clathrates I. Topics in Current Chemistry*, **1987**, vol 140, 107, Springer, Berlin Heidelberg New York.

[42] M. C. Etter, G. M. Frankenbach, *Chem. Mater*., **1989**, 1, 10.

[43] G. M. Frankenbach, M. C. Etter, *Chem. Mater*., **1992**, 4, 272.

[44] M. Bailey, C. J. Brown, *Acta Crystallogr*., **1967**, 22, 387.

[45] R. Alcala, S. Martinez-Carrera, *Acta Crystallogr., B*, **1972**, 28, 1671.

[46] D. J. Duchamp, R. E. March, *Acta Crystallogr., B*, **1969**, 25, 5.

[47] O. Ermer, *J. Am. Chem. Soc*., **1988**, 110, 3747.

[48] J. Yang, J. –L. Marendaz, S. J. Geib, A. D. Hamilton, *Tetrahedron Lett*., **1994**, 35, 3665.

[49] J. Yang, PhD thesis, 1996, University of Pittsburgh.

[50] S. Valiyaveettil, V. Enkelmann, K. Müllen, *J. Chem. Soc. Chem. Commun*., **1994**, 2097.

[51] K. Eichhorst-Gerner, A. Stabel, G. Moessner, D. Declerq, S. Valiyaveettil, V. Enkelmann, K. Müllen, J. P. Rabe, *Angew Chem. Int. Ed. Eng*., **1996**, l35, 1492.

[52] F. H. Herbstein, M. Kapon, G. M. Reisner, *J. Inclusion. Phenom*., **1987**, 5, 211.

[53] S. V. Kolotuchin, E. E. Fenlon, S. R. Wilson, C. J. Loweth, S. C. Zimmerman, *Angew Chem. Int. Ed. Engl*., **1995**, 34, 2654.

[54] R. E. Melendez, C. V. K. Sharma, M. J. Zaworotko, C. Bauer, R. D. Rogers, *Angew Chem. Int. Ed. Engl*., **1996**, 35, 2213.

[55] V. Berl, M. J. Chrische, I. Huc, J. –M. Lehn, M. Schmutz, *Chem. Eur. J*., **2000**, 6, 1938.

[56] J.A. Zerkowski, C.T. Seto, D.A. Wierda, G.M. Whitesides, *J. Am. Chem. Soc*. **1990**, 112, 9025.

[57] P. Coppens, A. Vos, *Acta Crystallog.* **1971**, B 27, 146.

[58] C. Chang-Zhang, S. Jian-Qiu, L. Zhou-Bin, G. Dong-Shou, H.X.L. Ding, *J. Struct. Chem.* **1995**, 14, 241.

[59] A. Ranganathan , V.R. Pedireddi , G. Sanjayan , K.N. Ganesh , C.N.R. Rao, *J. Mol. Struct*., **2000**, 522, 87.

Chapter 2 Self-assembly of dicarboxylic acid in the presence and absence of bases in the crystalline phase

2.1 Introduction

Crystal engineering is becoming a hot research area in the recent decades because it can help us with the "understanding of intermolecular interactions in the context of crystal packing and in the utilization of such understanding in the design of new solids with desired physical and chemical properties" [1]. The design of new architectures for the purpose of crystal engineering has generated great interest in recent years. In particular, organic compounds have been the focus of many studies due to the presence of functional groups that can form strong and stable intermolecular interactions [2]. Molecular building blocks or supramolecular synthons [3] are the core part of such architectures. Design of building blocks will be favorable to the creation of three dimensional crystal structures, which can lead to novel functional materials such as microporous materials [4].

Carboxylic acid group is one of the most commonly used functional groups in the design of building blocks because of its strong and specific interactions with other functional groups such as carboxylic acid, alcohol and pyridine (Scheme 2.1).

Since carboxylic acid groups can give rise to well-defined discrete structures (Scheme 2.1), it will be interesting to extend these motifs using polycarboxylic acid building blocks to design unusual supramolecular architectures in the crystal lattices. For example, terephthalic acid, isophthalic acid and trimesic acid have been extensively explored as building blocks in supramolecular chemistry. Terephtahlic acid forms a one-dimmensional linear ribbon-type structure [5], isophthalic acid forms crinkled tape structure [6], whereas

trimesic acid gives more complicated intertwined honeycomb-type structures [7, 8] in the crystal lattice. It is conceivable from the above three structure types that the position, orientation and the number of acid functional groups have a significant influence on self-assembly in the crystal lattice.

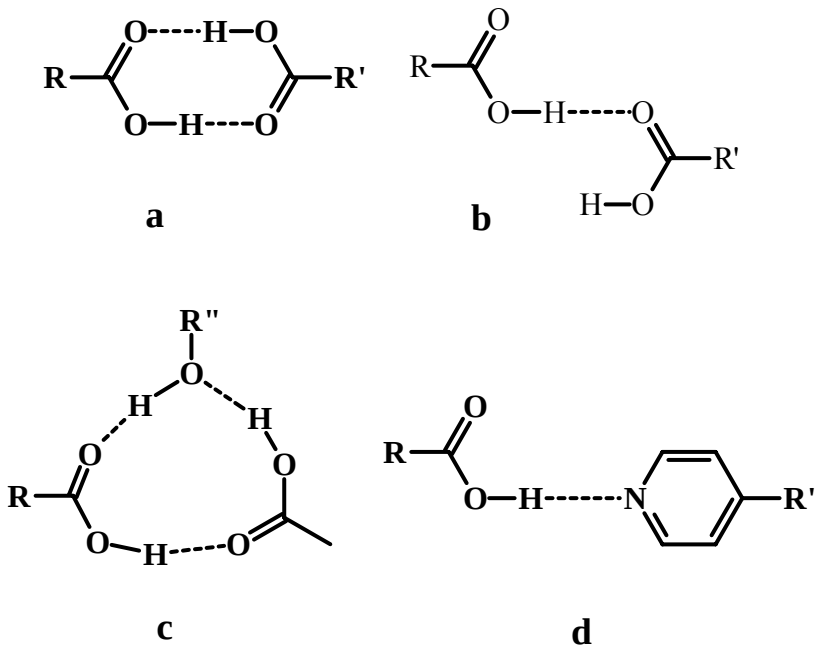

Scheme 2.1 Interactions between benzoic acid and other functional groups

We have been exploring the role of constitutional isomers and the interplay of weak interactions such as hydrogen bonds and alkyl chain crystallization on self-assembly in the solid state. Here we discuss our research efforts using a few dicarboxylic acids and their stoichiometric complexes with aromatic bases such as bipyridine (2,2'-bipyridine, 4,4'-bipyridine etc.). Our building blocks are designed to show that the influence of spacer groups, in particular the flexibility on the diacids or the dibase (e.g. 1,2-di(4-pyridyl) ethylene) and the directionality of the functional groups with respect to the spacer or the

molecular axis also plays an important role. A schematic representation of building blocks used in this study is given below.

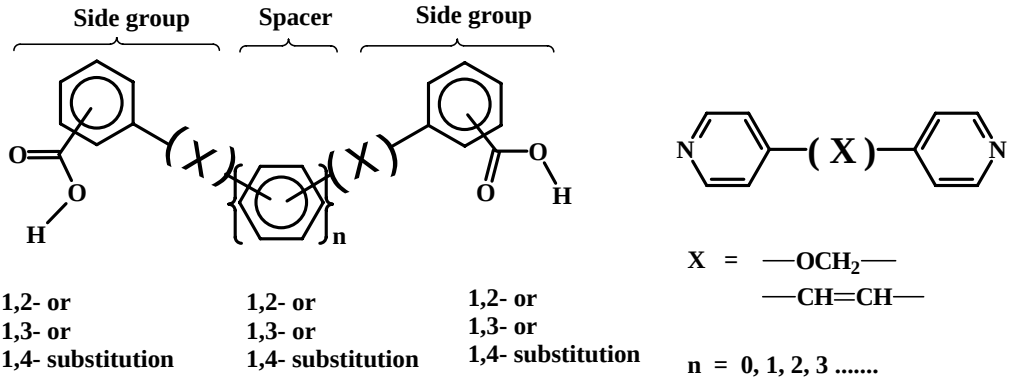

Scheme 2.2 A schematic representation of various dicarboxylic acid targets.

Some of the dicarboxylic acid molecules (**1**, **2**, **3**, and **4**, Scheme 2.3) and their stoichiometric complexes with bipy or dipet are investigated to examine the characteristic features of self-assembly in the solid state. They are discussed below with examples.

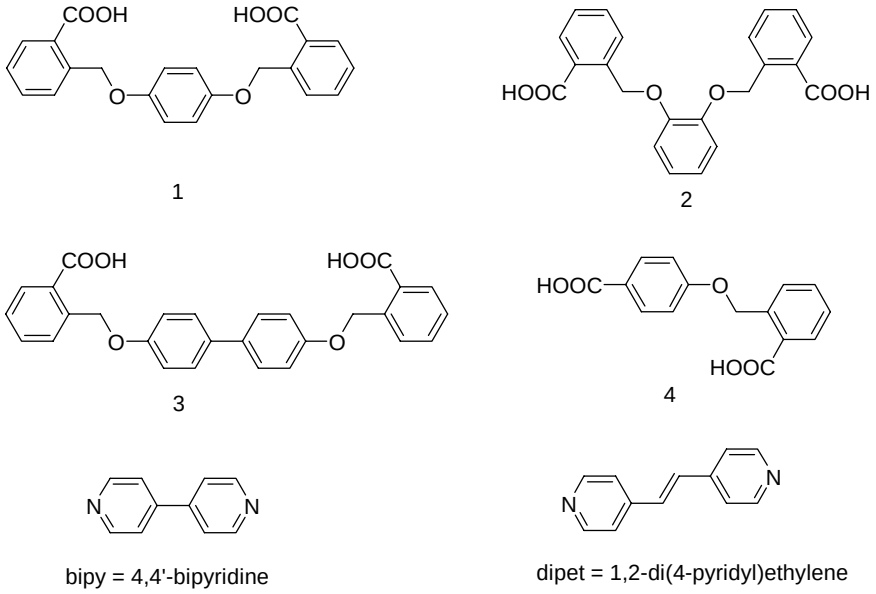

Scheme 2.3 Diacid building block structures: **1**, **2**, **3**, **4** and bridge molecule structures: bipy and dipet.

2.2 Results and discussion

2.2.1 Structure of pure diacids: **1** and **2**

2.2.1.1 Structure of compound **1**

Good quality single crystals of diacid **1** were obtained from a solution of methanol/THF (1:1), and exist in the monoclinic crystal system with the space group of $P2_1/n$. With the 1,4-substituted benzene group as spacer, a wavy ribbon-type structure in the crystal lattice is formed (Figure 2.1**)**. The molecules interact through the formation of carboxylic acid dimer (graph set $R_2^2(8)$ [9]), forming a zigzag ribbon. All molecules of a ribbon are in the same plane. The distance of the repeat unit along the ribbon orientation is about 15 Å. The acid-dimer formation in the crystal is the only strong interaction and bond distances of the dimer are as follows: O2-H2 1.09 Å, H2ΛO1 1.56 Å, O1ΛO2 2.65 Å, <O2-H2ΛO1 173º. Besides the weak van der Waal's interaction, there is no strong interaction found between the ribbons.

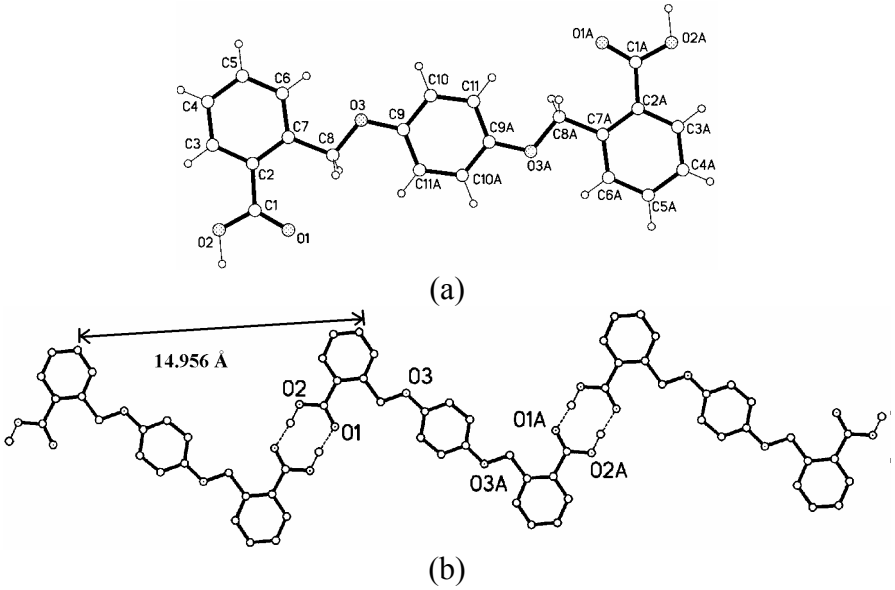

Figure 2.1 Compound of **1**: (a) molecular structure with atom numbers; (b) ribbon like structure formed by the acid dimer hydrogen bonds; H atoms are omitted for clarity.

The ribbons are in two different orientations and orthogonal to each other. A schematic representation of the packing in the lattice is shown in Figure 2.2. Ribbons stack parallel to each other to form a wave-type plane. Two such set of parallel planes are sandwiched by another set of planes in which the molecules are stacked in an almost perpendicular direction (see Figure 2.2b). The angle (θ) between the two nearly orthogonal set of planes is about 81.0 degree.

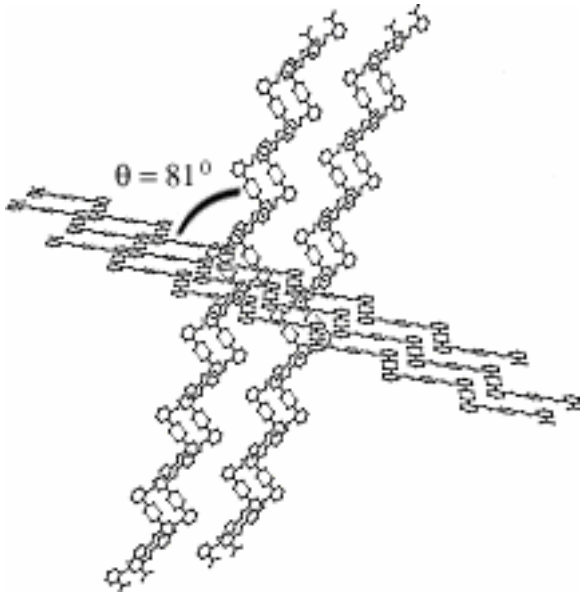

Figure 2.2 Crystal structure of **1**: illustration of orthogonal packing of the ribbons. (each plate stands for the plane formed by one ribbon and the wave in the plate stands for the ribbon; all H atoms are omitted for clarity).

Since the 1,4-substituted benzene produces a planar wave-type morphology, we decided to explore the 1,2-substituted benzene as spacer group, compound **2**, with the intention to induce a non-planar supramolecular architecture.

2.2.1.2 Structure of diacid **2**

Single crystals of diacid **2** were grown from a solution of the compound in methanol/acetone (2:1) mixture and found to have the monoclinic crystal system with the space group of $P2_1/n$ (Figure 2.3). Due to the use of 1,2-substituted benzene as spacer, the planarity of the molecule of compound **1** is absent. The crystal structure of compound **2** is shown in Figure 2.3. The molecules are connected through carboxylic acid dimers (graph set $R_2^2(8)$), and form a distorted wave-type ribbon. Owing to the unique conformation of the molecules, the two dimers formed from carboxyl groups on either side of the spacer are not equivalent. The bond distances and angles of the hydrogen bonds are given as follows: O2-H2 (0.83 Å), H2ΛO1 (1.79 Å), O2ΛO1 (2.62 Å), <O2-H2ΛO1 (73 º) and the other one O6-H6 (0.88 Å), H6ΛO5 (1.77 Å), O6ΛO5 (1.65 Å), <O6-H6ΛO5 (175º). Such acid group dimers alternate along the ribbon. Adjacent ribbons in one plane interact with the weak van der Waal's forces only.

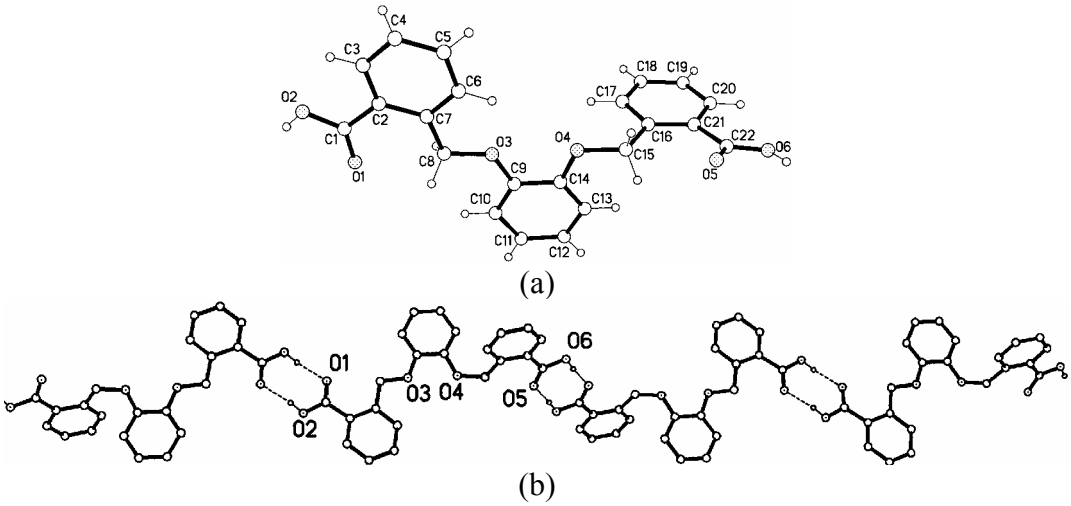

Figure 2.3 Crystal structure of compound **2**: (a) a schematic structure; (b) a distorted wave-type ribbon; H atoms are omitted for clarity.

The packing of the distorted wave-like ribbons is shown in Figure 2.4a, which is similar to the crystal structure of compound **1** (Figure 2.2). They are stacked on top of each other along the *b* axis (Figure 2.4b) and form layers that are parallel to each other.

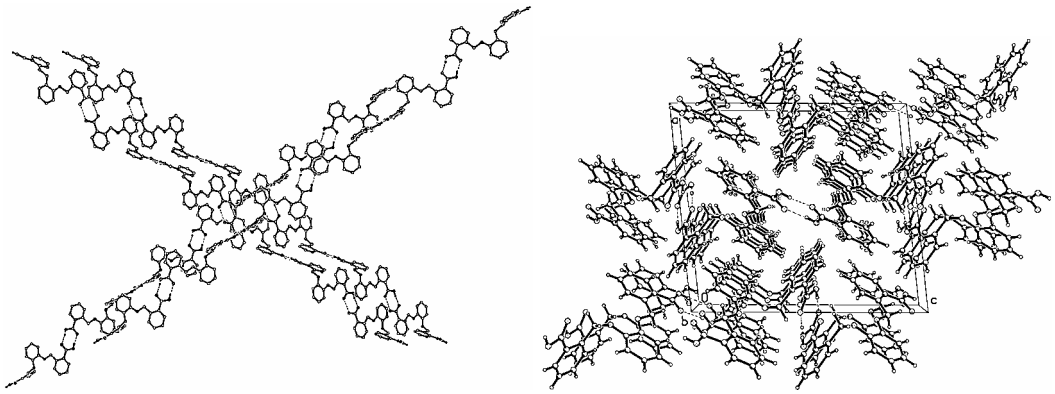

(a) (b)

Figure 2.4 Crystal structures of **2**: (a) cross packing of the ribbons, most H atoms are omitted for clarity (b) packing of ribbons in the crystal lattice (viewed along the *b* axis).

Self-assembly of stoichiometric molecular complexes of carboxylic acid and diamines has been an interesting area of research in crystal engineering. Knowing the similarities and differences of the above two structures and the influence of spacer groups, we explored the self-assembly of 1:1 complexes of these compounds with diamines such as 4,4'-bipyridine and 1,2-di(4-pyridyl)ethylene.

2.2.2 Self-assembly of stoichiometric complexes from diacids and bases

2.2.2.1 Structure of complex **1·bipy**

Good quality single crystals of **1·bipy** were grown from a solution of the complex in methanol/THF (1:1); they have the triclinic crystal system with the P(-1) space group. The diacid and bipyridine molecules are connected together by intermolecular O-HΛN interactions and thus form wave-type ribbons (Figure 2.5). The distance between the

repeating units along the ribbon orientation is 22.58 Å. The parameters of this hydrogen bonding are as follows: O1-H1 0.98 Å, H1ΛN1 1.68 Å, O1ΛN1 2.67 Å, <O1-H1ΛN1 175°. Similar to the crystal structures of **1** and **2**, there are no strong interactions between the ribbons. As evident from Figure 2.6, the diacid building block maintains its planarity. All the carbon atoms from the diacid molecule are located in the same plane. The wave-type pattern is changed slightly compared with that in the crystal lattice of **1** due to the insertion of 4,4'-bipyridine. The torsion angle for the V-type monomer unit along the ribbon is around 70 degrees.

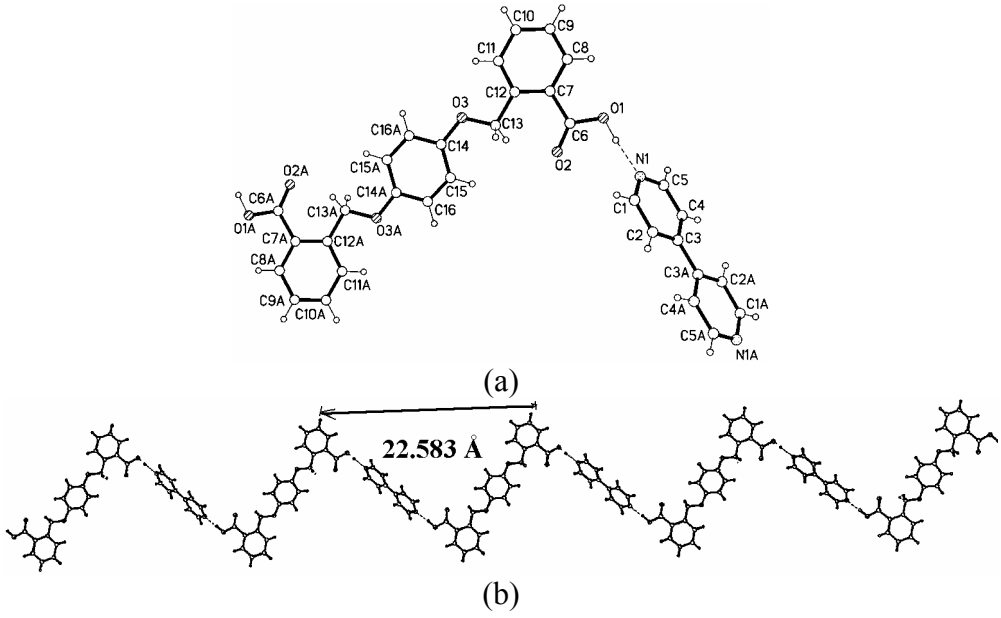

Figure 2.5 Crystal structure of **1·bipy**: (a) a molecular structure with atom numbering; (b) wave-like ribbon formed by O-H…N hydrogen bonding.

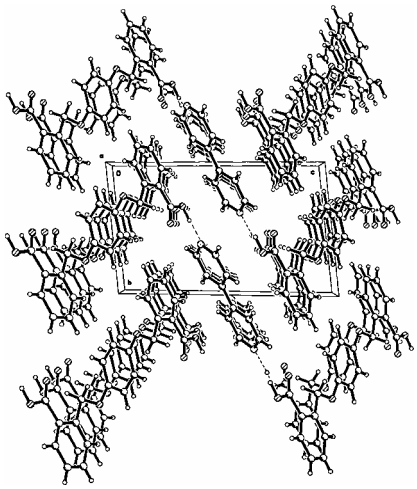

Figure 2.6 Packing diagram of **1·bipy**: crystal pattern viewed along the *a* axis.

The packing of the ribbons is shown in Figure 2.6. The ribbons are stacked one on top of each other along the *a* axis and form wave-type planes. These planes are parallel to each other. The ribbons in different wave-type planes are exactly the same, which is different from that in the crystal structure of **1** and **2**.

By comparing the lattice structure of **1** and the lattice of **1·bipy**, it is clear that the **bipy** molecule expanded the lattice and provided a different packing arrangement. In order to elaborate on this, we used 1,2-bis(4-pyridyl)ethylene (**dipet**), which is longer than the 4,4'-bipyridine molecule.

2.2.2.2 Structure of complex **1·dipet**

Single crystals of the stochiometric complex between compound **1** and 1,2-di(4-pyridyl)ethylene were grown from a solution of DMSO/H_2O via vapor diffusion method. X-ray investigation revealed a monoclinic crystal lattice with space group $P2_1/c$. The diacid and the bipyridine molecules are connected together by O-HΛN hydrogen bonding and thus form a wave-type ribbon (Figure 2.7). The distance between the repeating units

along the ribbon orientation is 22.23 Å. The hydrogen bonding parameters are as follows: O(1)-H(1) 0.83 Å, H(1)ΛN(1) 1.81 Å, O(1)ΛN(1) 2.63 Å, <O(1)-H(1)ΛN(1) 170°. There are no hydrogen bonds between the ribbons.

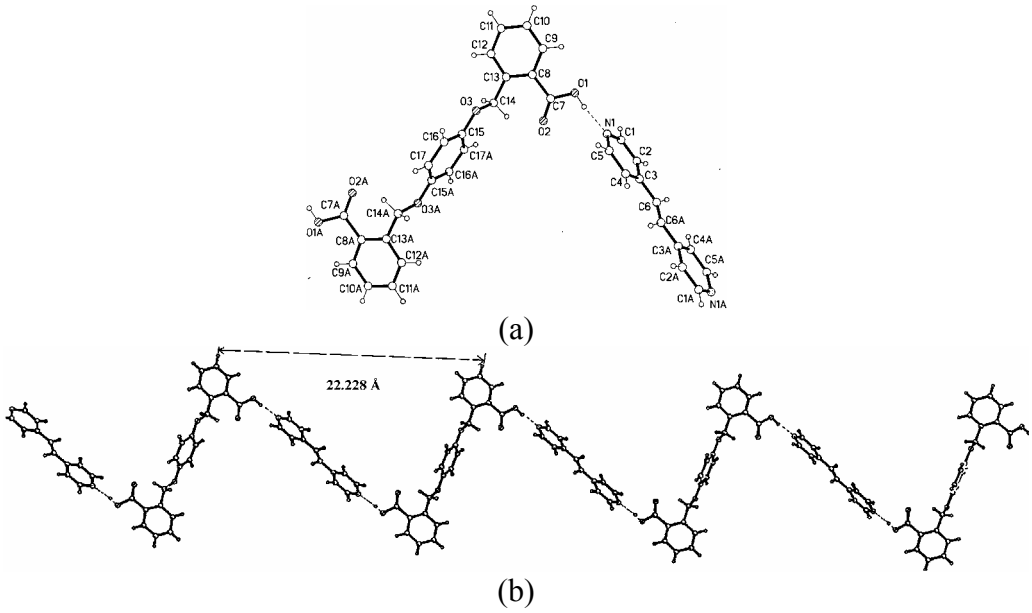

Figure 2.7 Crystal structure of **1·dipet**, wave-like ribbon formed by the O-H…N hydrogen bond.

The ribbons are packed along the *b* axis. Adjacent ribbons formed planes (along *b* axis) were tilted by an angle to achieve maximum close packing inside the lattice (Figure 2.8a). These ribbons stack along the *b* axis, which results in the formation of layers along the *b* axis (Figure 2.8b). The layers are parallel along the *a* axis.

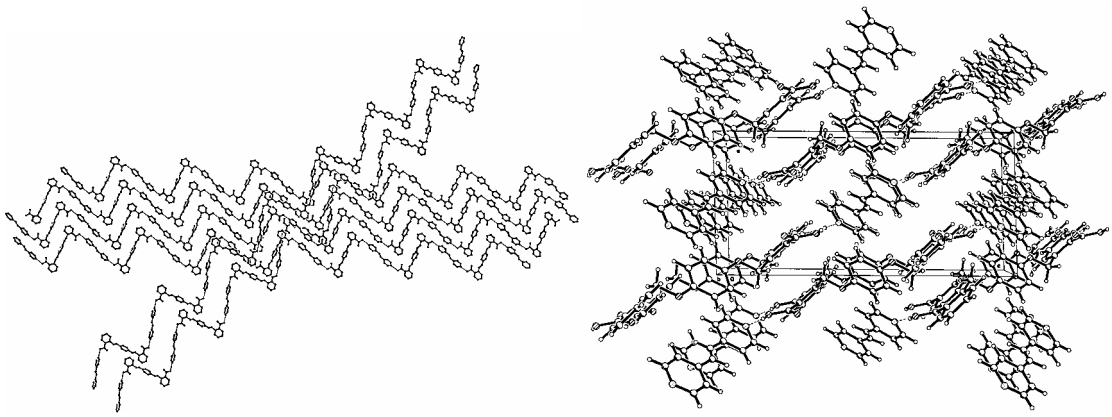

(a) (b)

Figure 2.8 (a) Crystal structure of **1·dipet** showing tilted ribbon packing (b) packing in the crystal lattice of **1·dipet** seen along the *b* axis.

Growing single crystals of diacarboxylic acids **3** and **4** were not successful (Scheme 2.1). However single crystals of 1:1 stoichiometric complexes of these diacids with bipyridine were readily obtained and analyzed.

2.2.2.3 Structure of complex **3·bipy**

Good quality single crystals of stoichiometric complex **3·bipy** were grown from a solution of DMSO/H_2O through vapor diffusion method. Single crystal X-ray analysis reveals a triclinic crystal lattice with the P(-1) space group. The molecules are connected by intermolecular O-H…N hydrogen bonds and thus form a wave-like chain (Figure 2.9). The distance between the repeating units along the ribbon is 24.90 Å, which is longer than that in the other two crystals discussed above. This is obviously due to the presence of the biphenyl moiety at the center of the molecule. The hydrogen bonding parameters include the distances O(1)-H(1) 1.04 Å, H(1)ΛN(1) 1.66 Å, O(1)ΛN(1) 2.68 Å and the <O(1)-H(1)ΛN(1) 165° angle.

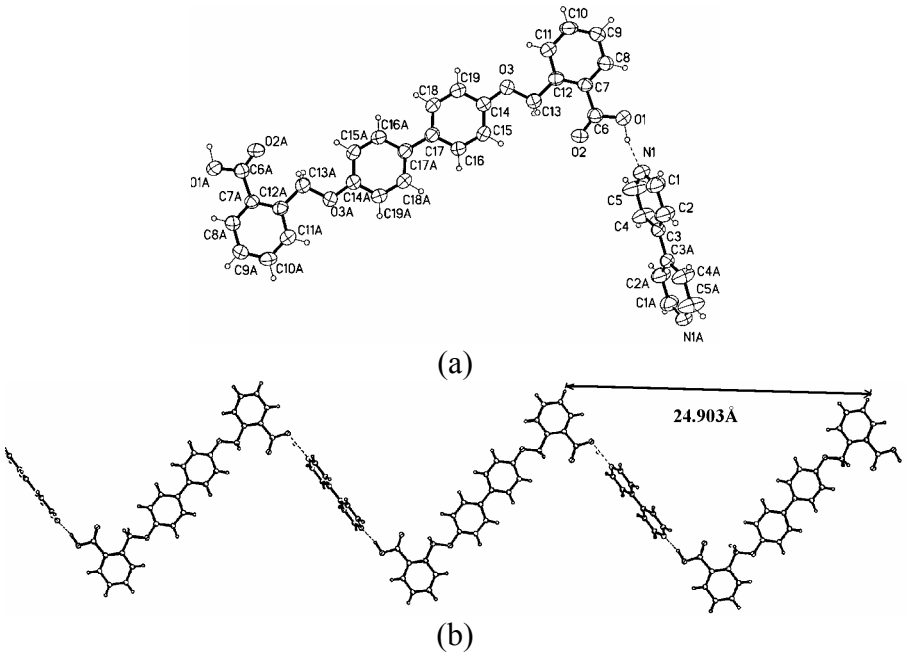

Figure 2.9 Crystal structure of complex **3·bipy**: (a) a schematic structure; (b) wave-like ribbons are formed by intermolecular O-H…N hydrogen bonding.

The crystal packing of **4** indicates that its structure is quite similar to that of complex **1·bipy**. All the carbon atoms from the same diacid molecules lie on the same plane. One significant difference is that crystal **4** has inter-ribbon C-HΛO interactions, which is the glue for ribbons to form 2-D wave-type plane (Figure 2.11a). There is no strong interaction between the 2-D wave-like planes (Figure 2.11b) and unlike the previous structures here all the planes are parallel to each other.

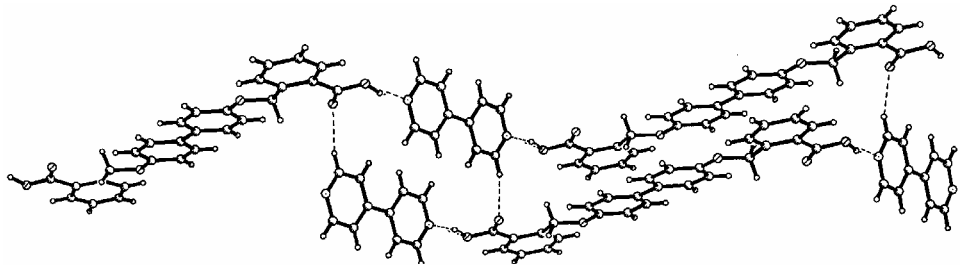

Figure 2.10 Crystal structure of complex **3·bipy** ribbons connected together by C-HΛO interactions.

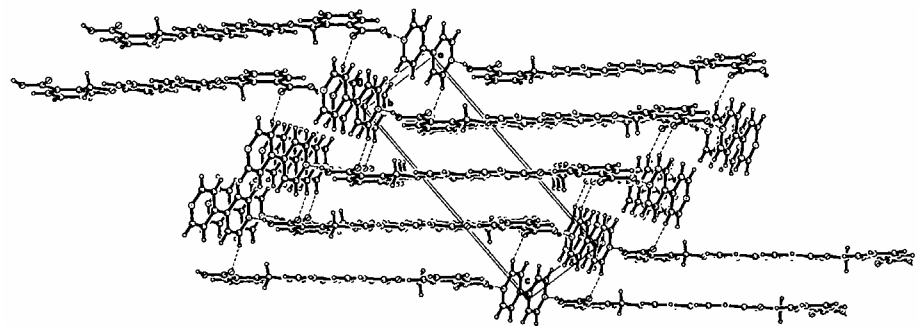

(a)

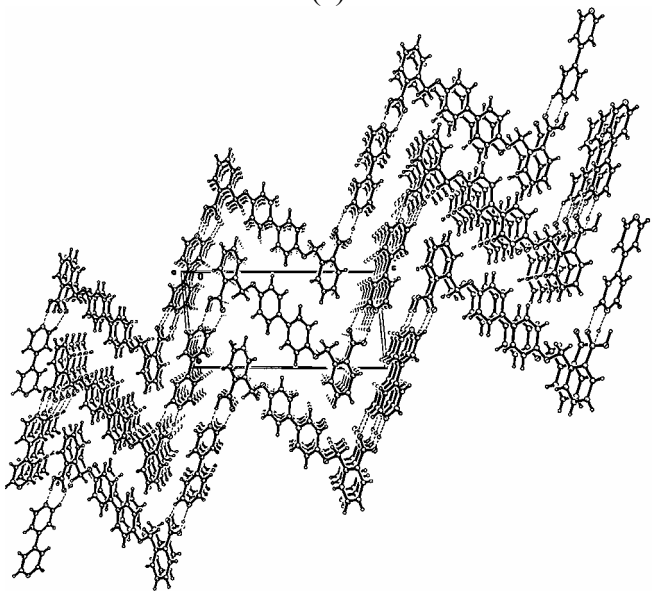

(b)

Figure 2.11 (a) Packing diagram of complex **3·bipy** viewed along the *b* axis. (b) Crystal structure of complex **3·bipy** viewed along the *a* axis showing no strong intermolecular interactions.

2.2.2.4 Structure of complex **4·bipy**

Single crystals of molecular complex **4·bipy** were grown from a solution of DMSO/H_2O through vapor diffusion. It has a monoclinic crystal lattice with the $P2_1/c$ space group. The molecules are connected by intermolecular hydrogen bonding O-HΛN to form a wave-like ribbon (Figure 2.12). The distance between the repeating units along the direction of the ribbon is 26.74 Å. Similar to that found in the crystal structure for **3·bipy**, the ribbons are connected by two kinds of C-HΛO weak hydrogen bonding. One is formed between oxygen atoms from carboxylic acid groups and H atoms from the aromatic ring

of the bipyridine bridge molecule (Figure 2.13a). Another one is formed between the oxygen atom from carboxylic acid and an H atom from benzene ring of diacid molecule (Figure 2.13b).

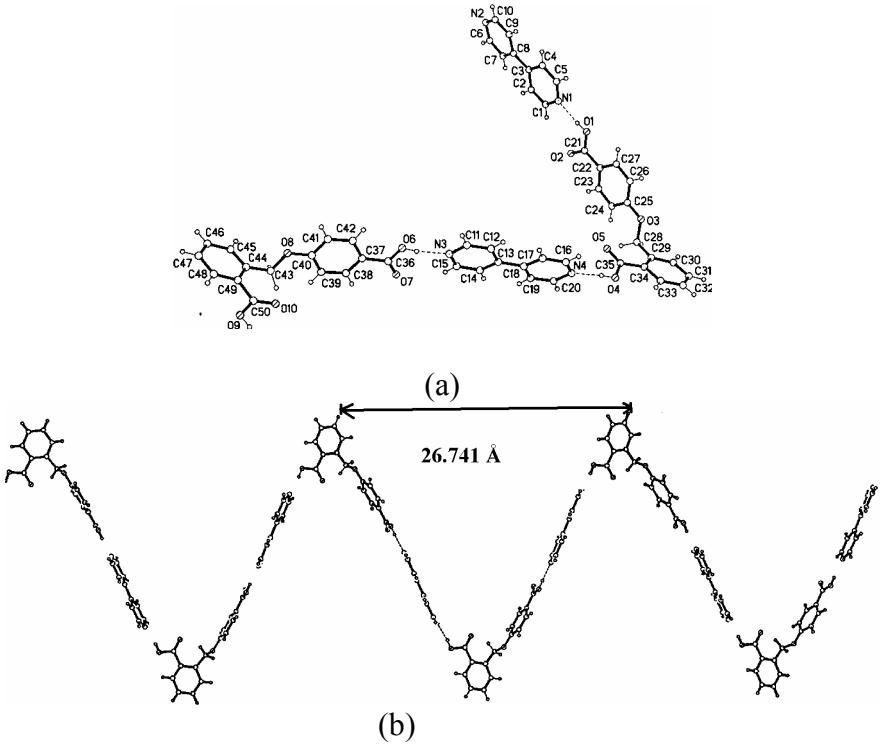

Figure 2.12 Crystal structure of complex **4·bipy**: (a) a schematic structure; (b) ribbons are formed by intermolecular O-H…N hydrogen bonding.

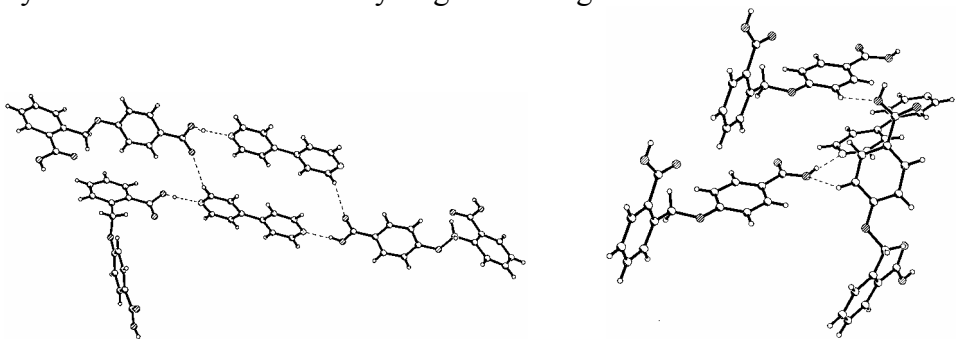

Figure 2.13 Crystal structure of complex **4·bipy**: weak inter-ribbon hydrogen bond C-HΛO between (a) bipyridine and carboxylic acid group and (b) carboxylic acid group and H atoms from another diacid molecule.

The ribbons are stacked along the *b* axis (Figure 2.14), forming 2-D planes that are parallel to each other. Compared to the lattice structure of complexes mentioned above, the ribbons in different planes are not aligned parallel to each other and four orientations or intersect pattern were found in the unit cell.

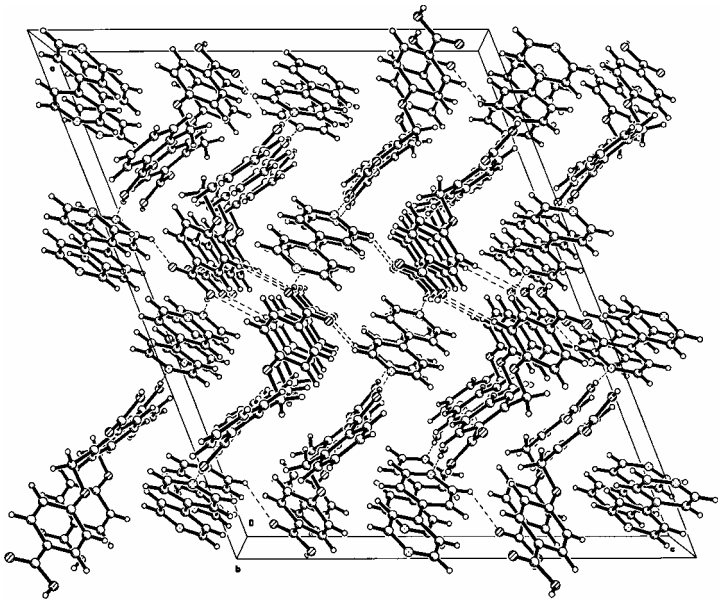

Figure 2.14. Packing diagram of complex **4·bipy**: crystal structure showing inter-ribbon interactions (viewed along the *b* axis).

Table 1. Hydrogen bond distances and angles in **4·bipy**.

D-H	d (D-H)	d (HΛA)	<DHA	D (DΛA)	A
O1-H1	0.83	1.86	172	2.68	N1
O4-H4	0.83	1.84	171	2.66	N4
O6-H6	0.83	1.86	171	2.68	N3
O9-H9	0.83	1.81	173	2.64	N2

2.3 Conclusion

All the six structures from two pure diacids and four complexes have wave-like pattern. And all the structures have ribbons formed by acid dimers in pure acid structures,

or O-HΛN hydrogen bonds (between acid group and pyridine group) in complexes. The dimension and direction of the ribbons were slightly modified according to the spacer group of diacids (Scheme 2.2). The similar pattern from different diacids with similar conformation show that these diacids are good potential building blocks in crystal engineering.

2.4 Experimental

All solvents and reagents were of reagent quality, purchased commercially, and used without further purification, unless otherwise noted. Column Chromatography was carried out with Merck silica gel (230- 400 mesh) for flash column chromatography. Merck silica gel 60 F_{254} plastic backed plates (20 x 20 cm) were used for thin layer chromatography (TLC). NMR spectra were recorded on a Brucker ACF-300 spectrometer. A general synthetic scheme is given below.

2.4.1 Synthesis scheme:

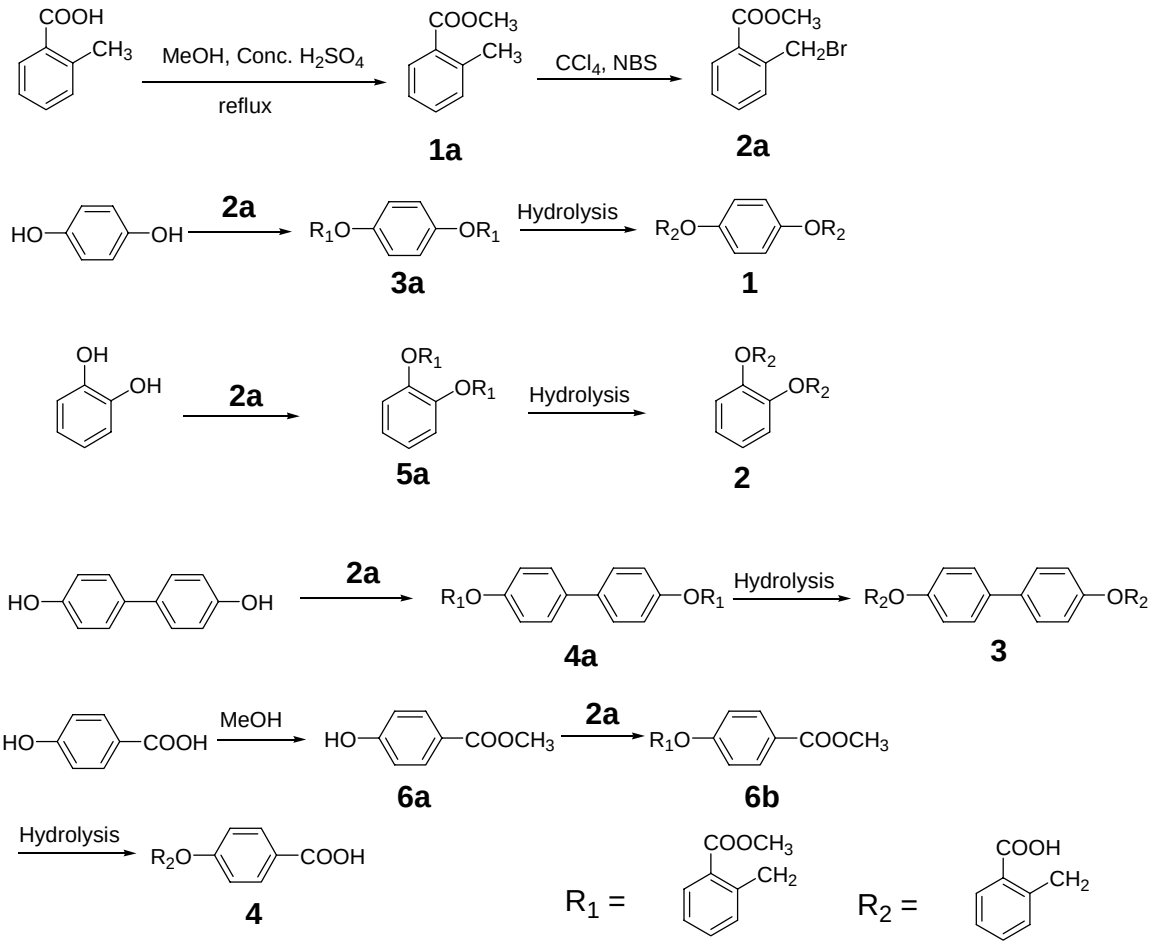

Scheme 2.4 Synthetic routes for diacid molecules.

2.4.2 Synthesis

2.4.2.1. Methyl-2-methylbenzoate (**1a**)

2-methyl benzoic acid (30g, 0.2 mol), methanol (250 ml), and Conc. H_2SO_4 (4 ml) were placed in a 500 ml round bottom flask. The solution was refluxed for 3 hr and cooled to room temperature. The solvent was removed by distillation under reduced pressure. The residue was dissolved in CH_2Cl_2 (100 ml), washed with water (3 x 100 ml) until the aqueous layer was neutral. The organic solvent was removed under reduced pressure. A white solid was obtained after drying. Yield: 33.0 grams (100 %); ^{1}H NMR (300 MHz, $CDCl_3$, δ ppm) 2.6 (s, 3H, CH_3), 3.9 (s, 3H, OCH_3), 7.25 (m, 2H, Ph), 7.4 (t, *J*

= 6.8 Hz, 1H, Ph), 7.94 (d, *J* = 7.0 Hz, 1H, Ph); ^{13}C NMR ($CDCl_3$, δ ppm) 167.0 (C=O); 138.9, 132.7, 131.2, 129.6, 129.1 and 125.4 (Ar); 50.0 (OCH_3); 14.1 (CH_3); ESI-MS (M+1) 151.

2.4.2.2. Methyl 2-bromomethylbenzoate (**2a**)

Compound **1a (**7 g, 46.6 mmol), AIBN (200 mg, 1.2 mmol), NBS (7.48 g, 42.0 mol), and CCl_4 (150 ml) were placed in 250 ml round bottom flask. The solution was refluxed at 80°C for 1.5 hours. The solution was filtered and excess solvent was removed under reduced pressure to give orange oil. The product was recrystallised from hexane on cooling. Yield: 8.2 g (85 %); ^{1}H NMR (300 MHz, $CDCl_3$, δ ppm) 3.93 (s, 3H, OCH_3), 4.95 (s, 2H, CH_2Br), 7.34 (t, *J* = 7.6 Hz, 1H, Ph), 7.48 (m, 2H, Ph), 7.95 (d, *J* = 7.8 Hz, 1H, Ph); ^{13}C NMR ($CDCl_3$, δ ppm) 167.0 0 (C=O); 139.2, 133.1, 131.2, 130.0, 129.1 and 128.6 (Ar); 50.0 (OCH_3); 31.6 (CH_2Br); MS (M+1) 229.

2.4.2.3. 1,4-Bis(2-methoxycarbonylbenzyloxy)benzene (**3a**)

Hydroquinone (2.0 g, 18.2 mmol), **2a** (8.3 g, 36.4 mmol), anhydrous potassium carbonate (5 g, 36.23 mmol) and dimethyl formamide (DMF 150 ml) were placed in a 250 ml round bottom flask equipped with a stirrer under argon. The mixture was left heating at 75 °C overnight. After filtering, the solvent was removed under reduced pressure and a yellow residue was obtained. The residue was poured into water (100 ml), a white solid was obtained which was filtered, and washed with cold methanol (3 x 10 ml) to give pure **3a** (6.5 g, 88%): ^{1}H NMR (300 MHz, $CDCl_3$, δ ppm) 3.87 (s, 6H, $COOCH_3$), 5.41 (s, 4H, OCH_2), 6.89 (s, 4H, OPhO), 7.32 – 7.50 (m, 4H, Ph), 7.71 (t, *J* = 6.8 Hz, 2H, Ph), 7.97 (d, *J* = 7.2 Hz, 2H, Ph); ^{13}C NMR ($CDCl_3$, δ ppm) 167.0 (C=O);

154.3, 142.1, 133.0, 129.9, 129.3, 127.3, 127.2 and 115.1 (Ar); 71.0 (OCH_2); 49.8 (OCH_3); MS (M+1) 407.

2.4.2.4. 1,4-Bis(2-carboxybenzyloxy)benzene (**1**)

Compound **3a** (3.0 g, 7.4 mmol), EtOH/H_2O (2 : 1, 90 ml), and NaOH (3 g, 75 mmol) were placed in a 150 ml round bottom flask equipped with a stirrer. The solution was refluxed for an hour and concentrated under reduced pressure. Then 100 ml of water was added and cooled down to nearly 0°C with ice. Conc. HCl was added drop by drop with constant stirring until the solution was acidic (pH = 1). Pink solid was washed with water until the filtrate was neutral. The solid was dried at 40 °C under high vacuum. Yield: 2.4 g (86 %); ^{1}H NMR (300 MHz, DMSO-d_6, δ ppm) 5.37 (s, 4H, OCH_2), 6.91 (s, 4H, OPhO), 7.42 (t, *J* = 7.4 Hz, 2H, Ph), 7.45 – 7.66 (m, 4H, Ph), 7.91 (d, *J* = 7.6Hz, 2H, Ph); ^{13}C NMR (DMSO-d_6, δ ppm) 172.0 (COOH); 154.3, 142.5, 133.9, 130.3, 129.4, 127.3, 127.2 and 115.2 (Ar); 71.0 (OCH_2); ESI-MS (M-1) 377. $C_{22}H_{18}O_6$ (378.1): calcd. C 69.83, H 4.79; found C 69.66, H 4.72%.

2.4.2.5. 4,4'-Bis(2-methoxycarbonylbenzyloxy)biphenyl (**4a**)

With a procedure similar to that used for **3a**, 4,4'-biphenol (2 g, 10.7 mmol) and **2a** (4.9 g, 21.4 mmol) afforded **4a** (4.5 g, 87 %): ^{1}H NMR (300 MHz, $CDCl_3$, δ ppm) 3.91 (s, 6H, $COOCH_3$), 5.54 (s, 4H, OCH_2), 7.02 (s, 4H, Ph), 7.36 (t, *J* = 7.4 Hz, 3H, Ph), 7.46 (d, *J* = 7.0 Hz, 2H, Ph), 7.53 (t, *J* = 7.6 Hz, 2H, Ph), 7.77 (d, *J* = 7.4 Hz, 4H, Ph), 8.01 (d, *J* = 7.2 Hz, 2H, Ph); ^{13}C NMR ($CDCl_3$, δ ppm) 167.3 (C=O); 160.8, 142.0, 133.7, 129.9, 129.3, 128.9, 128.4, 127.3, 127.2 and 114.6 (Ar); 71.0 (OCH_2); 49.8 (OCH_3); MS (M+1) 483.

2.4.2.6. 4,4'-Bis(2-carboxybenzyloxy)biphenyl (**3**)

With a procedure similar to that used for **1**, **4a** (3 g, 6.2 mmol) afforded **3** (2.3 g, 81 %): ^{1}H NMR (300 MHz, DMSO-d_6, δ ppm) 5.47 (s, 4H, OCH_2), 7.02 (d, *J* = 8.4 Hz, 4H, Ph), 7.43 – 7.66 (m, 10H, Ph), 7.92 (d, *J* = 7.6 Hz, 2H, Ph); ^{13}C NMR (DMSO-d_6, δ ppm) 178.3 (COOH); 170.2, 142.5, 133.9, 130.3, 129.4, 128.9, 128.4, 127.3, 127.2 and 114.6 (Ar); 69.8 (OCH_2); ESI-MS (M-1) 453. $C_{28}H_{22}O_6$ (454.5): calcd. C 74.00, H 4.88; found C 73.65, H 4.77%.

2.4.2.7. 1,2-Bis(2-methoxycarbonylbenzyloxy)benzene **(5a)**

With a procedure similar to that used for **3a**, pyrocatechol (2 g, 18.2 mmol) and **2a** (8.3 g, 36.2 mmol) afforded **5a** (5.6 g, 76 %): ^{1}H NMR (300 MHz, $CDCl_3$, δ ppm) 3.89 (s, 6H, $COOCH_3$), 5.60 (s, 4H, OCH_2), 6.87 – 6.95 (m, 4H, Ph), 7.33 (t, *J* = 7.3 Hz, 2H, Ph), 7.51 (t, *J* = 7.6 Hz, 2H, Ph), 7.90 (d, *J* = 7.4 Hz, 2H, Ph), 8.01 (d, *J* = 7.4 Hz, 2H, Ph); ^{13}C NMR ($CDCl_3$, δ ppm) 166.9 (C=O); 163.1, 142.1, 133.2, 130.5, 129.8, 129.3, 127.3, 127.2, 106.3 and 99.7 (Ar); 72.1 (OCH_2); 50.2 (OCH_3); MS (M+1) 407.

2.4.2.8. 1,2-Bis(2-carboxybenzyloxy)benzene (**2**)

With a procedure similar to that used for **1**, **5a** (4g, 9.8 mmol) afforded **2** (3.1 g, 83 %): ^{1}H NMR (300 MHz, $CDCl_3$, δ ppm) 5.49 (s, 4H, OCH_2), 6.89 – 6.93 (m, *J* = 3.6 Hz, 2H, Ph), 6.97 - 7.01 (m, *J* = 3.6 Hz, 2H, Ph), 7.43 (t, *J* = 7.4 Hz, 2H, Ph), 7.59 (t, *J* = 7.6 Hz, 2H, Ph), 7.75 (d, *J* = 7.6 Hz, 2H, Ph), 7.95 (d, *J* = 7.6 Hz, 2H, Ph); ^{13}C NMR (DMSO-d_6, δ ppm) 172.3 (C=O); 163.1, 142.5, 133.9, 130.4, 130.1, 129.6, 127.4, 127.1,

106.3 and 99.6 (Ar); 69.8 (OCH_2); ESI-MS (M-1) 377. $C_{22}H_{18}O_6$ (378.1): calcd. C 69.83, H 4.79; found C 69.52, H 4.63%.

2.4.2.9. Methyl 4-hydroxy benzoate (**6a**)

4-hydroxybenzoic acid (15 g, 0.11 mol), methanol (150 ml) and Conc. H_2SO_4 (4 ml) were placed in a 250 ml round bottom flask equipped with a stirrer. The solution was left refluxing for overnight followed by the removal of solvent under reduced pressure. The residue was dissolved in CH_2Cl_2 and then washed with H_2O (3 x 100 ml). After the solvent was removed, a white solid was obtained which was dried in vacuo. Yield: 16.3 g (99 %); ^{1}H NMR (300 MHz, $CDCl_3$, δ ppm) 3.90 (s, 3H, $COOCH_3$), 5.62 (s, 1H, OH), 6.89 (d, *J* = 8.4 Hz, 2H, Ph), 7.95 (d, *J* = 7.0 Hz, 2H, Ph); ^{13}C NMR ($CDCl_3$, δ ppm) 166.3, 161.4, 131.0, 123.1, 115.6, 50.3; ESI-MS (M-1) 151.

2.4.2.10. Methyl 4-(2-methoxycarbonylbenzyloxy)-benzoate **(6b)**

With a procedure analogue to that used for **3a**, **6a** (1.5 g) was converted to a white solid to afford **6b** (2.5 g, 85 %): ^{1}H NMR (300 MHz, $CDCl_3$, δ ppm) 3.88 (s, 3H, $COOCH_3$), 3.90 (s, 3H, $COOCH_3$), 5.56 (s, 2H, OCH_2), 7.01 (d, *J* = 8.8 Hz, 2H, Ph), 7.38 (t, *J* = 7.6 Hz, 1H, Ph), 7.55 (t, *J* = 7.2 Hz, 1H, Ph), 7.71 (d, *J* = 7.6 Hz, 1H, Ph), 7.96 – 8.05 (m, 3H, Ph); ^{13}C NMR ($CDCl_3$, δ ppm) 166.7 (C=O); 166.3, 142.1, 133.0, 130.7, 129.9, 129.3, 127.3, 127.2, 122.8 and 114.0 (Ar); 71.0 (OCH_2); 50.0 (OCH_3); MS (M+1) 299.

2.4.2.11. 4-(2-Carboxybenzyloxy)-benzoic acid **(4)**

With a procedure analogue to that used for **1**, **6a** (2.0 g) was converted to a white solid to afford **4** (1.71 g, 95 %): ^{1}H NMR (300 MHz, DMSO-d_6, δ ppm) 5.53 (s, 2H, OCH_2), 7.06 (d, *J* = 8.0 Hz, 2H, Ph), 7.46 (t, *J* = 7.6 Hz, 1H, Ph), 7.57 – 7.65 (m, 2H, Ph), 7.9 – 7.96 (m, 3H, Ph); ^{13}C NMR (DMSO-d_6, δ ppm) 172.0 (C=O); 167.1, 142.6, 133.9, 131.0, 130.3, 129.3, 127.3, 127.2, 122.8 and 114.0 (Ar); 71.2 (OCH_2); ESI-MS (M-1) 271. $C_{15}H_{12}O_5$ (272.3): calcd. C 66.17, H 4.44; found C 66.03, H 4.61%.

2.4.3 Crystal growth

2.4.3.1. 1,4-Bis(2-carboxybenzyloxy)benzene (**1**)

1,4-bis(2-carboxybenzyloxy)benzene (75 mg, 0.20 mmol) was dissolved in 5 ml hot methanol/THF (1:1) in a test tube. The test tube was sealed with para film for 6 days, colorless crystals were formed at the bottom of the test tube and were collected and analyzed.

2.4.3.2. 1,4-Bis(2-carboxybenzyloxy)benzene 4,4'-bipyridine (**1·bipy**):

1,4-Bis(2-carboxybenzyloxy)benzene (60 mg, 0.16 mmol) and 4,4'-bipyridine (26 mg, 0.17 mmol) were dissolved in 4 ml hot methanol/THF (1:1) in a test tube. The test tube was sealed with parafilm for 10 days. Colorless crystals were formed and were collected and analyzed.

2.4.3.3. 1,4-Bis(2-carboxybenzyloxy)benzene 1,2-Di(4-pyridyl) ethylene (**1·dipet**)

1,4-Bis(2-carboxybenzyloxy)benzene (48 mg, 0.13 mmol) and 1,2-Di(4-pyridyl)ethylene (23 mg, 0.13 mmol) were dissolved together in 2 ml DMSO in a small test tube. The test tube then was placed in a large bottle with water inside. The bottle was

sealed and left undisturbed for 7 days. Colorless crystals were formed on the walls of the small test tube.

2.4.3.4. 4,4'-Bis(2-carboxybenzyloxy)biphenyl 4,4'-bipyridine (**3·bipy**)

4,4'-Bis(2-carboxybenzyloxy)biphenyl (**3**) (81 mg, 0.18 mmol) and 4,4'-bipyridine (27 mg, 0.17 mmol) were dissolved together in DMSO (1.5 ml) in a small test tube. The test tube was then placed in a large bottle. The bottle was sealed and left undisturbed for 11 days. Colorless crystals were formed on the walls of the small test tube.

2.4.3.5. 1,2-Bis(2-carboxybenzyloxy)benzene **(2)**

1,2-bis(2-carboxybenzyloxy)benzene (60 mg, 0.16 mmol) was dissolved in 3 ml methanol/acetone (2:1) in a test tube. The test tube was sealed by para film for 5 days. Colorless crystals were formed and collected for analysis.

2.4.3.6. 4-(2-Carboxybenzyloxy)benzoic acid 4,4'-bipyridine (**4·bipy**)

4-(2-Carboxybenzyloxy)benzoic acid (37 mg, 0.14 mmol) and 4,4'-bipyridine (21 mg, 0.13 mmol) were dissolved together in DMSO (1.5 ml) in a small test tube. The test tube then was placed in a large bottle with water inside. The bottle was sealed and left undisturbed for 10 days. Colorless crystals were formed on the walls of the small test tube.

2.4.4. *X-ray crystallography*

X-ray crystallographic data were collected on a Bruker AXS SMART CCD 3-circle diffractometer with a Mo Kα sealed tube. The softwares used were: SMART [10] for

collecting frames of data, indexing reflections and determination of lattice parameters; SAINT [10] for integration of intensity of reflections and scaling; SADABS [11] for empirical absorption correction; and SHELXTL [12] for space group determination, structure solution and least-squares refinements on F^2. Structures were obtained by direct methods and non-hydrogen atoms were refined anisotropically. Hydrogen atoms were placed on calculated positions (C-H 0.96 Å) and assigned isotropic thermal parameters riding on their parent atoms. The crystal data and experimental details are given in Table 1.

Table 1 Crystal data and structure refinement parameters.

Compound	**1**	**2**	**1·bipy**	**1·dipet**	**3·bipy**	**4·bipy**
Chemical formula	$C_{22}H_{18}O_6$	$C_{22}H_{18}O_6$	$C_{22}H_{18}O_6 \cdot C_{10}H_8N_2$	$C_{22}H_{18}O_6 \cdot C_{12}H_{10}N_2$	$C_{28}H_{22}O_6 \cdot C_{10}H_8N_2$	$C_{15}H_{12}O_6 \cdot C_{10}H_8N_2$
Formula weight	378.36	378.36	534.55	560.58	610.64	428.43
Crystal system	monoclinic	monoclinic	Triclinic	monoclinic	triclinic	monoclinic
Space group	P2(1)/n	P2(1)/n	P(-1)	P2(1)/c	P(-1)	P2(1)/c
a [Å]	5.1580(2)	15.1936(2)	6.1009(7)	8.9416(11)	5.6121(7)	25.886(2)
b [Å]	10.8283(5)	7.2404	8.0739(9)	8.1164(10)	8.1416(10)	8.0974(6)
c [Å]	15.6703(7)	17.3198	13.4904(15)	18.832(2)	16.492(2)	21.2008(16)
α [^{0}]	90	90	83.523(2)	90	84.294(3)	90
β [^{0}]	91.135(1)	96.105(1)	80.384(1)	91.627(3)	86.691(3)	111.625(2)
γ [^{0}]	90	90	87.233(2)	90	88.555(3)	90
V [Å]	875.05(7)	1894.51(4)	650.70(13)	1366.1(3)	748.41(16)	4131.1(5)
Z	2	4	1	2	1	8
ρ_{Calcd} [g cm^{-3}]	1.436	1.327	1.364	1.363	1.355	1.378
Crystal size [mm]	0.18x0.16x0.10	0.6x0.6x0.5	0.44x0.14x0.03	0.26x0.20x0.10	0.34x0.31x0.20	0.5x0.36x0.16
μ [mm^{-1}]	0.105	0.097	0.095	0.094	0.092	0.097
Temperature [K]	293(2)	293(2)	293(2)	223(2)	295(2)	223(2)
Measured reflns	4650	9897	4072	7675	6184	22180
Indep. Reflns	1771	3765	2441	2409	2640	7274
θ max [^{0}]	2.29<2θ<26.37	1.89<2θ<26.36	2.54<2θ<26.37	2.16<2θ<24.99	2.49<2θ<25.00	1.69<2θ<25.00
Refinement on	F^2	F^2	F^2	F^2	F^2	F^2
Final R ind (I > 2σ(I))	R1 = 0.0488 wR2 = 0.1138	R1 = 0.0443 wR2 = 0.1193	R1 = 0.0527 wR2 = 0.1300	R1 = 0.0981 wR2 = 0.2763	R1 = 0.0688 wR2 = 0.1918	R1 = 0.0672 wR2 = 0.1578
R indices (all data)	R1 = 0.0724 wR2 = 0.1230	R1 = 0.0625 wR2 = 0.1296	R1 = 0.0887 wR2 = 0.1480	R1 = 0.1171 wR2 = 0.2994	R1 = 0.0963 wR2 = 0.2266	R1 = 0.0952 wR2 = 0.1687
Data/restraints /parameters	1771/0/164	3765/0/324	2441/0/186	2409/0/207	2640/0/227	7274/0/582
Absorption corr.	Sadabs	Sadabs	Sadabs	Sadabs	Sadabs	Sadabs
Residual electron density [e Å^{-3}]	0.206/ -0.221	0.259/ -0.227	0.234/ -0.190	0.755/ -0.646	0.327/ -0.325	0.381/ -0.2944
GoF	0.951	1.059	1.035	1.075	1.023	0.964

2.5 References

[1] Gautam R. Desiraju, *Crystal Engineering-the Design of Organic Solids*, Elsevier, Amsterdam**, 1989**.

[2] R. E. Meléndez, A. D. Hamilton, in *Design of Organic Solids.* Ed. E. Weber, P. 97 (Topics in Current Chemistry, 198, Ed. A. de Meijere, K. N. Houk, H. Kessler, J.-M. Lehn, S. V. Ley, S. L. Schreiber, J. Thiem, B. M. Trost, F. Vögtle, H. Yamamoto), Springer, Germany, **1998**.

[3] Introduction about supramolecular chemistry: J.-M. Lehn, *Supramolecular Chemistry: Concepts and Perspectives,* VCH, Weinhem, 1995.

[4] A recent review about porous materials: T. J. Barton, Lucy M. Bull, W. G. Klemperer, D. A. Loy, B. McEnaney, M. Misono, P. A. Monson, G. Pez, G. W. Scherer, J. C. Vartuli, O. M. Yaghi, *Chem. Mater.* **1999**, 11, 2633 – 2656.

[5] M. Bailey, C. J. Brown, *Acta Crystallogr.* **1967**, B 22, 238.

[6] (a) R. Alcala, S. Martinez-Carrera, *Acta Crystallogr.* **1972**, B 28, 1671; (b) J. L. Derissen,, *Acta Crystallogr.* **1974**, B. 30, 2764.

[7] D. J. Duchamp, R. E. Marsh, *Acta Crystallogr.* **1969**, B 25, 5-19.

[8] S. V. Kolotuchin, P. A. Thiessen, E. E. Fenlon, S. R. Wilson, C. J. Loweth, S. C. Zimmerman, *Chem. Eur. J.* **1999**, 5, 2537- 2547.

[9] M. C. Etter, *Acc. Chem. Res*. **1990**, 23, 120 – 126.

[10] SMART & SAINT Software Reference Manuals, Version 4.0, Siemens Energy & Automation, Inc., Analytical Instrumentation, Madison, Wisconsin, USA, **1996**.

[11] G.M. Sheldrick, SADABS, software for empirical absorption correction, University of Gottingen, Gottingen, Germany, **1996**.

[12] SHELXTL Reference Manual, Version 5.03, Siemens Energy & Automation Inc., Analytical Instrumentation, Madison, Wisconsin, USA, **1996**.

Chapter 3 Self-assembly from trimesic acid and cyanuric acid

3.1 Introduction

Trimesic acid (Benzene-1,3,5-tricarboxylic acid; TMA) is a versatile building block for designing supramolecular architectures. It can form a sheet type framework (shown in Figure 3.1) with interpenetration to fill the 14 Å cavity [1].

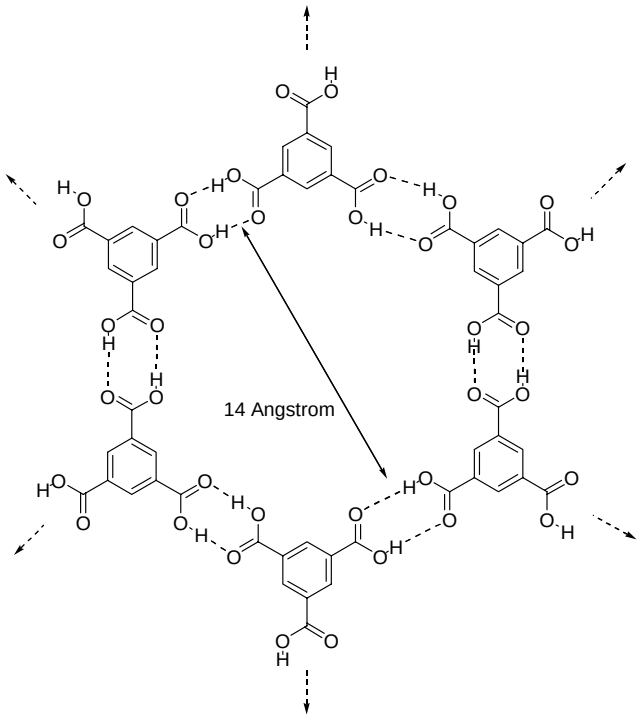

Figure 3.1 Extensively hydrogen-bonded chicken-wire network formed by *syn*-*syn* cetrosymmetrical $R_2^2(8)$ hydrogen bond in trimesic acid (TMA).

Some micro-porous structures formed from TMA have been mentioned in introduction part (Chapter 1: Carboxylic acids). This kind of structures has attracted many research groups' interest such as Zimmerman [2], Yaghi [3] etc in recent years. Cyanuric acid (Scheme 3.1) has similar geometry as TMA and thus absorbs our interest (see

Chapter 1: cynauric acid) in pursuing some similar target as TMA. In this Chapter, two complexes from TMA and cyanuric acid are discussed in details.

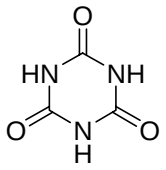

Scheme 3.1 Structure of cyanuric acid.

5-alkoxyl-isophthalic acid (CnISA) molecules were synthesized and explored previously by Valiyaveettil [4, 5] and Hamilton [6], and have some interesting pattern and liquid crystalline properties. A general structure of 5-alkoxyl-isophthalic acid molecules is shown in Scheme 3.2. In CnISA, two meta-disposed carboxyl groups form the head and the alkyl group at C-5 position forms the tail. Obviously, the hydrogen bonds from the head group and the van der Waals interactions of the tail groups are deciding factors for controlling the supramolecular structures. From the previous studies, it is not difficult to conclude that the head group may form a ribbon-like structure or a cyclic one [4]. For example, isophthalic acid forms a ribbon-like structure [7], and 1,3,5-benzenetricarboxylic acid forms a six-membered cyclic structure [8]. Actually, from the results published by Hamilton [6] and Müllen's [4] group, CnISA can form cyclic or ribbon like structures with interesting properties. For example, CnISA (n = 16, 18) has liquid crystalline property; CnISA (n = 12) can form stable monolayer, which can be analyzed under STM [5]. Based on these results, it may be possible to combine TMA and 4-alkoxypyridine, to obtain a similar structure with interesting properties. Consequently, crystals from combining TMA

and ddpy (mole ratio = 1:1) were obtained. A detailed analysis of structure and properties are given in this chapter.

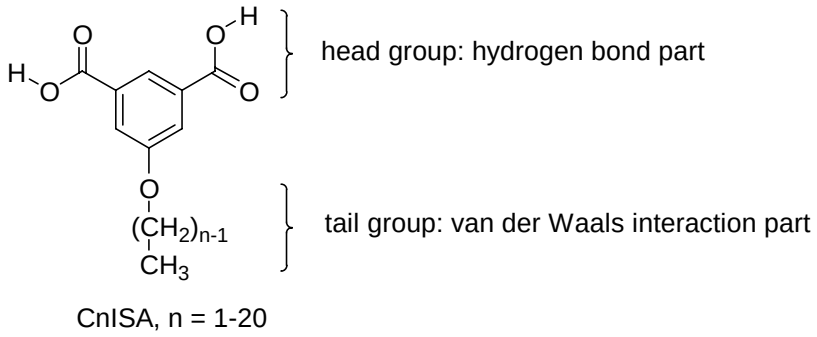

Scheme 3.2 A general formula of 5-alkoxyl-isophthalic acids.

3.2 Results and discussion

3.2.1 Crystal structure of TMA•1/2THB

The α-polymorph crystal structure of TMA [1] contains approximately 14 Å diameter holes (Figure 3.1), which are occupied by triple concatenation to meet the close packing requirement. Because the 14 Å channel in TMA is significantly larger than that found in others channel clathrates, it is interesting to design a structure of TMA without interpenetration. Herbstein et al. reported [9] the first noncatenated TMA structures containing disordered alkane guests. Zimmerman designed a plan to prevent interpenetration of the TMA networks by including a large and relatively non-flexible guest molecule such as pyrene molecules and they succeeded to get a pyrene incorporated expanded hexamer [10]. Recently, Kolotuchin et al. [2] observed a series of crystal structures that generate clathrates from substituted TMA molecule.

Some method can be used to generate clathrates from TMA molecule and its analogues. Zimmerman et al. designed three strategies [10] to realize it: (a) crystallization of TMA and organic guests, (b) synthesis and crystallization of substituted analogues of TMA, and (c) replacement of a carboxylic acid dimer with a covalent linkage of similar geometry. And he has explored the strategy (**b**) in his recent work [5]. Here we report a non-penetrating, planar and distorted chicken-wire structure from TMA in which strategy (**a**) is used.

The conformation of organic guest compound is very important consideration in generating a clathrate structure instead of interpenetrated one. THB molecule is a good guest molecule for TMA clathrate because of its planar rigid backbone and three hydroxyl functional groups, which can form strong interactions between host and guest by hydrogen bonding. Crystallization from a solution of methanol containing 1 and 0.5 equiv. of TMA and phloroglucinol, respectively, afforded the desired cocrystal TMA•1/2THB upon slow evaporation at room temperature.

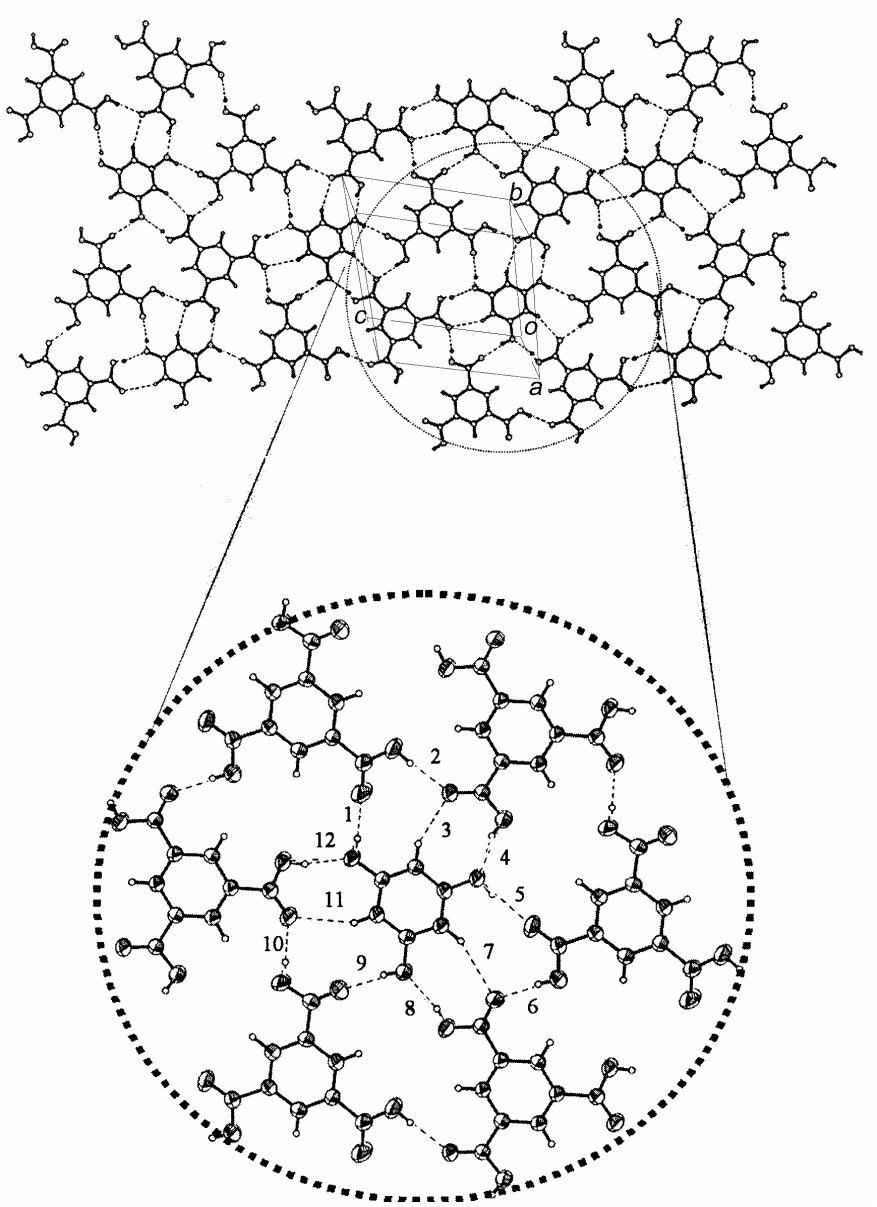

Figure 3.2 Crystal structure of TMA•1/2THB showing one layer and one enlarged roulette, the hydrogen bonding graph set between THB and surrounded TMA are $R_2^2(8)$, $R_3^2(10)$.

The crystal packing of TMA•1/2THB is shown in Figure 3.2. Six TMA molecules rotate away from their positions in the common chicken-wire motif, form a distorted six-membered ring. The central part, occupied by THB molecule, is much smaller compared that in common TMA cavity (diameter 14 Å). TMA molecules self-assemble in such a

manner so that the smaller guest molecule such as THB molecules can fill inside the cavity.

Table 3.1 Hydrogen bonding parameters (Figure 3.2)

HB No. *	D (D-H)	d (HΛA)	<DHA	d (DΛA)
1	0.82	1.88	170	2.69
2	0.82	1.86	173	2.68
3	0.93	2.55	156	3.42
4	0.82	1.85	165	2.65
5	0.82	1.90	170	2.71
6	0.82	1.85	173	2.67
7	0.93	2.55	157	3.43
8	0.82	1.86	164	2.66
9	0.82	1.90	170	2.71
10	0.82	1.87	171	2.68
11	0.93	2.56	156	3.43
12	0.82	1.85	164	2.65

* HB = Hydrogen Bonding, the number is same as that in Figure 3.2.

The twelve different hydrogen bonds between THB and six surrounding TMA molecules are also shown in Figure 3.2, and their detailed parameters are given in Table 3.1. There are two different types of hydrogen bond graph sets: $R_2^2(8)$ (formed by **3** and **4**; **7** and **8**; **11** and **12**), $R_3^2(10)$ (formed by **1**, **2** and **3**; **5**, **6** and **7**; **9**, **10** and **11**) in the structure. There are nine hydrogen bonds in total formed between the central THB molecule and the neighboring six TMA molecules. Three are C-HΛO weak hydrogen bonds; the other six are strong O-HΛO hydrogen bonds. The six TMA molecules are connected together by only 6 hydrogen bonds to form a hexameric ring structure. The ring stability is much weaker than the common honeycomb structures, in which the graph set is $R_2^2(8)$ (acid dimer). Such ring packing could be due to the close packing requirement. Because the guest molecule (THB) is relatively small, when the TMA common motif is slightly distorted, a relatively small pore size suitable for THB can be formed. Another reason for such a deviation from standard graph sets for carboxylic acid may be due to the

lowering of energy from the formation of the 9 hydrogen bonds between the guest molecule (THB) and the six-surrounding TMA molecules. Although such deviation entails higher energy, this is compensated by the 9 hydrogen bonds between THB and the six TMA molecules.

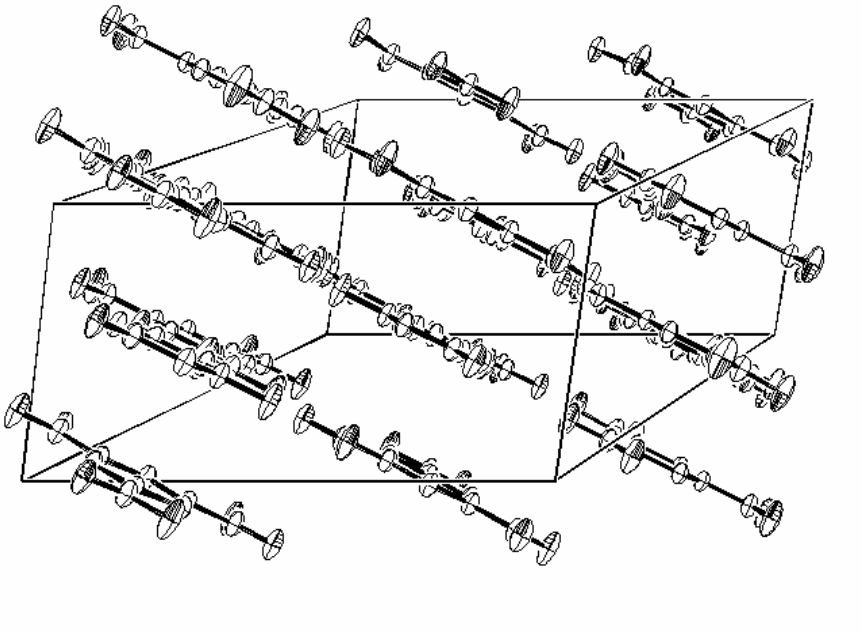

Figure 3.3 An ORTEP view of the crystal structure showing different layers, which is parallel to each other.

A side view showing different layers in TMA·1/2THB is shown in Figure 3.3, from which it can be seen that the layers are planar and parallel to each other. However, the layers do not stack on top of each other to form a channel but is shifted slightly from one another. The packing relationship between the different layers is illustrated in Figure 3.4. The distance between layers is about 3.3 Å. Two ellipses (black and grey), standing for the basic six-membered ring unit in the two layers respectively, are out of alignment from another. The orientations of the two units are different and have a relationship of rotation of about 60 degree.

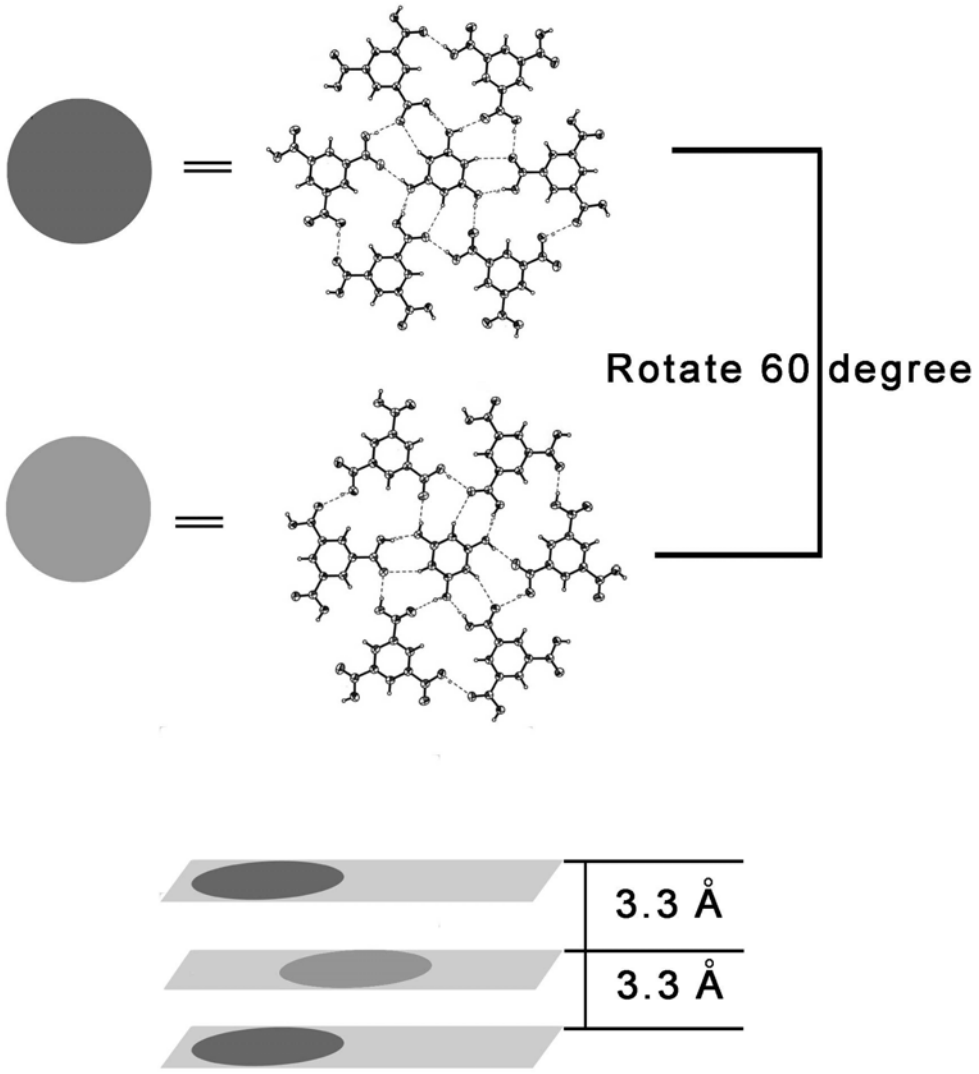

Figure 3.4 A diagram showing the layer packing and the relative position of the six-membered ring unit.

The reason of the slight shift may be that, if the cavity forms a channel, there will be three void places formed between two neighboring TMA molecules, and thus cannot meet the close requirement.

Two different geometries **A** and **B** (Figure 3.5) for a complex of isophthalic acid and THB were studied by molecular modeling in order to know the details about why the molecules forms a distorted six-membered ring unit. Two possible geometries **A** and **B**

were examined. In geometry **A**, six isophthalic acid molecules form a standard hexamer with $R_2^2(8)$ hydrogen bonding graph set, and a THB molecule is located in the center of the ring. All the molecules are on the same plane. In geometry **B**, the structure is very close to that found in X-ray crystallography. The difference is that all the molecules form a bowl-like structure instead of a coplanar one inside the crystal. This is possible because of no interaction surrounding the ring unit, and in such geometry, the six hydrogen bond surrounding the ring can be stronger. Both geometries are the optimized results under Spartan SGI version 5.1.3 OpenGL built under IRIX 6.2 using the AM1 [11] and none solvent model [12] and interestingly the energy difference is only $\Delta E = 0.7$ KJ/mol. The observed geometry is not in total agreement with either one of them. But when the non-hydrogen-bonded functional groups from the six surrounded isophthalic acid are considered, the six newly formed hydrogen bonds may lower the energy of the **B** geometry. Thus **B** geometry is more likely structure in the solid-state, which is confirmed by crystal structure analysis.

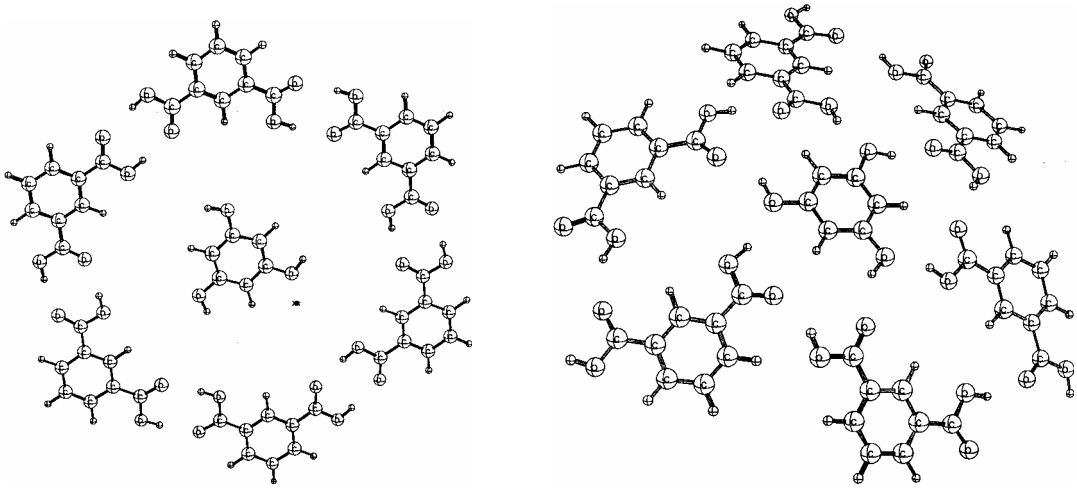

(A) (B)

Figure 3.5 Geometry A and B optimized with Spartan version 5.1.3.

3.2.2 Crystal structure of cyanuric acid with 4,4'-dithiodipyridine (CA·ddpy)

In Chapter 1 (cyanuric acid part), we showed some cyanuric acid (CA) crystal structures and works done by other people [13,14, 15]. We are interested in examining whether the pattern will be different from the structure of cyanuric acid with 4,4'-bipyridine (bipy), when employing other different bridge molecules such as 4,4'-dithiodipyridine (ddpy).

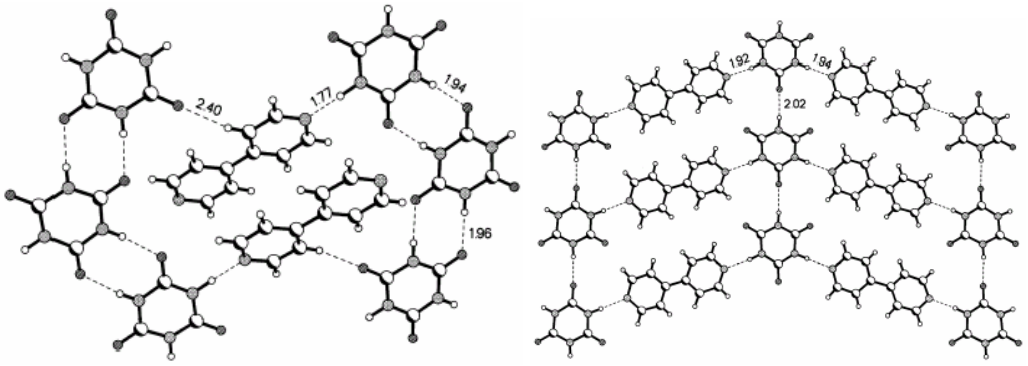

(a) (b)

Figure 3.6 (a) Arrangement of 2CA·bipy obtained from methanol. Notice the presence of cyclic hydrogen bonds. (b) Two-dimensional arrangement of CA·bipy obtained from water. Notice the presence of only single hydrogen bonds (and the absence of cyclic hydrogen bonds).

Co-crystallization of CA and bipy from methanol yields a 2:1 adduct, 2CA·bipy, while co-crystallization from water gives a 1:1 adduct, CA·bipy [16]. In 2CA·bipy, CA molecules were held together by two different cyclic N–HΛO hydrogen-bonded dimers (HΛO, 1.94 and 1.96 Å) as shown in Figure 3.6a. The bipy molecules interact with CA through an N–HΛN hydrogen bond (HΛN, 1.77 Å). There is also some C–HΛO interaction between bipy and CA (HΛO, 2.40 Å). The structure of CA·bipy, crystallized from water is different from that of 2CA·bipy complex, crystallized from methanol. In this structure, the CA molecules form a chain through N-HΛO hydrogen bonds (HΛO, 2.02

Å). The bipy molecules hold the chains together by N-HΛO hydrogen bonds (NΛH, 1.92, 1.94 Å). The N-HΛO bonds forming the chains in CA·bipy are very much longer than in 2CA·bipy. The N-HΛN bond is also considerably longer than in 2CA·bipy.

In our case, good quality single crystals of CA·ddpy were obtained from a solution of DMSO/H_2O, and exist in the orthorhombic crystal system with the space group of C222(1). The crystal structure of CA·ddpy is shown in Figure 3.7. The adjacent CA molecules are held together and form a chain by N-HΛO hydrogen bonds (HΛO, 2.02 Å, see in Figure 3.9), which is similar to the reported complex of CA·bipy (Figure 3.6b). The ddpy molecules hold the chains together through one N-HΛN (HΛN, 2.06 Å) hydrogen bond and two C-HΛO (HΛO, 2.31, 2.47 Å) weak hydrogen bonds. The two C-HΛO hydrogen bonds are formed between ddpy and the two adjacent CA molecules (Figure 3.7), which were not observed in the complexes 2CA·bipy and CA·bipy. The N-HΛN bonds between the CA and bipy are quite longer than in the structure of CA·bipy. The hydrogen bonds details are shown in Figure 3.8b and Table 3.2.

The chain structure of the 1:1 adduct between the CA and ddpy is comparable to that of CA·bipy (see Figure 3.6b) and CA·H_2O (Figure 1.15b, in Chapter 1), wherein the ddpy molecules are replaced by bipy molecules and water molecules, respectively. In CA·bipy, the CA molecules formed chains are connected by bipy through N-HΛN hydrogen bonds, however, only one hydrogen bond was found between the CA molecule and bipy molecule. In CA·H_2O, CA molecules form very similar chains as that in CA·ddpy with a N-HΛN hydrogen bond (HΛN, 2.01 Å, in CA·ddpy: HΛN, 2.02 Å). And two water molecules locating between two neigbouring CA molecules from different chains form three hydrogen bonds, which are similar as in CA·ddpy.

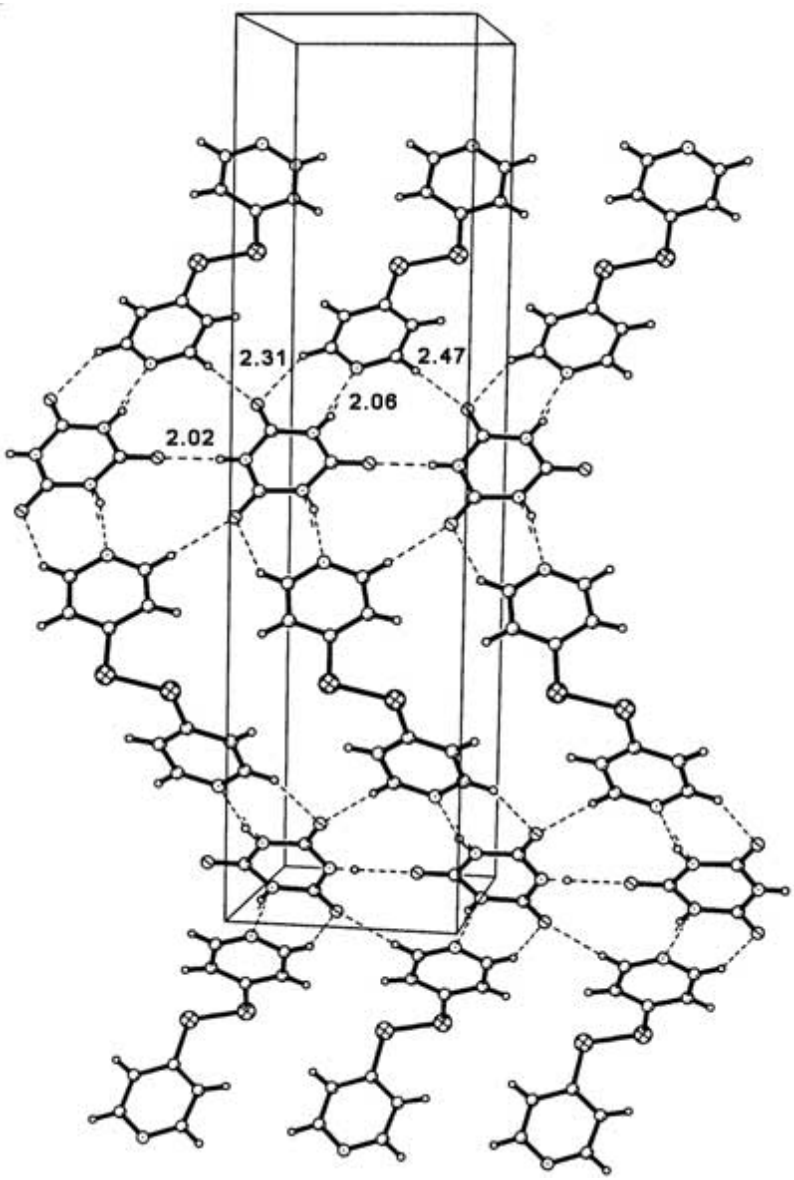

Figure 3.7 Crystal structure of CA·ddpy. The CA molecules form chains by N-HΛO hydrogen bonds, and the ddpy molecules connect the chains together through one N-HΛN hydrogen bond and two C-HΛO hydrogen bonds with adjacent two CA molecules.

The structure of CA·ddpy is obviously different from CA·bipy and CA·H_2O because of the quite different bridge molecule conformation of ddpy. When ddpy molecule replaces the bipy and H_2O molecules, the structure changed from sheet type to a zigzag structure, which was shown in Figure 3.8a. The layers are quite planar and stack on top another. No hydrogen bond or other strong interactions were found between the zigzag layers.

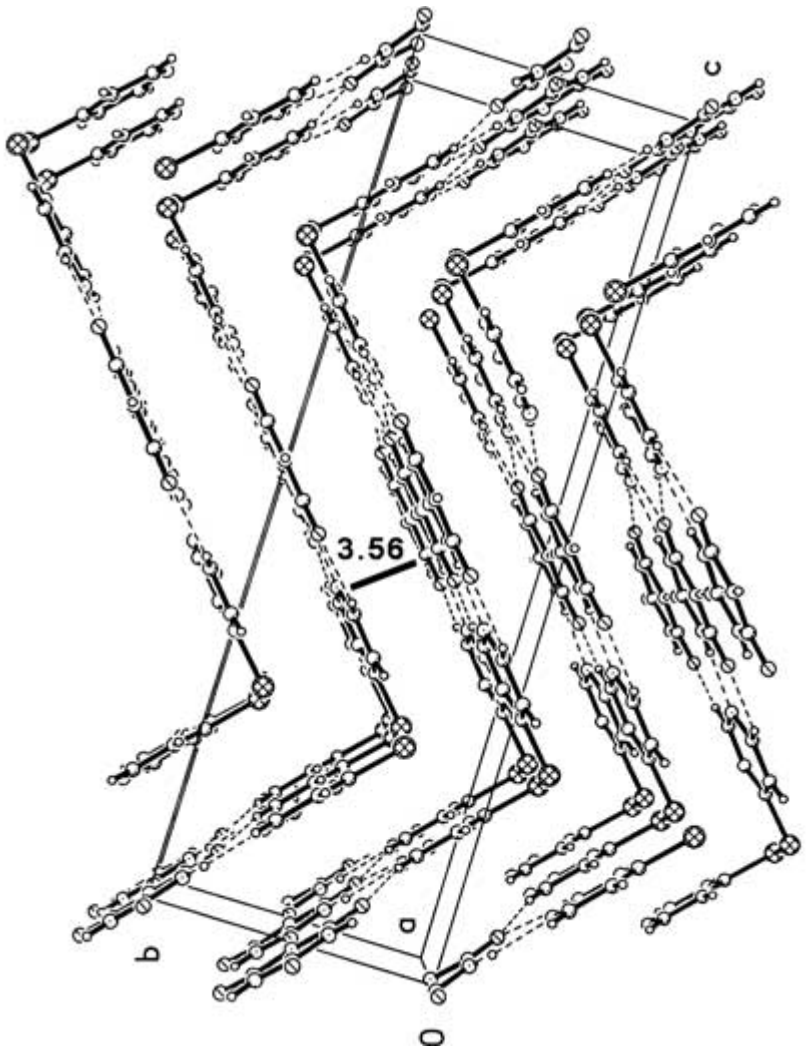

Figure 3.8a A perspective view of the crystal structure of CA·ddpy.

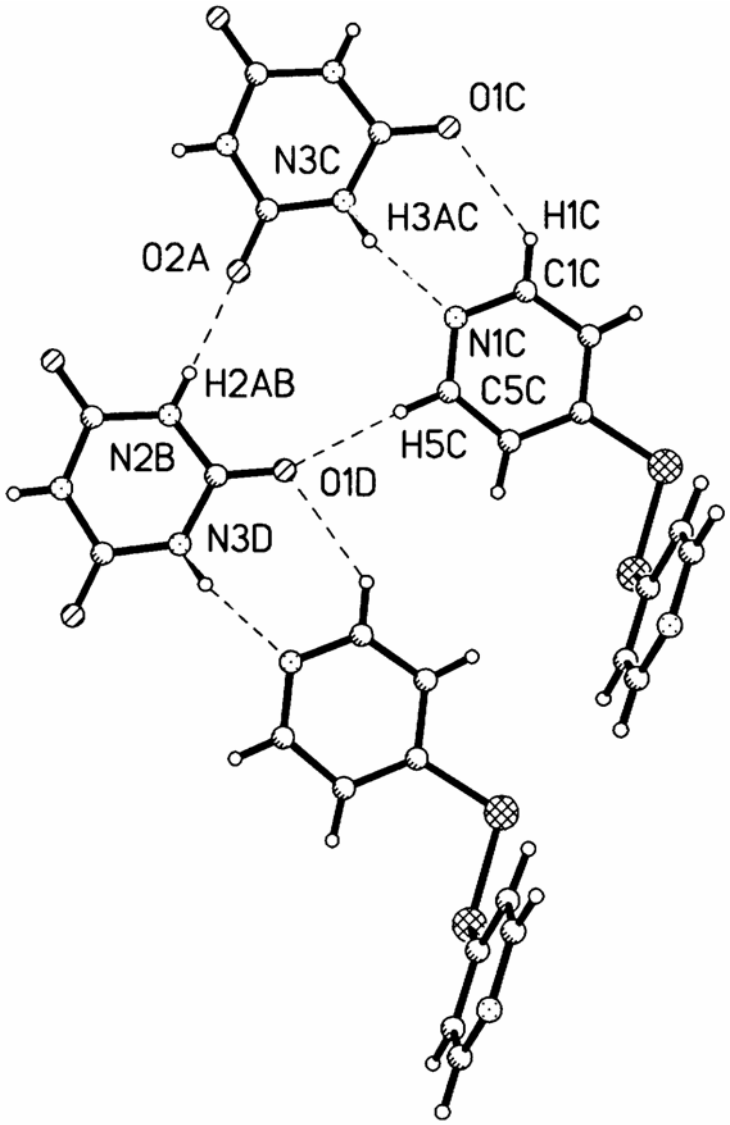

Figure 3.8b Crystal structures of CA·ddpy showing four different hydrogen bonds.

Table 3.2 Hydrogen bond parameters of CA·ddpy.

D-H	d(D-H)	d(HΛA)	<DHA	A
N3C-H3AC	0.85	2.06	164	N1C
C1C-H1C	0.94	2.47	138	O1C
N2B-H2B	0.82	2.02	180	O2A
C5C-H5C	0.93	2.31	172	O1D

3.2.3 Self-assembly of TMA and 4-dodecyloxy-pyridine complex

In the introduction part of this chapter, we showed some interesting properties from 5-alkoxyisophthalic acid (CnISA). We combine the 4-alkoxypyridine and TMA molecules with the 1:1 mole ratio with the hope of getting a similar supramolecular structure of CnISA and some similar interesting properties. We synthesized a few 4-alkoxy-pyridine compounds with different alkyl chains, and we obtained one single crystal from TMA and 4-dodecyloxypyridine (C_{12}Py). The crystal structure was obtained and thermal behavior was investigated at variable temperatures.

3.2.3.1 Crystal structure of the TMA and 4-dodecyloxy-pyridine complex (TMA·C_{12}Py)

The crystal structure of TMA·C_{12}Py with the two components is given in Figure 3.9. The TMA molecule and the C_{12}Py molecule are connected through N-HΛO hydrogen bond. The acidic hydrogen atom, a part of the acid group of TMA molecule, is shifted to the base (pyridine) side and attached to the N atom of C_{12}Py. The two-component supramolecular system resembles the structure of CnISA (Scheme 3.2).

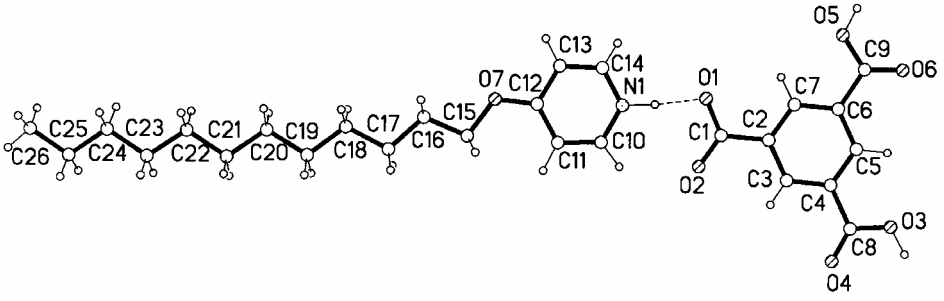

Figure 3.9 The two components in crystal structure of TMA·C_{12}Py.

In TMA·C_{12}Py, there are four kinds of hydrogen bonds present in this crystal and their parameters are listed in Table **3.3**. The distance of N1-H1 is 1.03 Å, which shows that the proton originally attached to the TMA molecule moves over to the N atom of the pyridyl group. And thus the alkoxypyridine forms salts with TMA. The two kinds of cyclic hydrogen bonds in $R_2^2(7)$ graph sets are responsible for the connection between the salt molecules.

Table 3.3. Hydrogen bonding in crystal TMA·C_{12}Py

D-H	d(D-H)	d(HΛA)	<DHA	d(DΛA)	A
O(3)-H(3)	0.96	1.71	160	2.64	O6[-x,-y,-z]
O(5)-H(5)	0.96	1.54	171	2.49	O1[-x+1,-y+1,-z]
N(1)-H(1)	1.03	1.63	175	2.65	O1
N(1)-H(1)	1.03	2.47	124	3.17	O2

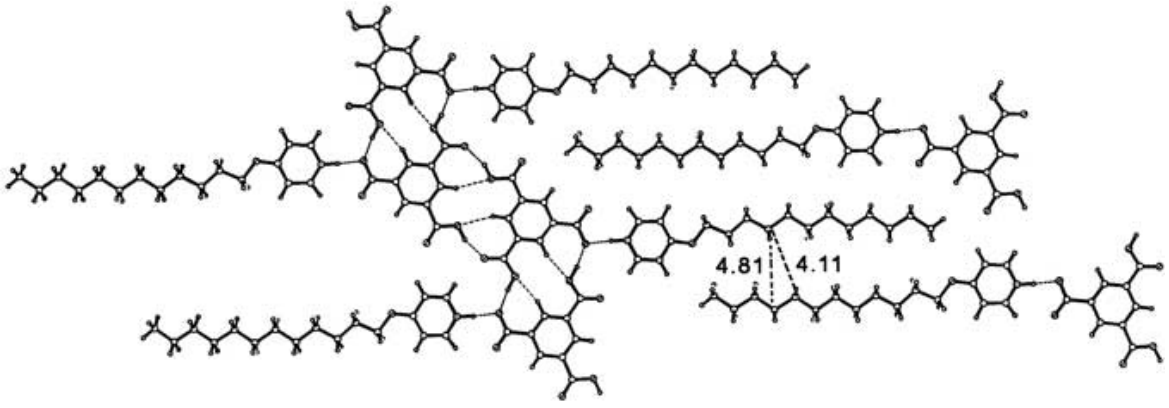

Figure 3.10 Crystal structure of TMA·C_{12}Py: the two adjacent alkyl chains interdigitate to each other through van der Waals interactions. The distance of alkyl chain carbon atom from nearest carbon atoms of adjacent alkyl chain are 4.11 and 4.81 Å.

The crystal packing is shown in Figure 3.10. The sheet-type structure involves a hydrogen-bonded ribbon of the TMA side that is much different from CnISA. In CnISA (Figure 1.11d, Chapter 1), ribbon is formed by bidentate of isophthalic acid. The alkyl substituents from the adjacent hydrogen-bonded chain interdigitate and crystallize to form a sheet interacting with those from the sheets above and below through weak van der Waals forces. Here, one acid group from TMA molecule forms salt with pyridine through proton transfer, and the other two undissociated acid groups form hydrogen bonds with each other and form more close packing by two cyclic $R_2^2(7)$ hydrogen bonds. In the case of CnISA, only acid dimers were observed and the alkyl chains pack in a 3D lattice. In the structure reported here, no acid dimer was observed. All the alkyl chains are on the same plane as the trimesic acid molecules.

3.2.3.2 Variable Temperature (VT) study of the complex: TGA, DSC, VT-powder XRD

The TGA results of TMA·C_{12}Py are shown in Figure 3.11. The crystal starts to decompose at 140 °C, and the decomposition is complete at 413 °C with a residue of 1.9%. Obviously there are at least two decomposition regions. The first one starts from 140 °C and ends at 280 °C with a decomposition of 37%, the second one starts from 280 °C and ends at 413 °C with a decomposition of 61%. Based on the results, the first decomposition region is probably due to the leaving of the side chain of the ddpy molecule. This is because the weight percentage of the $C_{12}H_{25}$ side (mass 169) is 36% of the molecular mass of TMA·C_{12}Py (473).

The thermal properties of the compound were analyzed by differential scanning calroimetry (DSC) at a heating rate of 10 °C /min. the DSC curve of complex is shown in figure 3.12. The melting temperature of complex was observed at 111 °C. Two other small

thermal transition appear at 43 ^{o}C, 67 ^{o}C respectively. Isotropic transition was not observed due to the decomposition of the complex before the isotropic point.

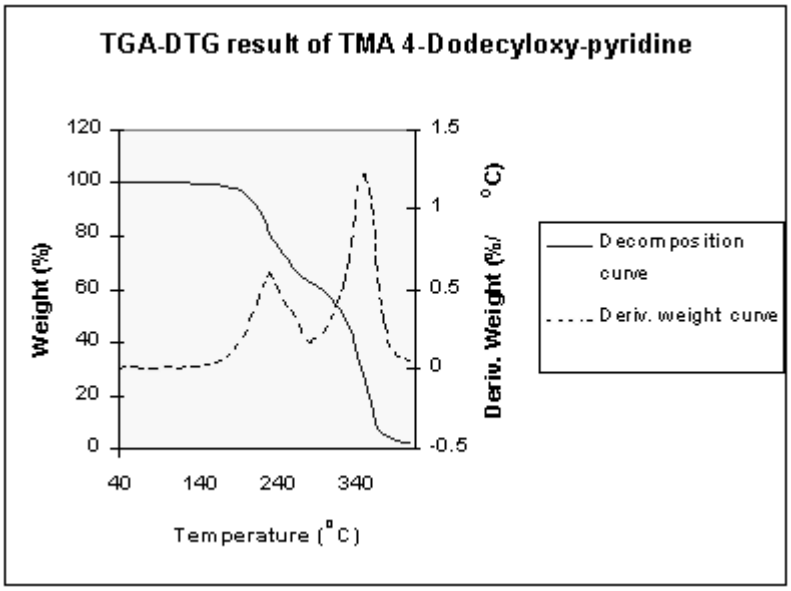

Figure 3.11 Thermo gravimetric analysis (TGA) results of crystal TMA 4-dodecyl-pyridine.

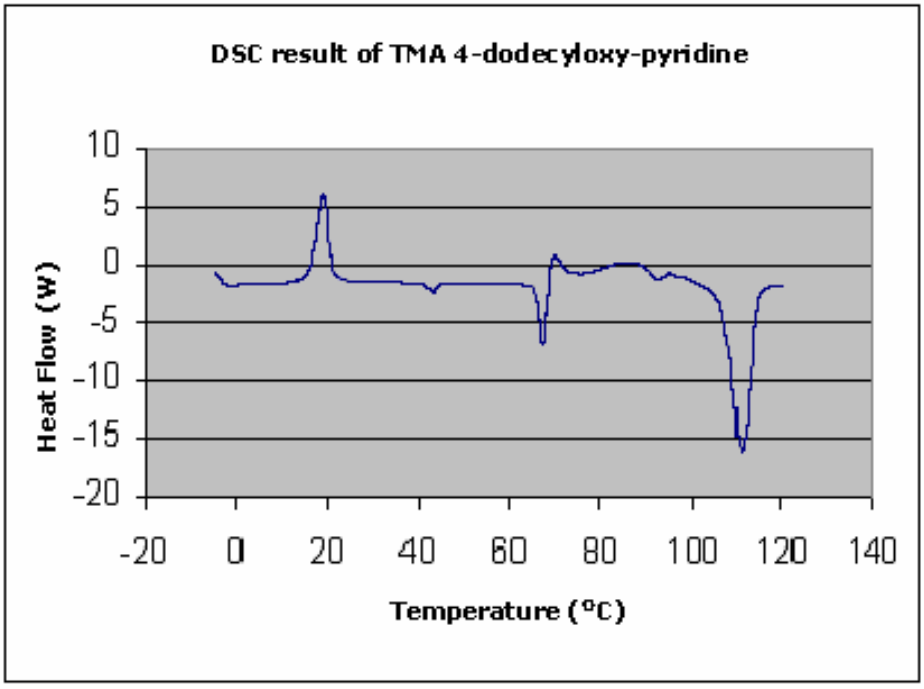

Figure 3.12 Differential Scanning Calorimetry (DSC) result of crystal state TMA 4-dodecyloxy-pyridine: the second heating at 5 degree per minutes; sample weight 13 mg.

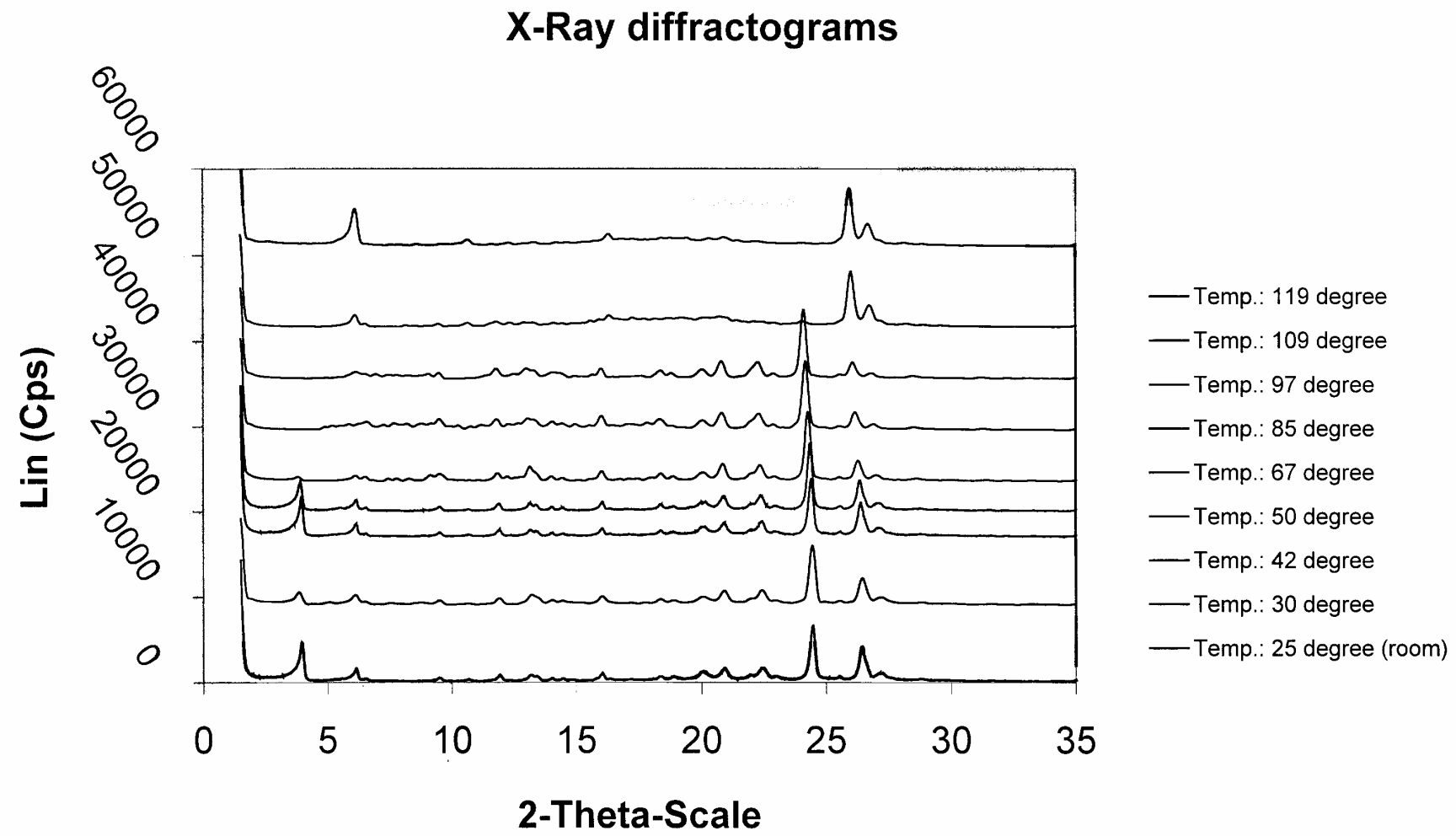

Figure 3.13 X-Ray Diffractograms (XRD) of crystal TMA 4-dodecyloxyl-pyridine powder: the record is under different temperatures of second heating process. The 2θ range is from 1.5 degree to 35 degree.

Variable Temperature Powder X-Ray Diffraction (VT-powder XRD) spectra are shown in Figure 3.13. The powder of the crystal TMA·C_{12}Py was heated from room temperature to 120 °C in air, and then it was cooled to room temperature. During the second heating scan, diffractions from 1.5 degree to 35 degree of 2θ were measured as shown in Figure 3.13.

The nature of the crystalline phase at low temperature examined by XRD allows us to investigate the supramolecular architecture of this complex. The temperature dependent changes in the layer spacing, is indicated by the intermolecular reflection in the small-angle region (0 – 5 degree). The 3D arrangement of the structure is given by the intermolecular reflection in the wide-angle region of 5 – 35 degree.

In Figure 3.13 at 25 ^{o}C (room temperature) the diffraction pattern of the crystalline phase of the crystal after first cooling exhibits Bragg reflections at 22.4 Å (2θ of 3.9 degree), consistent with the existence of the 2D lamellar ordering of the molecules with non-interdigitated alkyl chain. The calculated distance of the alky chains between two hydrogen bond areas (Scheme 3.3 left) is about 23 Å.

In the case reported by Pfaadt et. al. [4], the thermal behavior of C_{18}ISA (5-octadecyloxyisophthalic acid) crystal at different temperatures is discussed. During the cooling process, the interdigitated alkyl chain pattern changed to non-interdigitated. And during the heating process, the pattern is converted back to interdigitated one.

TMA·C_{12}Py exhibites a different pattern compared to C_{18}ISA. From Figure 3.13, it can be seen that a Bragg distance of 22.4 Å (2θ of 3.9 degree) is present at the temperature range from 25 °C to 67 °C (at 67 °C, the reflection is weak but the peak is still present), and disappears at 85 °C. The result indicated that the non-interdigitated alkyl chain becomes disordered. From Figure 3.12, the pattern changed from an order state to disordered one at 67 °C.

Also as shown in Figure 3.13, the intermolecular reflection of Bragg distance of 3.4 Å (2θ of 26.4 degrees) is observed from room temperature to 119 °C. This reflection should come from the distance between the layers. The heating pattern mode above 67 °C is suggested in Scheme 3.3. The non-interdigitated alkyl chains kept till 67 °C, above that, the alkyl chain become disorder. However, the layers are still kept as existence of the Bragg distance of 3.4 Å (2θ of 26.4 degrees) from room temperature to 119 °C.

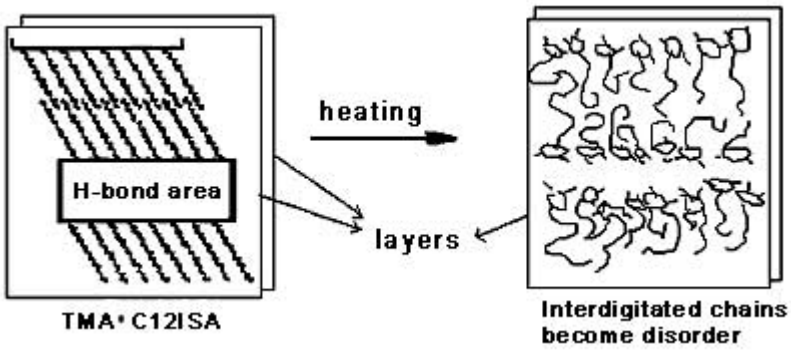

Scheme 3.3 Schematic representations of the different arrangements of TMA·C_{12}Py at different temperatures. After cooling of the first heating process, the crystal exhibits a pattern as shown on the left, and when a second heating process is conducted, the non-interdigitated alkyl chains is broken and changed to a disordered state, but the layers are still kept.

3.3 Conclusion

Three structures (TMA·1/2THB, TMA·C_{12}Py and CA·ddpy) were obtained and characterized. When cocrystillized with compound THB, TMA molecules gave a planar, sheet-type, and close packed structure with a much smaller cavity compared with normal honeycomb structure of TMA. When TMA molecules cocrystallized with C_{12}Py molecule, the observed solid-state structure was very similar to that found from 5-hexadecyl isophthalic acid. Among the three acid protons of TMA (-CO_2H), one acid proton was transferred to the N atom of C_{12}Py, which resulted in the formation of a salt. The remaining two undissociated carboxyl groups formed H-bonds with neighboring acid functional groups. Its thermal analysis showed that the structure has much different patterns at different temperatures. The structure from the complex of CA molecule and ddpy molecule is composed of ribbons formed by CA molecules, and the ribbons are connected by the bridge molecule of ddpy.

3.4 Experimental

All solvents and reagents were of reagent quality, purchased commercially, and used without further purification, unless otherwise noted. Column Chromatography was carried out with Merck silica gel (230- 400 mesh) for flash column chromatography. Merck silica gel 60 F_{254} plastic backed plates (20 x 20 cm) were used for thin layer chromatography (TLC). NMR spectra were recorded on a Brucker ACF-300 spectrometer. All solvents were dried prior to use and all reactions were carried out under nitrogen atmosphere.

3.4.1 X-ray crystallography

X-ray crystallographic data were collected on a Bruker AXS SMART CCD 3-circle diffract meter with a Mo Kα sealed tube at 23 °C. Softwares used were: SMART [17] for collecting frames of data, indexing reflections and determination of lattice parameters;

SAINT [12] for integration of intensity of reflections and scaling; SADABS [18] for empirical absorption correction; and SHELXTL [19] for space group determination, structure solution and least-squares refinements on F^2. Structures were obtained by direct methods and non-hydrogen atoms were refined anisotropically. Hydrogen atoms were placed on calculated positions (C-H 0.96 Å) and assigned isotropic thermal parameters riding on their parent atoms. The crystal data and refinement details were given in Table 3.4.

Table 3.4 Crystal data and structure refinement parameters.

Compound	**TMA•1/2THB**	**CA•ddpy**	**TMA·C_{12}Py**
Chemical formula	$C_{24}H_{18}O_{15}$	$C_{13}H_{11}O_3N_5S_2$	$C_9H_6O_6 \cdot C_{17}H_{29}NO$
Formula weight	546.38	349.39	473.55
Crystal system	triclinic	orthohombic	triclinic
Space group	P(-1)	C222(1)	P(-1)
a [Å]	7.1504(1)	6.8042(3)	9.3263(2)
b [Å]	13.5269(2)	8.4317(4)	10.0384(1)
c [Å]	13.5587(2)	25.8389(11)	14.3866(2)
α [^{0}]	63.756(1)	90	107.000(1)
β [^{0}]	80.888(1)	90	99.907(1)
γ [^{0}]	81.243(1)	90	98.223(1)
V [Å]	1156.39(3)	1482.40(11)	1241.82(3)
Z	2	4	2
ρ_{Calcd} [g cm^{-3}]	1.569	1.565	1.266
Crystal size [mm]	0.36x0.26x0.18	0.44x0.24x0.20	0.5x0.4x0.36
μ [mm^{-1}]	0.134	0.382	0.091
Temperature [K]	293(2)	223(2)	223(2)
Measured reflns	4453	1730	3101
Indep. Reflns	5447	1842	4164
θ max [^{0}]	1.80<2θ<28.26	1.58<2θ<29.30	2.17<2θ<25.00
Refinement on	F^2	F^2	F^2
Final R ind (I > 2σ(I))	R1 = 0.0368 wR2 = 0.1069	R1 = 0.0306 wR2 = 0.0643	R1 = 0.0690 wR2 = 0.1403
R indices (all data)	R1 = 0.0447 wR2 = 0.1112	R1 = 0.0275 wR2 = 0.0628	R1 = 0.0518 wR2 = 0.1296
Data/restraints /parameters	5447/0/352	1842/0/128	4164/0/448
Absorption corr.	Sadabs	Sadabs	Sadabs
GoF	1.062	1.088	0.987

3.4.2 Synthesis of 4-dodecylpyridine

The synthesis of 4-dodecyloxypyridine is shown in Scheme 3.4. 4-hydroxypyridine (4.75 g, 49.9 mmol), 1-bromododcyane (12.44 g, 49.9 mmol), anhydrous potassium carbonate (6 g, 0.1 mol) and dimethylformamide (DMF, 150 ml) were placed in a 250 ml round bottom flask (RBF) equipped with a condenser and purged with nitrogen. The solution was heated at 70 °C for 3 hours. The solvent was removed under reduced pressure and the residue dissolved in dichloromethane. The organic layer was washed with brine water. The solvent was removed to afford a white solid. Yield: 5.2 g (43 %). ^{1}H-NMR (300 MHz in $CDCl_3$, δ ppm), 0.87 (t, J = 3.2 Hz, 3H, $O(CH_2)_{11}CH_3$), 1.22 – 1.46 (m, 18H, $OCH_2CH_2(CH_2)_9CH_3$), 1.78 (q, 2H, $OCH_2CH_2(CH_2)_9CH_3$), 3.96 (t, J = 3.0 Hz, 2H, $OCH_2(CH_2)_{10}CH_3$), 6.79 (d, J = 3.4 Hz, 2H, OC_5H_4N), 8.40 (d, J = 6.9 Hz, 2H, OC_5H_4N); ^{13}C NMR ($CDCl_3$, δ ppm) 164.9, 150.7, 109.8 (OC_5H_4N); 72.3, 32.5, 30.6, 30.3, 30.2, 30.1, 30.0, 26.6, 23.1 and 14.0 ($OC_{12}H_{25}$).

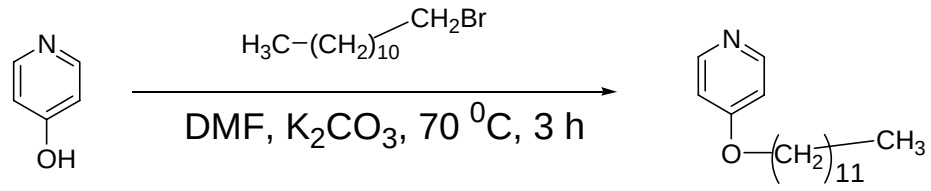

Scheme 3.4 Synthesis of 4-dodecylpyridine.

3.4.3 Crystal growth

3.4.3.1 TMA 1,3,5-trihydroxylbenzene

1,3,5-trimesic acid (TMA, 135.1 mg, 0.8 mmol) and phloroglucinol (100 mg, 0.8 mmol) were dissolved in 8 ml methanol in a test tube. The test tube was sealed with para film. 3 days later, colorless crystal formed.

3.4.3.2 TMA 4-dodecyloxyl-pyridine

1,3,5-trimesic acid (TMA, 40.6 mg, 0.2 mmol) and 4-dodecyloxypyridine (53.5 mg, 0.2 mmol) were dissolved in methanol (6 ml) in a test tube. The test tube was sealed with Para film. 6 days later, colorless crystal formed.

3.4.3.2 Cyanuric acid 4,4'-dithiodipyridine

Cyauric acid and 4,4'-dithiodipyridine (mole ratio: 2: 3) were dissolved in DMSO in a small test tube. The test tube was then placed in a large bottle containing some water at the bottom. The bottle was sealed and left undisturbed for 10 days. Colorless crystals were formed on the walls of the small test tube.

3.5 Reference

[1] D. J. Duchamp, R. E. Marsh, *Acta Crystallogr.* **1969**, B 25, 5.

[2] S. V. Kolotuchin, P. A. Thiessen, E. E. Fenlon, S. R. Wilson, C. J. Loweth, S. C. Zimmerman, *Chem. Eur. J.* **1999**, 5, No 9, 2537.

[3] O. M. Yaghi, G. Li, H. Li, *Nature*, **1995**, 378, 703.

[4] M. Pfaadt, G. Moessner, D. Pressner, S. Valiyaveetil, C. Boeffel, K. Mullen, H. W. Spiess, *J. Mater. Chem.,* **1995**, 5(12), 2265.

[5] S. Valiyaveettil, K. Mullen, *New J. Chem.*, **1998**, 89.

[6] J. Yang, J. L. Marendaz, S. J. Geib, A. D. Hamilton, *Tetrahedron Lett*. **1994**, 35, 3665.

[7] (a) R. Alcala, S. Martinez-Carrera, *Acta Crystallogr. Sect. B* **1972**, 28, 1671; (b) J. L. Derissen,, *Acta Crystallogr*. **1974**, 30 B, 2764.

[8] For a recent extensive discussion of the crystal packing behavior of trimesic acid and its derivatives see: S.V. Kolotuchin, P. A. Thiessen, E. E. Fenlon, S. R. Wilson, C. J. Loweth, and S. C. Zimmerman, *Chem. Eur. J.* **1999**, 5, 2537; F. H. Herbstein, *Comprehensive Supramolecular Chemistry*, Pergamon Press, Oxford. Volume 6, **1996**.

[9] F. H. Herbstein, M. Kapon, G. M. Reisner, *J. Inclusion Phenom.* **1987**, 5, 211-214; see also: F. H. Herbstein, *Top. Curr. Chem.* **1987**, 140, 107-140; F. H. Herbstein, in *Comprehensive Supramolecular Chemistry*, *Vol 6* (Eds.: J. L. Atwood, J. E. D. Davies, D. D. MacNicol, F. Vögtle), Pergamon, New York, **1996**, Ch. 3.

[10] S. V. Kolotuchin, E. E. Fenlon, R. W. Wilson, C. J. Loweth, S. C. Zimmerman, *Angew. Chem.*. **1995**, 107, *Angew. Chem. Int. Ed. Engl.* **1995**, 34, 2654.

[11] M. J. S. Dewar, E. G. Zoebisch, E. F. Healy, J. J. P. Stewart, *J. Am. Chem. Soc*., **1985**, 107, 3902.

[12] Both geometries **A** and **B** are optimized results with Spartan SGI version 5.1.3 OpenGL built under IRIX 6.2 using the AM1 force field and none solvent model. **A** was initially drawn as cyclic hexamer (six isophthalic acids) with a THB molecule located in its center. **B** was initially drawn as a structure with all the atoms posited in the similar relevant positions as the distorted hexamer in the crystal lattice.

[13] V. Berl, M. J. Chrische, I. Huc, J. –M. Lehn, M. Schmutz, *Chem. Eur. J*., **2000**, 6, 1938.

[14] J.A. Zerkowski, C.T. Seto, D.A. Wierda, G.M. Whitesides, *J. Am. Chem. Soc*. **1990**, 112, 9025.

[15] P. Coppens, A. Vos, *Acta Crystallog.* **1971**, B 27, 146.

[16] A. Ranganathan , V.R. Pedireddi , G. Sanjayan , K.N. Ganesh , C.N.R. Rao, *J. Mol. Struct*., **2000**, 522, 87.

[17] SMART & SAINT Software Reference Manuals, Version 4.0, Siemens Energy & Automation, Inc., Analytical Instrumentation, Madison, Wisconsin, USA, **1996**.

[18] G.M. Sheldrick, SADABS, software for empirical absorption correction, University of Gottingen, Gottingen, Germany, **1996**.

[19] SHELXTL Reference Manual, Version 5.03, Siemens Energy & Automation Inc., Analytical Instrumentation, Madison, Wisconsin, USA, **1996**.

Chapter 4 Approaches to nanoporous structure

4.1 Introduction

Organic solid state and molecular architectures providing nano- or mesoporous space for the inclusion of guest species open up new opportunities for the synthesis of materials showing designed chemical and physical properties. Microporous materials such as zeolites find widespread application in heterogeneous catalysis, adsorption and ion exchange processes. The rigidity and stability of such frameworks allow for shape- and size-selective inclusion of organic molecules and ions [1-2]. Recently, the construction of porous materials by linking transition metal ions with bridging ligands other than oxygen attracted great interest, which has potential for the synthesis of new types of tailored porous materials [3]. For example, Yaghi et al. synthesized an interesting microporous metal-organic framework (see Figure **4.1**) with the help of trimesic acid as ligand, Co^{2+} as metal ion and pyridine as spacer unit (U layer) [4].

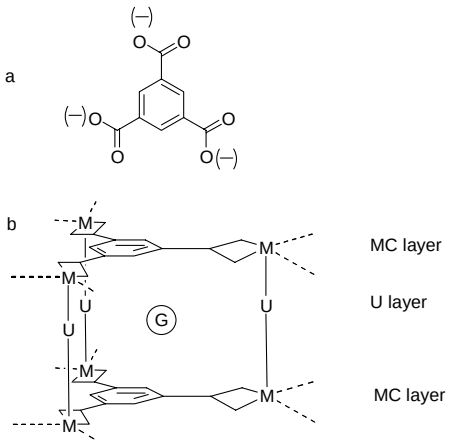

Figure 4.1 (a) Structural formula of 1,3,5-benzenetricarboxylate (BTC), and (b) its coordination to a metal ion to form alternating metal-carboxylate and spacer unit layers to form voids where guest are accommodated.

In our project, we would like to utilize some simple building blocks as ligands such as isophthalic acid to construct micoroporous structures. We also designed and synthesized a series of triacids as possible ligands. Not only pure organic compound inclusion structures were attempted, but also porous metal-organic framework using the deprotonated acid, such as isophthalate (IPA), were explored. The transitional metals used for such complexes are Cu, Co, Zn etc. After many attempts, single crystals suitable for X-ray diffraction experiments were obtained, in which the crystal structure is different as in Yaghi's case [4]. The complex formed between Cu^{2+} and organic ligand IPA together with 2,2'-bipyridine (bpy) was obtained. Another single crystal from one of synthesized triacids was isolated; we were unable to solve its structure after collecting its diffraction data.

In this chapter, the structural details of the copper complex is discussed. Some information of the incomplete structure from one of the synthesized triacids 5-(2-carboxybenzyloxy)isophthalic acid **(12)** is given. All synthetic procedure for triacids is given at the end of this chapter.

4.2 Results and discussion

4.2.1 Crystal structure of $[Cu_2(bpy)_2(IPA)Cl(H_2O)_3][Cu_2(bpy)_2(IPA)Cl_2(H_2O)_2]$-$[Cl][H_2O]$ (**11**)

The structure of **11** consists of two kinds of subunits in the crystal structure. As shown in Figure **4.2**, the four Cu^{2+} ions from the two subunits have different coordination environment. Three of Cu^{2+} atoms coordinate with one Cl atom, one water molecule, one 2,2'-bipyridine molecule and one carboxyl group from isophthalate, one Cu^{2+} ion

coordinates with two water molecule, one 2,2'-bipyridine and one carboxyl group from isophthalate. A crystallographic C_2 symmetry is presented in one subunit (Figure 4.2 right).

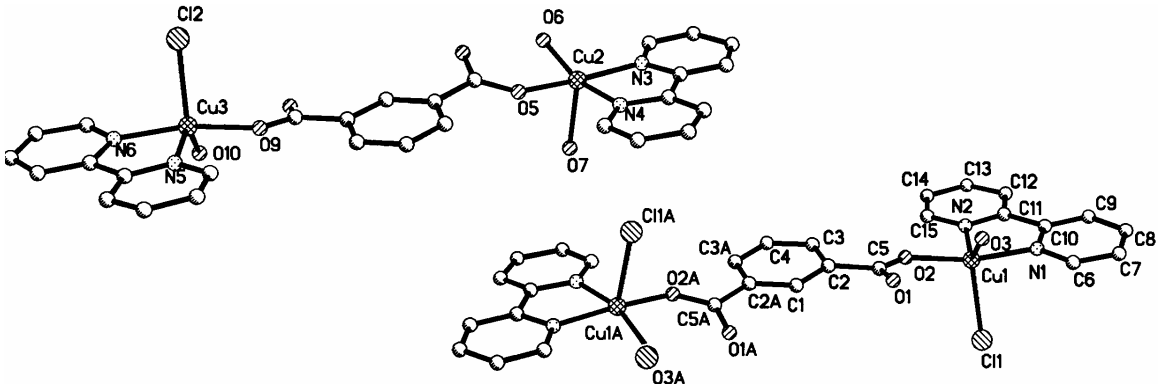

Figure 4.2 Repeating units of **11** with Cu, O from water molecules and Cl atom labeling scheme showing two different subunits in the crystal structure. $[Cu_2(bpy)_2(IPA)Cl(H_2O)_3]^+$ (above left subunit): one Cu atom coordinates with two water molecules and another Cu atom coordinates with one Cl atom and one water molecule; $[Cu_2(bpy)_2(IPA)Cl_2(H_2O)_2]$ (down right subunit) each of two Cu atoms coordinates with one Cl^- and one water molecule.

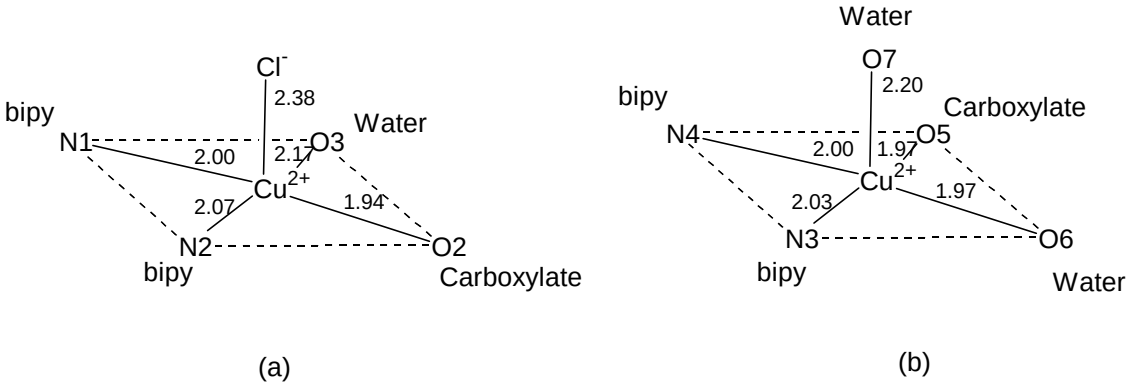

Figure 4.3 Comparison of Copper (II) coordination environments from **11**.

All copper(II) ions are five-coordinated. Five-coordinate copper(II) complexes are not uncommon; the geometry around the metal ion is trigonal bipyramidal or square pyramidal (Figure 4.3). Figure **4.3** shows the comparison of copper (II) coordination environment in crystal **11**. The geometries around copper(II) center are best described as distorted square pyramidal. Selected bond distances and angles are shown in Table **4.1**.

Table 4.1 Selected bond distances (Å) and angles (°) for **11**.

Cu1-Cl1	2.3758(6)	Cu1-O2	1.9426(14)
Cu1-N1	1.9987(16)	Cu1-O3	2.1682(16)
Cu1-N2	2.0679(16)	Cu2-N3	2.0257(17)
Cu2-N4	1.9983(17)	Cu2-O5	1.9735(14)
Cu2-O6	1.9727(16)	Cu2-O7	2.196(2)
N1-Cu1-Cl1	93.07(5)	O5-Cu2-N3	168.53(7)
N2-Cu1-Cl1	123.09(5)	N2-Cu1-N1	123.09(5)
O2-Cu1-N2	88.98(6)	O2-Cu1-Cl1	98.88(5)
O3-Cu1-N1	90.71(7)	O2-Cu1-N1	166.89(7)
O3-Cu1-O2	91.95(6)	O3-Cu1-Cl1	102.41(5)
N4-Cu2-N3	80.82(7)	O3-Cu1-N2	133.76(7)
O5-Cu2-N4	90.94(6)	O7-Cu2-N3	96.49(8)
O6-Cu2-N4	164.63(7)	O7-Cu2-O5	92.42(8)

The subunits are connected together by intermolecular hydrogen bonding (see Figure **4.4**, **4.5**). C-HΛCl$^-$ (C-H 0.93 Å, HΛCl 2.85 Å, ∠C-HΛCl 174°) and O-HΛCl$^-$ (O-H 0.76 Å, HΛCl 2.32 Å, ∠O-HΛCl 174°) are the main interactions in the crystal to connect the subunits. Also the free water molecule can form C-HΛO (C-H 0.93 Å, HΛO 2.58 Å, ∠C-HΛO 148°) hydrogen bonding with H atoms from 2,2'-bipyridine.

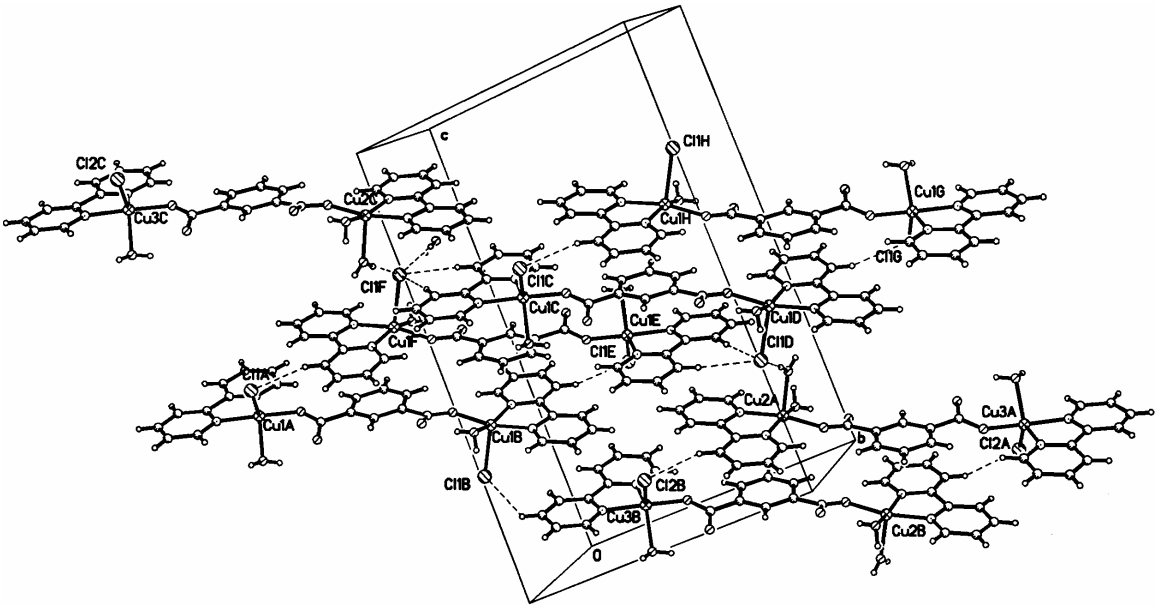

Figure 4.4 Partial packing diagram of **11** with special atom (Cu and Cl) labeling scheme showing the stacking interaction and hydrogen bonding.

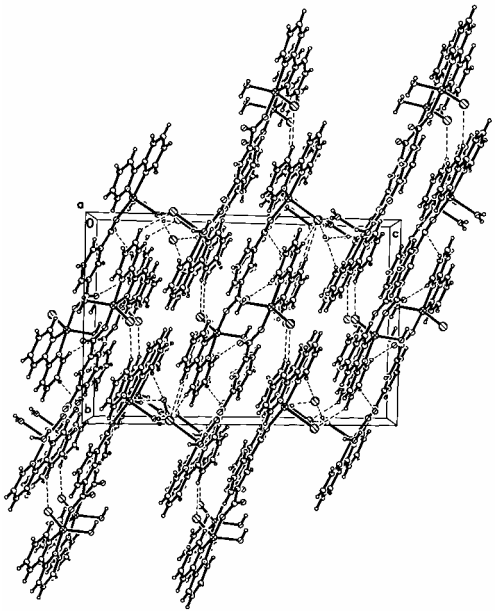

Figure 4.5 Packing diagram of **11** viewed along the *a* axis.

Although porous structures have been synthesized and explored by Yaghi et al. from 1,4-benzenedicarboxylic acid (terephthalic acid) [5] and trimesic acid [3], it seems that isophthalic acid (1,3-benzenedicarboxylic acid) is difficult to form porous structure under similar conditions.

4.2.2 Synthesized triacids as building blocks

As shown in Figure **4.6**, seven triacids were synthesized. All of them have been used to crystallize in order to get structures of the pure organic acids or complexes. Unfortunately, we obtained only one single crystal from methanol/THF solution of triacid (**3a)**.

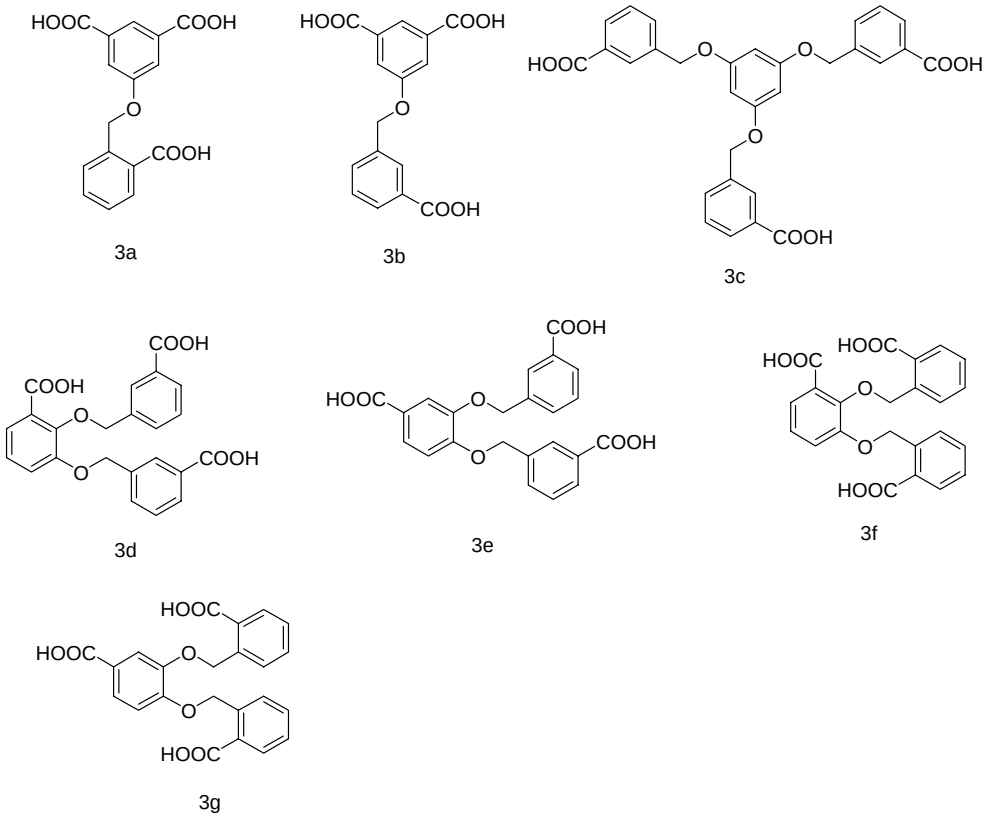

Figure 4.6 Structures of seven synthesized compounds.

Due to the quality of the crystal, the structure cannot be solved completely. Partially solved structure fragment (**12**) from the crystal diffraction is shown in Figure **4.7**.

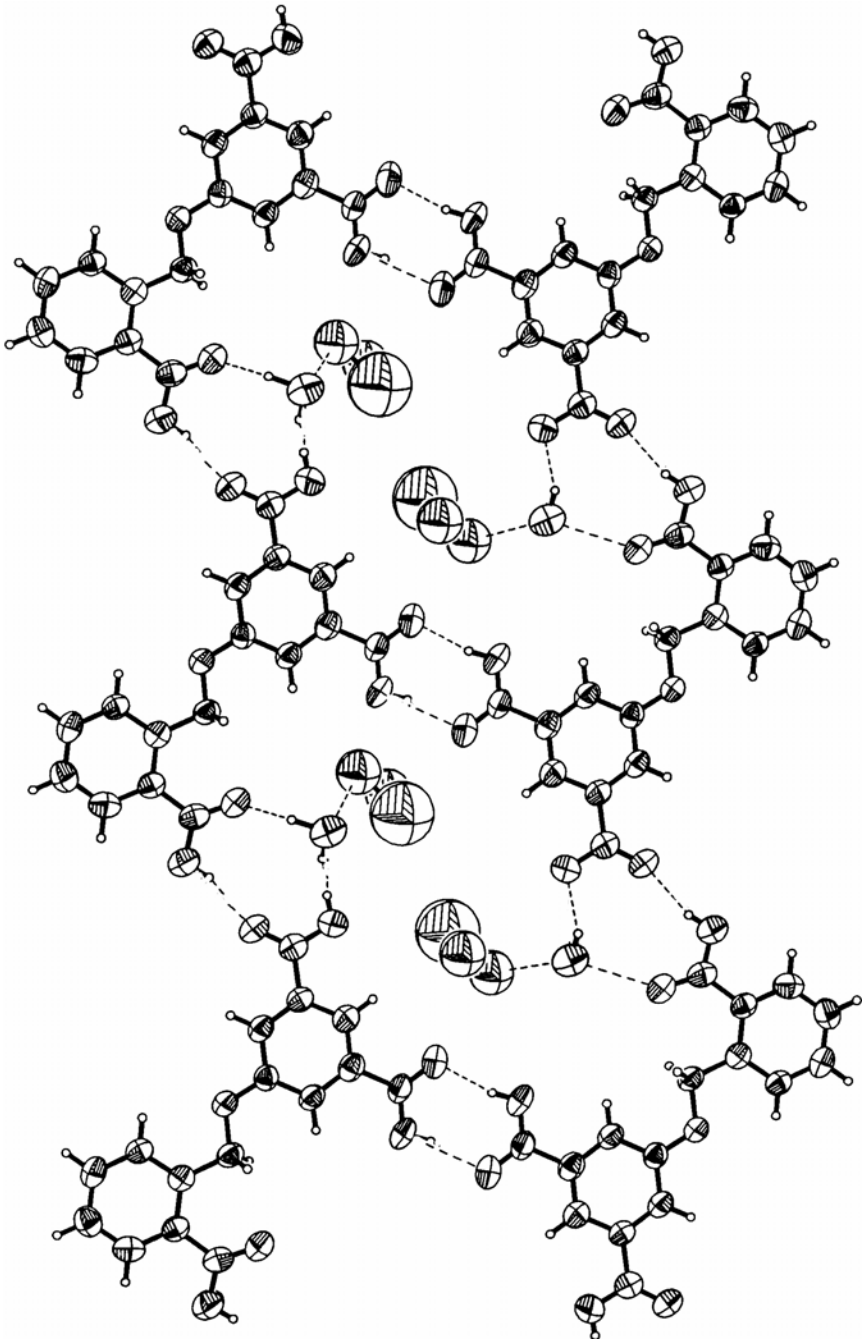

Figure 4.7 Partially solved structure: four triacid molecules (**3a**) form a channel and two water molecules and two methanol molecules inside the channel.

Although the structure is not fully solved, Figure **4.7** shows that an inclusion compound has been synthesized. The inclusion guest molecules included here are methanol and water molecules.

4.3 Conclusions

Starting from our synthesized triacids and some simple building blocks such as isophthalic acid, we tried several methods including cocrystallization and complexation to get porous structures or inclusion compounds. As a result one complex from isophthalic acid and copper(II) together with 2,2'-bipyridine was obtained. Two different coordination environments in three Cu(II) centers were found in **11**. It did not have the desired porous structure. Partially solved fragments of one triacid show that it may be a porous structure with water and methanol molecules as guest molecules in the channel formed by the four triacid molecules.

4.4 Experimental

All solvents and reagents were of reagent quality, purchased commercially, and used without further purification, unless otherwise noted. Column Chromatography was carried out with Merck silica gel (230- 400 mesh) for flash column chromatography. Merck silica gel 60 F_{254} plastic backed plates (20 x 20 cm) were used for thin layer chromatography (TLC). NMR spectra were recorded on a Brucker ACF-300 spectrometer. All solvents were dried prior to use and all reactions were carried out under nitrogen atmosphere. NBS was further purified by recrystallization from hot water.

4.4.1 X-ray crystallography

X-ray crystallographic data were collected on a Bruker AXS SMART CCD 3-circle diffractometer with a Mo Kα sealed tube at 23 °C. The softwares used were: SMART [6] for collecting frames of data, indexing reflections and determination of lattice parameters; SAINT [7] for integration of intensity of reflections and scaling, SADABS [7] for empirical absorption correction; and SHELXTL [8] for space group determination, structure solution and least-squares refinements on F^2. Structures were obtained by direct methods and non-hydrogen atoms were refined anisotropically. Hydrogen atoms were placed on calculated positions (C-H 0.96 Å) and assigned isotropic thermal parameters riding on their parent atoms. The crystal data and refinement were given in Table 3.4.

Table 3.4 Crystal data and structure refinement parameters.

Compound	**11**
Chemical formula	C14 H13 Cl Cu N2 O3.50
Formula weight	364.25
Crystal system	monoclinic
Space group	P2(1)/n
a [Å]	9.2610(5)
b [Å]	14.4793(7)
c [Å]	22.2070(11)
α [^{0}]	90.1460(10)
β [^{0}]	99.5540(10)
γ [^{0}]	90.0510(10)
V [Å]	2936.5(3)
Z	8
ρ_{Calcd} [g cm^{-3}]	1.648
Crystal size [mm]	Not measured
μ [mm^{-1}]	1.684
Temperature [K]	293(2)
Measured reflns	8363
Indep. Reflns	12556
θ max [^{0}]	1.86<2θ<27.09
Refinement on	F^2
Final R ind (I > 2σ(I))	R1 = 0.0302 wR2 = 0.0806
R indices (all data)	R1 = 0.0537 wR2 = 0.0894
Data/restraints/parameters	12556/0/812
Absorption corr.	Sadabs
GoF	0.994

4.4.2 Preparation of crystal:

$[Cu_2(bpy)_2(IPA)Cl(H_2O)_3][Cu_2(bpy)_2(IPA)Cl_2(H_2O)_2][Cl][H_2O]$ (**11**)

Isophthalic acid (74 mg, 0.4 mmol), 2,2'-bypyridine (69.5 mg, 0.4 mmol), $CuCl_2$ (0.1 M, 4.45 ml) were mixed and dissolved in methanol and stirred for 0.5 hours, then NaOH (0.2 M, 1.5 ml) was added. The mixture was left stirring for 4 hours under 70 °C. The mixture was left standing in a beaker. Several days later, blue crystals were formed and collected for analysis.

4.4.2 Synthesis of triacids

5-(2-Carboxybenyloxy)isophthalic acid (**3a**)

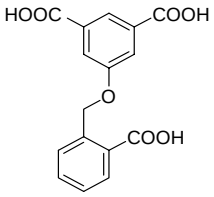

Procedure:

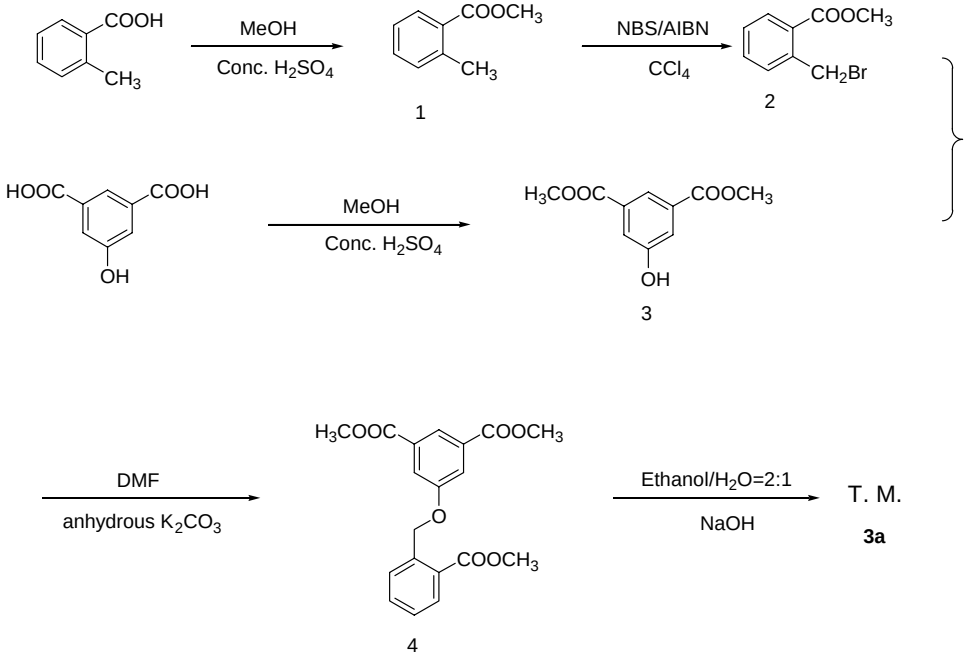

Scheme 4.1 Synthetic scheme of triacid **3a**.

2-Methylbenzoic acid methyl ester (**1**)

2-methylbenzoic acid (30 g, 0.2 mol), methanol (250 ml), and Conc. H_2SO_4 (4 ml) were placed in a 500 ml round bottom flask. The solution was refluxed for 3 hours and cooled to room temperature. The solvent was removed by distillation under reduced pressure. The residue was dissolved in CH_2Cl_2 (100 ml), washed with water (3 x 100 ml) until the aqueous layer was neutral. The organic solvent was removed under reduced pressure. A white solid was obtained which was dried in an oven. Yield: 33.0 grams (100 %); ^{1}H NMR (300 MHz, $CDCl_3$, δ ppm) 2.6 (s, 3H, CH_3), 3.9 (s, 3H, $COOCH_3$), 7.25 (m, 2H, Ph), 7.4 (t, *J* = 7.4 Hz, 1H, Ph), 7.94 (d, *J* = 7.2 Hz, 1H, Ph); ^{13}C NMR ($CDCl_3$, δ ppm) 167.0 (C=O); 138.9, 132.7, 131.2, 129.6, 129.1 and 125.4 (Ar); 50.0 ($COOCH_3$); 14.1 (CH_3) MS (M+1) 151.

2-Bromomethylbenzoic acid methyl ester (**2**)

Compound **1 (**7 g, 46.6 mmol), AIBN (200 mg, 1.2 mmol), NBS (7.48 g, 42.0 mmol), and CCl_4 (150 ml) were placed in 250 ml round bottom flask. The solution was refluxed at 80°C for 1.5 hours, cooled, filtered and excess solvent was removed under reduced pressure to give orange oil, which was recrystallised in hexane to obtain colorless crystalline solid. Yield: 8.2 g (85%); ^{1}H NMR (300 MHz, $CDCl_3$, δ ppm) 3.93 (s, 3H, $COOCH_3$), 4.95 (s, 2H, CH_2Br), 7.34 (t, *J* = 6.8 Hz, 1H, Ph), 7.48 (m, 2H, Ph), 7.95 (d, *J* = 7.2 Hz, 1H, Ph); ^{13}C NMR ($CDCl_3$, δ ppm) 167.0 (C=O); 139.2, 133.1, 131.2, 130.0, 129.1 and 128.6 (Ar); 50.0 (CH_3); 31.6 (CH_2Br) MS (M+1) 229.

5-Hydroxyisophthalic acid dimethyl ester (**3**)

The procedure is the same as for compound **1**. 5-hydroxyisophthalic acid (30 g, 0.16 mol), Conc. H_2SO_4 (5 ml), and methanol (250 ml) were placed in a 500 ml round bottom flask. Yield 34.1 g (99%); ^{1}H NMR (300 MHz, $CDCl_3$, δ ppm) 3.94 (s, 6H, $COOCH_3$), 6.65 (s, 1H, OH), 7.80 (s, 2H, Ph), 8.23 (s, 1H, Ph); ^{13}C NMR ($CDCl_3$, δ ppm) 167.0 (C=O); 157.3, 131.8, 123.5 and 121.2 (Ar), 50.0 (CH_3); MS (M+1) 211. $C_{10}H_{10}O_5$ (210.2): calcd. C 57.14, H 4.80; found C 56.71 H 4.47 %.

5-(2-Methoxycarbonylbenzyloxy)isophthalic acid dimethyl ester (**4**)

Compound **3** (5.9 g, 28.1 mmol), compound **2** (6.44 g, 28.1 mmol), DMF (150 ml), and anhydrous potassium carbonate (13 g, 0.2 mol) were placed in 250 ml of round bottom flask. The solution was heated at 80 °C for 8 hours. The solvent was removed under reduced pressure to give a black oil, then 1 ml of methanol was added inside, a solid was precipitated out. Then wash the solid with methanol several times (cold methanol, 1 ml per time). Yield 4.6 g (46%); ^{1}H NMR (300 MHz, $CDCl_3$, δ ppm) 3.93 (s, 9H, $COOCH_3$), 5.18 (s, 2H, OCH_2), 7.48 (t, J = 7.4 Hz, 1H, Ph), 7.64 (d, J = 6.9 Hz, 1H, Ph), 7.84 (s, 2H, Ph), 8.02 (d, J = 7.0 Hz, 1H, Ph), 8.13 (s, 1H, Ph), 8.30 (s, 1H, Ph); ^{13}C NMR ($CDCl_3$, δ ppm) 167.3 and 166.9 (C=O); 161.8, 142.1, 133.0, 131.4, 129.9, 129.3, 127.3, 127.2, 123.2 and 119.6 (Ar); 71.0 (OCH_2); 50.0 (CH_3); MS (M+1) 359. $C_{19}H_{18}O_7$ (358.3): calcd. C 63.58, H 5.06; found C 63.12 H 4.81 %.

5-(2-carboxybenzylboxy)isophthalic acid (**3a**)

4 (4 g, 11.2 mmol), ethanol (100 ml), deionised water (50 ml), and sodium hydroxide (2 g, 50 mmol) were added in a 250 ml round bottom flask. The solution was refluxed under 90 °C for 5 hours. After cooling down, conc. HCl was added drop by drop until the

pH was about 1. White solid obtained was filtered, washed with water. The solid was dried in vacuo. White solid. Yield: 3.3 g (94%); ^{1}H NMR (300 MHz, DMSO-d_6, δ ppm) 5.52 (s, 2H, OCH_2), 7.42 (t, *J* = 7.2 Hz, 1H, Ph), 7.57 (t, *J* = 7.4 Hz, 1H, Ph), 7.8 (m, 3H, Ph), 7.92 (d, *J* = 6.5 Hz, 1H, Ph), 8.09 (d, *J* = 7.6 Hz, 1H, Ph); ^{13}C NMR (DMSO-d_6, δ ppm) 172.4 and 172.0 (C=O), 161.8, 142.5, 133.9, 131.5, 130.3, 129.4, 127.3, 127.2, 124.0 and 120.9 (Ar); 71.0 (OCH_2); ESI-MS 315.4 (M-1). $C_{16}H_{12}O_7$ (316.3): calcd. C 60.76, H 3.82; found C 60.69 H 3.91 %.

5-(2-Carboxybenzyloxy)isophthalic acid (**3b**)

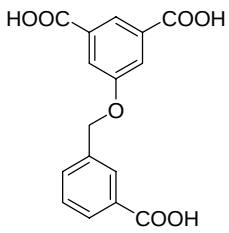

Procedure:

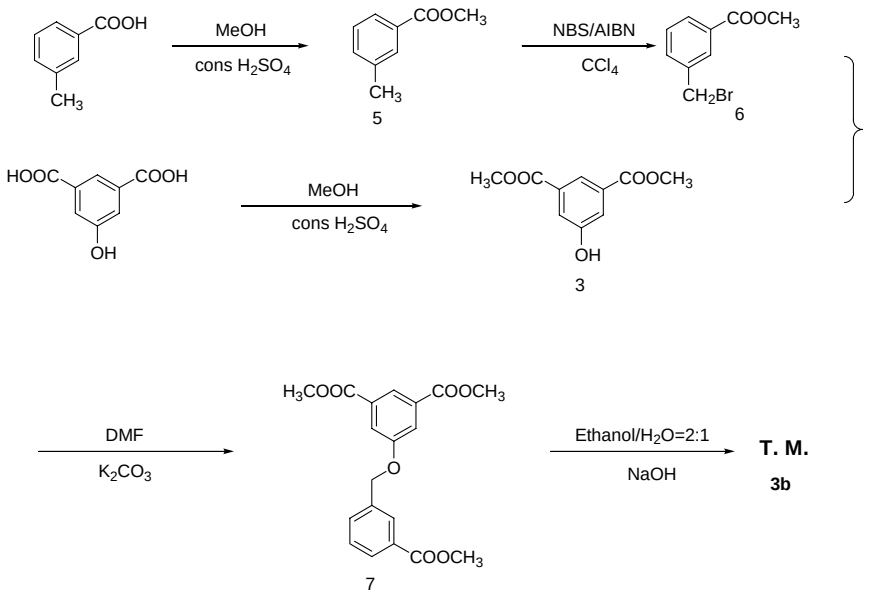

Scheme 4.2 Procedure for the preparation of triacid **3b**.

3-Methylbenzoic acid methyl ester (**5**)

3-Methylbenzoic acid (30 g, 0.22 mol), methanol (250 ml), and conc. H_2SO_4 (4 ml) were placed in a 500 ml round bottom flask. The solution was refluxed for 3 hours, after which the solvent was distilled under reduced pressure. The residue was dissolved in CH_2Cl_2 and water was used to wash the organic layer (3 x 100 ml) until the aqueous phase was neutral. The CH_2Cl_2 was distilled off under reduced pressure. A white solid was dried in vacuo. Yield: 33.5 g (100 %); ^{1}H NMR (300 MHz, $CDCl_3$, δ ppm) 2.39 (s, 3H, CH_3), 3.90 (s, 3H, $COOCH_3$), 7.34 (m, 2H, Ph), 7.83 (m, 2H, Ph); ^{13}C NMR ($CDCl_3$, δ ppm) 166.9 (C=O), 137.5, 133.5, 130.4, 128.3 and 126.7 (Ar); 49.9 (OCH_3); 20.9 (CH_3). MS (M+1) 151. $C_9H_{10}O_2$ (150.2): calcd. C 71.98, H 6.71; found C 71.53 H 6.97 %.

3-Bromomethylbenzoic acid methyl ester (**6**)

Compound **5** (14.43 g, 96.1 mmol), AIBN (200 mg, 1.2 mmol), NBS (17.13 g, 96.2 mmol), and CCl_4 (150 ml) were placed in 250 ml round bottom flask. The solution was refluxed at 80 °C for 1.5 hours. The solution was filtered, and distilled under reduced pressure. Orange oil was obtained which was recrystallised in hexane. Colorless crystalline solid was obtained. Yield: 18.7 g (85 %); ^{1}H NMR (300 MHz, $CDCl_3$, δ ppm) 3.92 (s, 3H, $COOCH_3$), 4.52 (t, *J* = 4.6 Hz, 2H, CH_2Br), 7.43 (t, *J* = 6.8 Hz, 1H, Ph), 7.59 (d, *J* = 7.3 Hz, 1H, Ph), 7.95 (d, *J* = 7.4 Hz, 1H, Ph), 8.09 (d, *J* = 7.6 Hz, 1H, Ph); ^{13}C NMR ($CDCl_3$, δ ppm) 167.3 (C=O), 137.9, 133.4, 130.8, 130.4, 129.9 and 128.7 (Ar), 50.0 (OCH_3); 38.4 (CH_2Br). MS (M+1) 230.

5-(3-Methoxycarbonylbenzyloxy)isophthalic acid dimethyl ester (**7**)

Compound **3** (5.82 g, 27.7 mmol), compound **6** (6.35 g, 27.7 mmol), DMF (150 ml), and anhydrous potassium carbonate (10 g, 178 mmol) were placed in 250 ml of round bottom flask. The solution was heated at 80 °C for 8 hours, after which the DMF was distilled off under reduced pressure. White solid was obtained by adding water, which was filtered and washed with methanol (3 x 10 ml). Yield 8.42 g (85%); ^{1}H NMR (300 MHz, $CDCl_3$, δ ppm) 3.92 (s, 9H, $COOCH_3$), 5.18 (s, 2H, OCH_2), 7.46 (t, *J* = 7.1 Hz, 1H, Ph), 7.62 (d, *J* = 7.3 Hz, 1H, Ph), 7.82 (s, 2H, Ph), 8.00 (d, *J* = 7.4 Hz, 1H, Ph), 8.11 (s, 1H, Ph), 8.28 (s, 1H, Ph); ^{13}C NMR ($CDCl_3$, δ ppm) 167.2 and 167.8 (C=O); 161.8, 140.8, 131.6, 131.4, 130.7, 128.6, 128.5, 123.2 and 119.6 (Ar); 77.8 (OCH_2); 50.0 and 49.7 (OCH_3); MS (M+1) 359.

5-(2-Carboxybenzylboxy)isophthalic acid (**3b**)

Compound **7** (8 g, 22.3 mmol), ethanol (100 ml), deionised water (50 ml), and sodium hydroxide (2 g, 50 mmol) were added into a 250 ml round bottom flask. The solution was refluxed below 90 °C for 5 hours. After the solution cooled down, Conc. hydrochloride was added drop by drop until the pH was about 1. A white solid appeared was distilled. Water was added again and the solid was filtered off and washed until the water was neutral. The white solid was dried in an oven. White solid. Yield: 6.64 g (94%); ^{1}H NMR (300 MHz, DMSO-d_6, δ ppm) 5.28 (s, 2H, OCH_2), 7.54 (t, J = 7.2 Hz, 1H, Ph), 7.13 (m, 3H, Ph), 7.89 (d, J = 7.1 Hz, 1H, Ph), 8.05 (m, 2H, Ph); ^{13}C NMR (DMSO-d_6, δ ppm) 172.7 and 172.1 (C=O); 161.8, 142.5, 133.9, 131.5, 130.3, 129.4, 127.3, 127.2, 124.0 and 120.9 (Ar); 76.4 (OCH_2); ESI-MS 315.4 (M-1). $C_{16}H_{12}O_7$ (316.3): calcd. C 60.76, H 3.82; found C 60.62 H 3.76 %.

1,3,5-Tris(3-carboxybenzyloxy)benzene (**3c**)

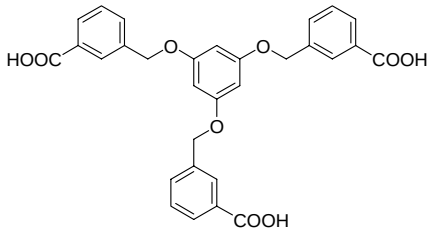

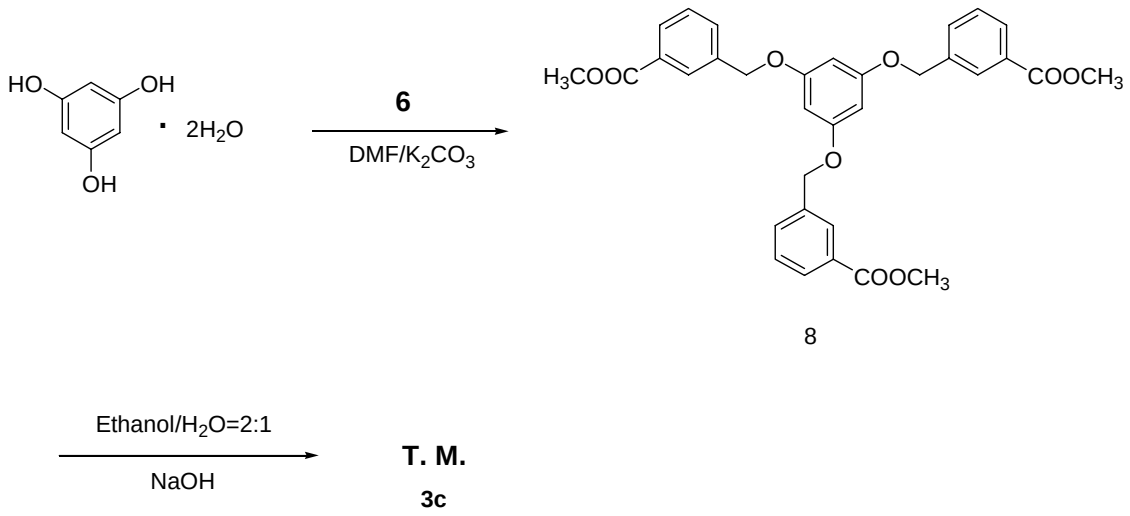

Scheme 4.3 Procedure for the synthesis of triacid **3c**.

1,3,5-Tris(3-Methoxylcarbonylbenyloxy)benzene (**8**)

Phloroglucinol dihydrate (1.5 g, 10.4 mmol), of **6** (6.4 g, 27.9 mmol), K_2CO_3 (10 g, 72 mmol), DMF (150 ml) were placed in 250 ml round bottom flask. The solution was heated at 80 °C for 5 hours and the solvent was distilled under reduced pressure. Water was added and after careful separation black oil was obtained which solidified overnight. The white solid was washed with methanol (3 x 10 ml). Yield: 1.0 g (19%); ^{1}H NMR (300 MHz, $CDCl_3$, δ ppm) 3.93 (s 9H, $COOCH_3$), 5.05 (s, 6H, OCH_2), 6.27 (s, 3H, Ph), 7.46 (t, *J* = 7.2 Hz, 3H, Ph), 7.62 (d, *J* = 7.4 Hz, 3H, Ph), 8.00 (d, *J* = 7.6 Hz, 3H, Ph), 8.10 (s, 3H, Ph); ^{13}C NMR ($CDCl_3$, δ ppm) 167.2 (C=O); 164.1, 140.8, 131.7, 130.7, 128.6, 128.5, 128.3 and 92.0 (Ar); 77.8 (OCH_2), 49.7 (CH_3); MS (M+1) 571.

1,3,5-Tris(3-carboxybenzoxyl)benzene (**3c**)

Compound **8** (1 g, 1.7 mmol), sodium hydroxide (0.5 g, 12.5 mmol), aqueous ethanol solution (90 ml, ethanol: H_2O = 2: 1) were added into a 150 ml round bottom flask. The solution was refluxed at 90 °C for 3 hours. When the solution was cooled down, the

solvent was distilled completely. Water was added to dissolve the residure and Conc. HCl to acidify the solution. A white solid formed which was filtered and washed with water until the washing was neutral. After drying, a white solid was obtained. (0.85 g, 91%) ^{1}H NMR (300 MHz, DMSO-d_6, δ ppm) 5.15 (s, 6H, OCH_2), 6.35 (s, 3H, Ph), 7.51 (t, J = 7.0 Hz, 3H, Ph), 7.67 (d, J = 7.4 Hz, 3H, Ph), 7.89 (d, J = 7.6 Hz, 3H, Ph); ^{13}C NMR (DMSO-d_6, δ ppm) 172.2 (C=O); 164.0, 140.8, 132.5, 130.8, 129.0, 128.9, 128.6 and 92.0 (Ar); 77.8 (OCH_2), ESI-MS 527 (M-1). $C_{30}H_{24}O_9$ (528.5): calcd. C 68.18, H 4.58; found C 67.73 H 4.47 %.

2,3-Di(3-carboxybenzyloxy)benzoic acid (**3d**)

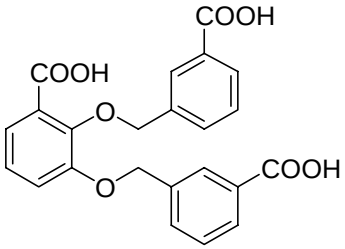

Procedure:

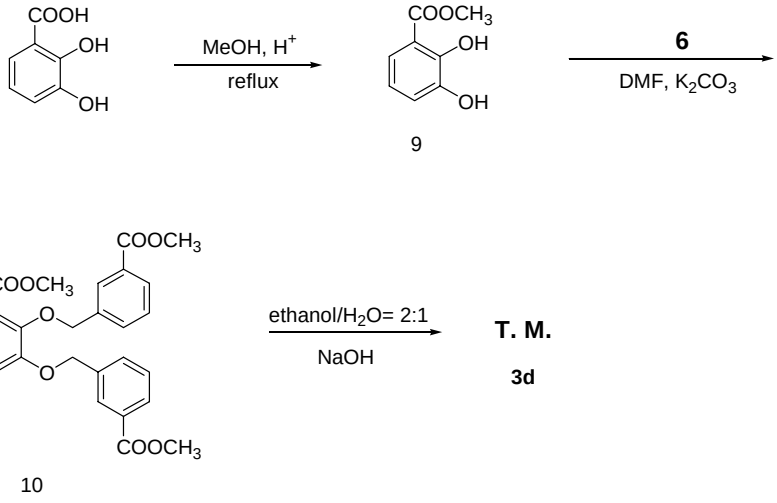

Scheme 4.4 Procedure for the synthesis of **3d**.

2,3-Dihydroxybenzoic acid methyl ester (**9**)

The procedure is same as for the preparation of **1**. 2,3-dihydroxy-benzoic acid (10 g, 59.5 mmol) gave a white solid **9 (**10.6 g, 97%) of; ^{1}H NMR (300 MHz, $CDCl_3$, δ ppm) 3.95 (s 3H, $COOCH_3$), 5. 70 (s, 1H, OH), 6.79 (t, *J* = 6.9 Hz, 1H, OH), 7.12 (d, *J* = 6.8 Hz, 1H, Ph), 7.37 (d, *J* = 7.0 Hz, 1H, Ph), 10.88 (s, 1H, Ph); ^{13}C NMR ($CDCl_3$, δ ppm) 167.3 (C=O); 145.7, 144.4, 123.7, 122.4, 121.4 and 119.1 (Ar); 49.9 (CH_3); MS (M+1) 169.

2,3-Bis(3-methoxycarbonylbenzyloxy)benzoic acid methyl ester(**10**)

The general procedure is same as for the preparation of **7**. Compound **9** (3 g, 17.8 mmol), compound **6** (8.15 g, 35.6 mmol) and DMF (150 ml) gave **10 (**2.3 g, 28%). ^{1}H NMR (300 MHz, $CDCl_3$, δ ppm) 3.89 (m, 9H, $COOCH_3$), 5.16 (m, 4H, OCH_2), 7.13 (m, 2H, Ph), 7.42 (m, 3H, Ph), 7.65 (t, *J* = 7.2 Hz, 2H, Ph), 8.10 (t, *J* = 7.4 Hz, 2H, Ph), 8.10 (s, 2H, Ph); ^{13}C NMR ($CDCl_3$, δ ppm) 167.3 (C=O); 167.2, 169.8, 148.8, 147.5, 140.9, 140.7, 131.8, 131.6, 130.7, 130.4, 128.7, 128.7, 128.6, 128.5, 128.5, 128.4, 123.0, 121.7, 119.4 and 117.1 (Ar); 78.3 and 78.1 (OCH_2), 50.1, 49.9 and 49.8 (CH_3); MS (M+1) 465.

2,3-Bis(3-Carboxybenzyloxy)benzoic acid (**3d**)

The procedure is same as that for **3a**. Compound **10** (2.2 g, 4.7 mmol) gave white solid of **3d** (1.78 g, 89%). ^{1}H NMR (300 MHz, DMSO-d_6, δ ppm) 5.08 (s, 2H, OCH_2), 5.28 (s, 2H, OCH_2), 7.17 (t, *J* = 7.6 Hz, 1H, Ph), 7.25-7.50 (m, 4H, Ph), 7.64 (d, *J* = 7.2 Hz, 2H, Ph), 7.70 (d, *J* = 7.1 Hz, 2H, Ph), 7.90 (t, *J* = 6.8 Hz, 2H, Ph), 8.07 (d, *J* = 7.3 Hz, 2H, Ph); ^{13}C NMR (DMSO-d_6, δ ppm) 172.0 (C=O); 149.2, 147.5, 140.8, 132.5, 130.8, 129.0,

128.9, 128.6, 123.4, 121.7, 120.3 and 117.2 (Ar); 78.0 and 78.7 (OCH_2); ESI-MS 420.9 (M-1). $C_{23}H_{18}O_8$ (422.4): calcd. C 65.40 H 4.30; found C 65.01 H 4.16 %.

3,4-Bis(3-carboxybenzyloxy)benzoic acid (**3e**)

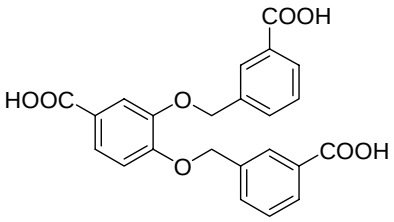

Procedure:

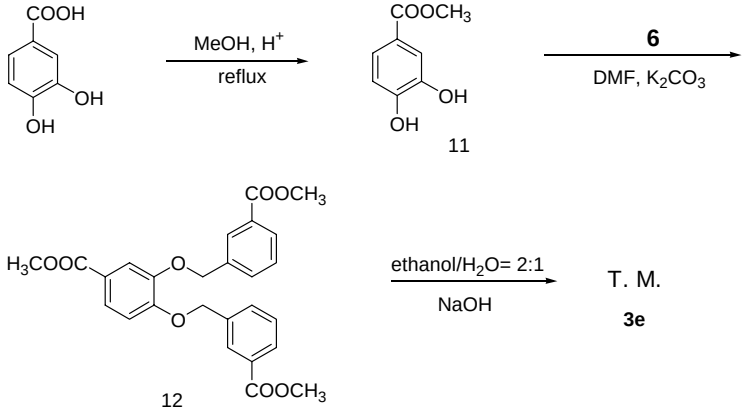

Scheme 4.5 Procedure for the synthesis of triacid **3e**.

3,4-Dihydroxybenzoic acid methyl ester (**11**)

The general procedure is same as that for **1**. 3,4-dihydroxy-benzoic acid (9.4 g, 61.0 mmol) gave white solid of **11** (10.02 g, 98 %). ^{1}H NMR (300 MHz, $CDCl_3$, δ ppm) 3.90 (s, 3H, $COOCH_3$), 6.02 (s, 1H, OH), 6.16 (s, 1H, OH), 6.92 (d, *J* = 7.2 Hz, 1H, Ph), 7.57 (d, *J* = 6.8 Hz, 1H, Ph), 7.66 (d, *J* = 6.9 Hz, 1H, Ph); ^{13}C NMR ($CDCl_3$, δ ppm) 167.3 (C=O), 148.8, 144.4, 124.5, 123.7, 118.3 and 117.0 (Ar); 49.8 (CH_3); MS (M+1) 169.

3,4-Bis(3-methoxycarbonylbenzyloxy)benzoic acid methyl ester (**12**)

The general procedure is the same as that for **7**. **11 (**2.70 g, 16.1 mmol), **6** (7.80 g, 34.1 mmol) gave white solid of **12** (6.2 g, 83 %). ^{1}H NMR (300 MHz, $CDCl_3$, δ ppm) 3.87 (s, 3H, $COOCH_3$), 3.90 (s, 6H, $COOCH_3$), 5.22 (s, 2H, OCH_2), 5.24 (s, 2H, OCH_2), 6.94 (d, *J* = 4.8 Hz, 1H, Ph), 7.45 (d, *J* = 6.8 Hz, 2H, Ph), 7.64-7.70 (m, 4H, Ph), 7.99 (d, *J* = 7.2 Hz, 2H, Ph), 8.13 (d, *J* = 7.3 Hz, 2H, Ph); ^{13}C NMR ($CDCl_3$, δ ppm) 167.3, 167.2 and 167.0 (C=O); 151.9, 147.5, 140.8, 140.7, 131.7, 131.6, 130.7, 130.6, 128.7, 128.6, 128.6, 128.5, 128.5, 128.4, 123.8 and 116.3 (Ar); 78.2 and 78.1 (OCH_2); 50.1, 49.9 and 49.8 (CH_3). MS (M+1) 465.

3,4-Bis(3-Carboxybenzyloxy)benzoic acid (**3e**)

The general procedure is the same as that for **3a**. Compound **12** (6 g, 12.9 mmol) gave white solid of **3e** (5.19 g, 95%). ^{1}H NMR (300 MHz, DMSO-d_6, δ ppm) 5.28 (s, 2H, OCH_2), 5.32 (s, 2H, OCH_2), 7.20 (d, *J* = 6.8 Hz, 1H, Ph), 7.50-7.59 (m, 4H, Ph), 7.73 (d, *J* = 6.9 Hz, 2H, Ph), 7.90 (d, *J* = 7.2 Hz, 2H, Ph), 7.90 (t, *J* = 6.9 Hz, 2H, Ph), 8.08 (d, *J* = 7.6 Hz, 2H, Ph); ^{13}C NMR (DMSO-d_6, δ ppm) 172.9, 172.5 and 172.3 (C=O); 152.8, 147.5, 140.8, 132.5, 130.8, 129.0, 128.9, 128.6, 123.9, 123.4, 116.7 and 115.0 (Ar); 78.1 (OCH_2); ESI-MS 420.9 (M-1). $C_{23}H_{18}O_8$ (422.4): calcd. C 65.40 H 4.30; found C 65.22 H 4.39 %.

2,3-Bis(2-carboxybenzyloxy)benzoic acid (**3f**)

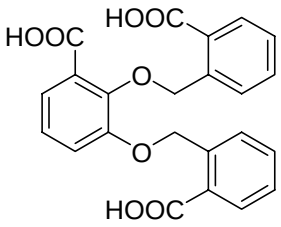

Procedure:

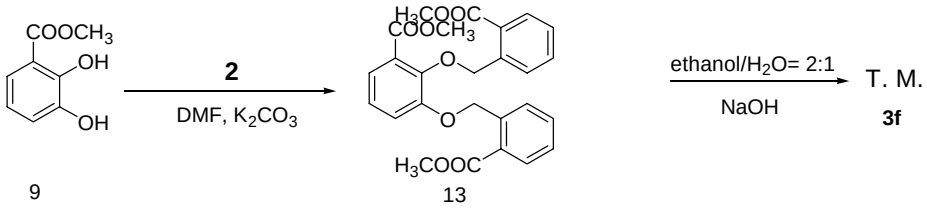

Scheme 4.6 Procedure for the synthesis of triacid **3f**

2,3-Bis(2-methoxycarbonylbenzyloxy)benzoic acid methyl ester (**13**)

The general procedure is the same as that for **4**. Compound **9** (1.67 g, 9.9 mmol) and compound **2** (4.56 g, 19.9 mmol) gave a white solid of **13** (2.23 g, 48%). ^{1}H NMR (300 MHz, DMSO-d_6, δ ppm) 3.40, and 3.38 (s, 9H, $COOCH_3$); 5.52 (s, 2H, OCH_2), 7.42 (t, *J* = 7.1 Hz, 1H, Ph), 7.57 (t, *J* = 6.9 Hz, 1H, Ph), 7.8 (m, 3H, Ph), 7.92 (d, *J* = 7.4 Hz, 1H, Ph), 8.09 (d, *J* = 7.5 Hz, 1H, Ph); ^{13}C NMR (DMSO-d_6, δ ppm) 167.3, 167.2 and 167.0 (C=O); 148.8, 147.5, 142.1, 142.0, 133.1, 133.0, 129.9, 129.8, 129.3, 129.2, 127.3, 127.2, 127.2, 127.1, 123.0, 121.7, 119.4 and 117.1 (Ar); 71.2 and 71.3 (OCH_2); 50.2, 50.1 and 49.9 (CH_3). MS (M+1) 465.

2,3-Bis(2-carboxybenzoxyl)benzoic acid (**3f**)

The general procedure is the same as that for **3a**. **13** (2 g, 4.3 mmol) gave a white solid of **3f** (1.45 g, 80%). ^{1}H NMR (300 MHz, DMSO-d_6, δ ppm) 5.54 (s, 2H, OCH_2), 5.59 (s, 2H, OCH_2), 7.10 (d, *J* = 6.9 Hz, 1H, Ph), 7.43-7.64 (m, 6H, Ph), 7.79 (t, *J* = 7.0 Hz, 2H,

Ph), 7.97 (d, *J* = 6.8 Hz, 2H, Ph); ^{13}C NMR (DMSO-d_6, δ ppm) 172.9, 172.3 and 172.0 (C=O); 147.8, 146.4, 142.5, 140.8, 133.9, 132.5, 130.8, 130.3, 129.4, 129.0, 128.9, 128.6, 127.5, 127.3, 127.2, 122.0, 120.6 and 114.0 (Ar); 78.1 and 77.7 (OCH_2), ESI-MS 420.9 (M-1). $C_{23}H_{18}O_8$ (422.4): calcd. C 65.40 H 4.30; found C 64.67 H 4.43 %.

3,4-Bis (2-carboxybenzyloxy)benzoic acid (**3g**)

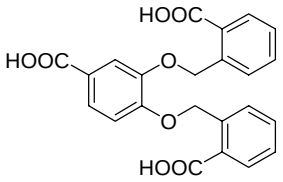

Procedure:

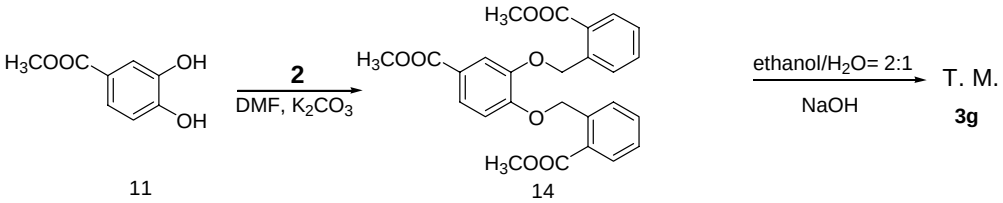

Scheme 4.7 Procedure for the synthesis of **3g**.

3,4-Bis(2-methylcarbonylbenzyloxy)benzoic acid methyl ester (**14**)

The general procedure is the same as that for **4**. Compound **11** (1.02 g, 6.1 mmol), compound **2** (2.78 g, 12.1 mmol) gave a white solid of **14** (1.76 g, 62%). ^{1}H NMR (300 MHz, $CDCl_3$, δ ppm) 3.89 (s, 3H, $COOCH_3$), 3.90 (s, 6H, $COOCH_3$), 5.63 (s, 2H, OCH_2), 5.64 (s, 2H, OCH_2), 6.99 (d, *J* = 6.2 Hz, 1H, Ph), 7.38 (t, *J* = 6.5 Hz, 2H, Ph), 7.55 (m, 2H, Ph), 7.67 (m, 2H, Ph), 7.88 (t, *J* = 6.3 Hz, 2H, Ph), 8.04 (d, *J* = 7.0 Hz, 2H, Ph); ^{13}C NMR ($CDCl_3$, δ ppm) 167.3, 167.2 and 167.0 (C=O), 152.0, 147.5, 142.2, 142.1, 133.1, 133.0,

129.9, 129.8, 129.4, 129.3, 127.4, 127.3, 127.2, 127.1, 123.8, 123.1, 116.3 and 115.0 (Ar), 71.3 and 71.2 (OCH_2); 50.1, 50.0 and 49.9 (CH_3); MS (M+1) 465.

3,4-Bis(2-carboxybenzyloxy)benzoic acid (**3g**)

The general procedure is the same as that for **3a**. **14** (1.7 g, 3.7 mmol) gave a white solid of **3g** (1.45 g, 94%). ^{1}H NMR (300 MHz, DMSO-d_6, δ ppm) 5.47 (s, 2H, OCH_2), 5.50 (s, 2H, OCH_2), 7.16-7.29 (m, 3H, Ph), 7.35-7.49 (m, 3H, Ph), 7.51 (d, J = 6.8 Hz, 1H, Ph), 7.60 (t, J = 7.2 Hz, 1H, Ph), 7.90-7.99 (m, 3H, Ph); ^{13}C NMR (DMSO-d_6, δ ppm) 172.7, 172.2 and 172.0 (C=O); 152.8, 147.5, 142.5, 140.8, 133.9, 132.5, 130.8, 130.3, 129.4, 129.0, 128.9, 128.6, 127.3, 127.2, 123.9, 123.4, 116.7 and 115.0 (Ar); 78.1 and 71.3 (OCH_2). $C_{23}H_{18}O_8$ (422.4): cacld. C 65.40 H 4.30; found C 65.26 H 4.34 %.

4.5 Reference

[1] S. Komarneni, D. M. Smith, J. S. Beck (eds) *Advances in Porous Materials*, Materials Research Scociety, Pittsburgh, **1995**.

[2] W. Holderich, M. Hesse, F. Naumann, *Angew Chem, Int. Ed. Engl*., **1998**, 27, 226.

[3] a) D. Venkataraman, S. Lee, M. S. Moore, P. Zhang, K. A. Hirsch, G. B. Gardner, A. C. Covery, C. L. Prentice, *Chem. Mater*. **1996**, 8, 2030; b) O. M. Yaghi In *Acess in Nanoporous Materials*, T. J. Pinnavaia, M. F. Thorpe, Eds., Plenum, New York, **1995**, p111; c) A. Stein, S. W. Keller, T. E. Mallouk, *Science*, 1993, 259, 1558; d) P. J. Fagan, M. D. Ward, *Sci. Am*., **1992**, 267, 48; e) *Supramolecular Architecture: Synthetic Control in Thin Films and Solids*, T. Bein Ed., ACS Symposium Series 499, American Chemical Society, Washington DC, **1992**; f) T.

Iwamoto, *Inclusion Compounds*, J. L. Atwood, J. E. D. Davies, D. D. MacNicol, Eds., Oxford, New York, **1991**, Vol. 5, 177.

[4] O. M. Yaghi, G. Li, H. Li, *Nature*, **1995**, 378, 703.

[5] a) H. Li, M. Eddaoudi, T. L. Groy, O. M. Yaghi, *J. Am. Chem. Soc*. **1998**, 120, 8571. b) T. M. Reineke, M. Eddaoudi, M. O'Keeffe, O. M. Yaghi, *Angew Chem. Int. Ed*. **1999**, 38, 2590.

[6] SMART & SAINT Software Reference Manuals, Version 4.0, Siemens Energy & Automation, Inc., Analytical Instrumentation, Madison, Wisconsin, USA, **1996**.

[7] G.M. Sheldrick, SADABS, software for empirical absorption correction, University of Gottingen, Gottingen, Germany, **1996**.

[8] SHELXTL Reference Manual, Version 5.03, Siemens Energy & Automation Inc., Analytical Instrumentation, Madison, Wisconsin, USA, **1996**.

Appendix – Bond Parameters

Bond parameters for **1**:

O1 C1 1.240(2)
O2 C1 1.306(2)
O3 C9 1.381(2)
O3 C8 1.430(2)
C1 C2 1.482(3)
C2 C3 1.403(2)
C2 C7 1.408(3)
C3 C4 1.375(3)
C4 C5 1.376(3)
C5 C6 1.392(3)
C6 C7 1.387(3)
C7 C8 1.519(2)
C9 C10 1.383(3)
C9 C11 1.389(3)
C10 C11 1.393(2)
C11 C9 1.389(3)

C9 O3 C8 117.16(14)
O1 C1 O2 121.53(18)
O1 C1 C2 123.16(17)
O2 C1 C2 115.32(16)
C3 C2 C7 119.49(17)
C3 C2 C1 117.54(17)
C7 C2 C1 122.96(15)
C4 C3 C2 121.32(19)
C3 C4 C5 119.24(18)
C4 C5 C6 120.4(2)
C7 C6 C5 121.45(19)
C6 C7 C2 118.10(16)
C6 C7 C8 119.58(17)
C2 C7 C8 122.28(16)
O3 C8 C7 108.08(15)
O3 C9 C10 116.01(16)
O3 C9 C11 124.54(16)
C10 C9 C11 119.44(16)
C9 C10 C11 121.09(17)
C9 C11 C10 119.46(18)

Bond parameters for **2**:

O1 C1 1.234(2)
O2 C1 1.298(2)
O3 C9 1.366(2)
O3 C8 1.4235(19)
O4 C14 1.377(2)
O4 C15 1.4340(19)
O5 C22 1.223(2)
O6 C22 1.301(2)
C1 C2 1.484(2)
C2 C3 1.390(3)
C2 C7 1.416(2)
C3 C4 1.383(3)
C4 C5 1.381(3)
C5 C6 1.378(3)
C6 C7 1.398(2)
C7 C8 1.506(3)
C9 C10 1.382(3)
C9 C14 1.403(2)
C10 C11 1.386(3)
C11 C12 1.367(3)
C12 C13 1.391(3)
C13 C14 1.375(2)
C15 C16 1.519(2)
C16 C17 1.389(2)
C16 C21 1.410(2)
C17 C18 1.383(3)
C18 C19 1.375(3)
C19 C20 1.375(3)
C20 C21 1.396(3)
C21 C22 1.481(2)

C9 O3 C8 118.79(14)
C14 O4 C15 117.48(13)
O1 C1 O2 122.62(17)
O1 C1 C2 122.36(15)
O2 C1 C2 115.02(17)
C3 C2 C7 119.89(16)
C3 C2 C1 118.37(16)
C7 C2 C1 121.75(16)
C4 C3 C2 121.24(19)
C5 C4 C3 119.1(2)
C6 C5 C4 120.62(18)
C5 C6 C7 121.55(18)
C6 C7 C2 117.58(17)
C6 C7 C8 119.95(15)
C2 C7 C8 122.47(15)
O3 C8 C7 106.96(14)
O3 C9 C10 126.35(15)
O3 C9 C14 113.83(15)
C10 C9 C14 119.82(16)
C9 C10 C11 120.06(18)
C12 C11 C10 119.96(19)
C11 C12 C13 120.65(19)
C14 C13 C12 119.94(18)
C13 C14 O4 125.74(15)
C13 C14 C9 119.56(16)
O4 C14 C9 114.69(14)
O4 C15 C16 112.32(14)
C17 C16 C21 117.84(16)
C17 C16 C15 119.71(15)
C21 C16 C15 122.44(14)
C18 C17 C16 121.53(18)
C19 C18 C17 120.29(19)
C18 C19 C20 119.7(2)
C19 C20 C21 120.81(18)
C20 C21 C16 119.84(16)
C20 C21 C22 119.25(15)
C16 C21 C22 120.84(15)
O5 C22 O6 122.11(16)
O5 C22 C21 123.00(15)
O6 C22 C21 114.87(16)

Bond parameters for **1·bipy**:

O1 C6 1.318(3)
O2 C6 1.207(3)
O3 C14 1.373(3)
O3 C13 1.425(2)
N1 C1 1.322(3)
N1 C5 1.322(3)
C1 C2 1.371(3)
C2 C3 1.371(3)
C3 C4 1.379(3)
C3 C3 1.488(4)
C4 C5 1.371(3)
C6 C7 1.490(3)
C7 C8 1.392(3)
C7 C12 1.409(3)
C8 C9 1.377(3)
C9 C10 1.368(3)
C10 C11 1.379(3)
C11 C12 1.386(3)
C12 C13 1.507(3)
C14 C15 1.381(3)
C14 C16 1.381(3)
C15 C16 1.380(3)
C16 C14 1.381(3)

C14 O3 C13 117.61(17)
C1 N1 C5 116.0(2)
N1 C1 C2 124.2(2)
C1 C2 C3 120.1(2)
C2 C3 C4 115.7(2)
C2 C3 C3 122.2(2)
C4 C3 C3 122.1(2)
C5 C4 C3 120.6(2)
N1 C5 C4 123.4(2)
O2 C6 O1 121.8(2)
O2 C6 C7 124.6(2)
O1 C6 C7 113.6(2)
C8 C7 C12 119.39(19)
C8 C7 C6 119.00(19)
C12 C7 C6 121.61(19)
C9 C8 C7 121.2(2)
C10 C9 C8 119.5(2)
C9 C10 C11 120.2(2)
C10 C11 C12 121.7(2)
C11 C12 C7 117.9(2)
C11 C12 C13 120.50(18)
C7 C12 C13 121.54(18)
O3 C13 C12 108.09(17)
O3 C14 C15 125.25(19)
O3 C14 C16 115.5(2)
C15 C14 C16 119.2(2)
C16 C15 C14 120.0(2)
C15 C16 C14 120.8(2)

Bond parameters for **1·dipet**:

O1 C7 1.302(4)
O2 C7 1.212(4)
O3 C15 1.382(4)
O3 C14 1.436(4)
N1 C5 1.326(5)
N1 C1 1.343(5)
C1 C2 1.355(6)
C2 C3 1.366(7)
C3 C4 1.385(8)
C3 C6 1.464(6)
C4 C5 1.392(6)
C6 C6 1.109(12)
C7 C8 1.501(4)
C8 C13 1.397(5)
C8 C9 1.401(5)
C9 C10 1.371(5)
C10 C11 1.381(6)
C11 C12 1.384(6)
C12 C13 1.394(5)
C13 C14 1.505(5)
C15 C17 1.377(5)
C15 C16 1.391(5)
C16 C17 1.389(5)
C17 C15 1.377(5)

C15 O3 C14 116.8(3)
C5 N1 C1 116.9(3)
N1 C1 C2 123.6(4)
C1 C2 C3 120.5(4)
C2 C3 C4 116.8(4)
C2 C3 C6 118.9(5)
C4 C3 C6 124.4(5)
C3 C4 C5 119.9(4)
N1 C5 C4 122.3(4)
C6 C6 C3 138.3(12)
O2 C7 O1 124.1(3)
O2 C7 C8 123.3(3)
O1 C7 C8 112.5(3)
C13 C8 C9 119.3(3)
C13 C8 C7 122.8(3)
C9 C8 C7 117.9(3)
C10 C9 C8 121.4(4)
C9 C10 C11 119.4(3)
C10 C11 C12 120.1(3)
C11 C12 C13 121.2(4)
C12 C13 C8 118.5(3)
C12 C13 C14 117.5(3)
C8 C13 C14 124.0(3)
O3 C14 C13 106.6(3)
C17 C15 O3 124.9(3)
C17 C15 C16 119.7(3)
O3 C15 C16 115.4(3)
C17 C16 C15 120.7(3)
C15 C17 C16 119.5(3)

Bond parameters for **3·bipy**:

O1 C6 1.317(3)
O2 C6 1.201(3)
O3 C14 1.355(3)
O3 C13 1.423(3)
N1 C1 1.298(4)
N1 C5 1.310(4)
C1 C2 1.389(4)
C2 C3 1.350(4)
C3 C4 1.366(4)
C3 C3 1.503(5)
C4 C5 1.375(4)
C6 C7 1.507(3)
C7 C8 1.380(3)
C7 C12 1.396(3)
C8 C9 1.393(4)
C9 C10 1.369(4)
C10 C11 1.387(4)
C11 C12 1.404(4)
C12 C13 1.494(3)
C14 C19 1.374(4)
C14 C15 1.385(4)
C15 C16 1.376(4)
C16 C17 1.400(3)
C17 C18 1.388(4)
C17 C17 1.477(5)
C18 C19 1.364(4)

C14 O3 C13 118.1(2)
C1 N1 C5 116.6(2)
N1 C1 C2 122.9(3)
C3 C2 C1 120.6(3)
C2 C3 C4 116.3(2)
C2 C3 C3 122.6(3)
C4 C3 C3 121.1(3)
C3 C4 C5 119.3(3)
N1 C5 C4 124.2(3)
O2 C6 O1 122.1(2)
O2 C6 C7 124.4(2)
O1 C6 C7 113.5(2)
C8 C7 C12 120.7(2)
C8 C7 C6 118.3(2)
C12 C7 C6 120.9(2)
C7 C8 C9 121.0(3)
C10 C9 C8 118.8(2)
C9 C10 C11 120.9(2)
C10 C11 C12 120.9(3)
C7 C12 C11 117.7(2)
C7 C12 C13 122.5(2)
C11 C12 C13 119.8(2)
O3 C13 C12 108.6(2)
O3 C14 C19 116.8(2)
O3 C14 C15 125.6(2)
C19 C14 C15 117.6(2)
C16 C15 C14 120.6(2)
C15 C16 C17 122.4(2)
C18 C17 C16 115.3(2)
C18 C17 C17 122.9(3)
C16 C17 C17 121.8(3)
C19 C18 C17 122.5(2)
C18 C19 C14 121.7(3)

Bond parameters for **4·bipy**:

N1 C5 1.330(3)	C5 N1 C1 116.2(2)
N1 C1 1.335(3)	N1 C1 C2 123.1(3)
C1 C2 1.369(4)	C1 C2 C3 121.0(2)
C2 C3 1.394(3)	C4 C3 C2 115.2(2)
C3 C4 1.388(3)	C4 C3 C8 121.9(2)
C3 C8 1.483(4)	C2 C3 C8 122.9(2)
C4 C5 1.369(4)	C5 C4 C3 120.2(2)
N2 C10 1.324(3)	N1 C5 C4 124.2(3)
N2 C6 1.338(4)	C10 N2 C6 116.0(2)
C6 C7 1.375(4)	N2 C6 C7 123.7(3)
C7 C8 1.387(3)	C6 C7 C8 120.3(3)
C8 C9 1.396(3)	C7 C8 C9 115.7(2)
C9 C10 1.375(4)	C7 C8 C3 122.6(2)
N3 C11 1.332(3)	C9 C8 C3 121.7(2)
N3 C15 1.334(3)	C10 C9 C8 119.8(2)
C11 C12 1.366(4)	N2 C10 C9 124.3(3)
C12 C13 1.388(3)	C11 N3 C15 116.0(2)
C13 C14 1.390(3)	N3 C11 C12 124.3(2)
C13 C18 1.494(3)	C11 C12 C13 120.1(2)
C14 C15 1.372(4)	C12 C13 C14 115.5(2)
N4 C20 1.332(3)	C12 C13 C18 121.8(2)
N4 C16 1.337(3)	C14 C13 C18 122.7(2)
C16 C17 1.368(4)	C15 C14 C13 120.7(2)
C17 C18 1.399(3)	N3 C15 C14 123.3(2)
C18 C19 1.392(3)	C20 N4 C16 116.4(2)
C19 C20 1.373(4)	N4 C16 C17 123.9(3)
C21 O2 1.216(3)	C16 C17 C18 120.1(2)
C21 O1 1.311(3)	C19 C18 C17 115.4(2)
C21 C22 1.474(4)	C19 C18 C13 122.4(2)
C22 C23 1.391(3)	C17 C18 C13 122.2(2)
C22 C27 1.407(3)	C20 C19 C18 120.7(2)
C23 C24 1.385(3)	N4 C20 C19 123.4(3)
C24 C25 1.395(3)	O2 C21 O1 121.9(3)
C25 O3 1.367(3)	O2 C21 C22 123.2(2)
C25 C26 1.390(3)	O1 C21 C22 114.9(2)
C26 C27 1.370(4)	C23 C22 C27 117.7(2)
C28 O3 1.444(3)	C23 C22 C21 120.4(2)
C28 C29 1.501(3)	C27 C22 C21 121.8(2)
C29 C30 1.399(3)	C24 C23 C22 121.8(2)
C29 C34 1.408(3)	C23 C24 C25 119.3(2)
C30 C31 1.385(4)	O3 C25 C26 115.8(2)
C31 C32 1.376(4)	O3 C25 C24 124.5(2)
C32 C33 1.385(4)	C26 C25 C24 119.7(2)
C33 C34 1.402(3)	C27 C26 C25 120.4(2)

Bond parameters for **4·bipy**: (continued)

C34 C35 1.496(3)
C35 O5 1.208(3)
C35 O4 1.319(3)
O6 C36 1.317(3)
O7 C36 1.219(3)
C36 C37 1.475(4)
C37 C38 1.392(3)
C37 C42 1.410(3)
C38 C39 1.388(4)
C39 C40 1.394(3)
C40 O8 1.361(3)
C40 C41 1.390(3)
C41 C42 1.372(3)
O8 C43 1.442(3)
C43 C44 1.496(3)
C44 C45 1.396(4)
C44 C49 1.408(3)
C45 C46 1.384(4)
C46 C47 1.371(4)
C47 C48 1.382(4)
C48 C49 1.403(4)
C49 C50 1.498(4)
C50 O10 1.202(3)
C50 O9 1.307(3)

C26 C27 C22 121.1(2)
O3 C28 C29 106.55(18)
C25 O3 C28 118.10(18)
C30 C29 C34 118.6(2)
C30 C29 C28 116.9(2)
C34 C29 C28 124.4(2)
C31 C30 C29 121.5(3)
C32 C31 C30 119.9(3)
C31 C32 C33 119.8(3)
C32 C33 C34 121.2(3)
C33 C34 C29 119.0(2)
C33 C34 C35 118.4(2)
C29 C34 C35 122.6(2)
O5 C35 O4 122.4(2)
O5 C35 C34 124.8(2)
O4 C35 C34 112.8(2)
O7 C36 O6 122.7(2)
O7 C36 C37 123.0(2)
O6 C36 C37 114.4(2)
C38 C37 C42 117.6(2)
C38 C37 C36 120.3(2)
C42 C37 C36 122.1(2)
C39 C38 C37 121.7(2)
C38 C39 C40 119.4(2)
O8 C40 C41 115.6(2)
O8 C40 C39 124.7(2)
C41 C40 C39 119.7(2)
C42 C41 C40 120.3(2)
C41 C42 C37 121.2(2)
C40 O8 C43 118.58(17)
O8 C43 C44 106.27(18)
C45 C44 C49 118.4(2)
C45 C44 C43 117.5(2)
C49 C44 C43 124.1(2)
C46 C45 C44 121.9(3)
C47 C46 C45 119.3(3)
C46 C47 C48 120.5(3)
C47 C48 C49 120.9(3)
C48 C49 C44 119.0(2)
C48 C49 C50 118.4(2)
C44 C49 C50 122.7(2)
O10 C50 O9 122.5(3)
O10 C50 C49 124.1(2)
O9 C50 C49 113.3(2)

Bond parameters for **TMA•1/2THB**:

C1A C2A 1.3942(15)
C1A C6A 1.3943(15)
C1A C7A 1.4887(15)
C2A C3A 1.3923(15)
C3A C4A 1.3949(15)
C3A C8A 1.4881(15)
C4A C5A 1.3915(15)
C5A C6A 1.3937(15)
C5A C9A 1.4891(15)
C7A O1A 1.2164(14)
C7A O2A 1.3183(14)
C8A O3A 1.2159(14)
C8A O4A 1.3163(14)
C9A O5A 1.2167(14)
C9A O6A 1.3143(14)
C10A O7A 1.3778(13)
C10A C11A 1.3867(16)
C10A C15A 1.3897(15)
C11A C12A 1.3892(15)
C12A O8A 1.3760(13)
C12A C13A 1.3885(15)
C13A C14A 1.3884(16)
C14A O9A 1.3757(13)
C14A C15A 1.3869(15)
C1B C2B 1.3944(15)
C1B C6B 1.3989(15)
C1B C7B 1.4915(15)
C2B C3B 1.3957(15)
C3B C4B 1.3933(15)
C3B C8B 1.4956(15)
C4B C5B 1.3976(15)
C5B C6B 1.3917(15)
C5B C9B 1.4934(16)
C7B O1B 1.2057(15)
C7B O2B 1.3162(14)
C8B O3B 1.2037(15)
C8B O4B 1.3154(14)
C9B O5B 1.2021(15)
C9B O6B 1.3084(15)

C2A C1A C6A 119.99(10)
C2A C1A C7A 120.75(10)
C6A C1A C7A 119.25(10)
C3A C2A C1A 120.04(10)
C2A C3A C4A 119.96(10)
C2A C3A C8A 119.37(10)
C4A C3A C8A 120.67(10)
C5A C4A C3A 120.01(10)
C4A C5A C6A 120.09(10)
C4A C5A C9A 119.23(10)
C6A C5A C9A 120.68(10)
C5A C6A C1A 119.91(10)
O1A C7A O2A 122.76(10)
O1A C7A C1A 124.46(10)
O2A C7A C1A 112.78(10)
O3A C8A O4A 122.73(11)
O3A C8A C3A 124.17(10)
O4A C8A C3A 113.11(10)
O5A C9A O6A 122.83(11)
O5A C9A C5A 124.28(11)
O6A C9A C5A 112.89(10)
O7A C10A C11A 116.95(10)
O7A C10A C15A 120.65(10)
C11A C10A C15A 122.41(10)
C10A C11A C12A 117.56(10)
O8A C12A C13A 116.97(10)
O8A C12A C11A 120.67(10)
C13A C12A C11A 122.36(10)
C14A C13A C12A 117.69(10)
O9A C14A C15A 117.20(10)
O9A C14A C13A 120.51(10)
C15A C14A C13A 122.28(10)
C14A C15A C10A 117.68(10)
C2B C1B C6B 119.96(10)
C2B C1B C7B 121.59(10)
C6B C1B C7B 118.45(10)
C1B C2B C3B 119.98(10)
C4B C3B C2B 120.17(10)
C4B C3B C8B 121.52(10)
C2B C3B C8B 118.31(10)
C3B C4B C5B 119.75(10)
C6B C5B C4B 120.27(10)
C6B C5B C9B 121.31(10)
C4B C5B C9B 118.43(10)

Bond parameters for **TMA•1/2THB**: (continued)

C5B C6B C1B 119.87(10)
O1B C7B O2B 123.55(11)
O1B C7B C1B 123.21(11)
O2B C7B C1B 113.24(10)
O3B C8B O4B 123.78(11)
O3B C8B C3B 122.82(11)
O4B C8B C3B 113.39(10)
O5B C9B O6B 123.42(12)
O5B C9B C5B 122.98(11)
O6B C9B C5B 113.60(10)

Bond parameters for **CA•ddpy**:

S1 C3 1.7781(16)
S1 S1 2.0341(8)
O1 C6 1.222(2)
O2 C7 1.214(3)
N1 C5 1.337(2)
N1 C1 1.344(2)
N2 C6 1.3718(17)
N2 C6 1.3718(17)
N3 C6 1.376(2)
N3 C7 1.3758(17)
C1 C2 1.391(2)
C2 C3 1.390(2)
C3 C4 1.388(2)
C4 C5 1.397(2)
C7 N3 1.3758(17)

C3 S1 S1 105.55(5)
C5 N1 C1 117.24(15)
C6 N2 C6 125.26(19)
C6 N3 C7 125.14(15)
N1 C1 C2 123.33(16)
C3 C2 C1 118.65(15)
C4 C3 C2 118.83(15)
C4 C3 S1 125.41(12)
C2 C3 S1 115.74(12)
C3 C4 C5 118.25(15)
N1 C5 C4 123.68(15)
O1 C6 N2 122.74(16)
O1 C6 N3 122.38(15)
N2 C6 N3 114.88(15)
O2 C7 N3 122.65(9)
O2 C7 N3 122.65(9)
N3 C7 N3 114.70(19)

Bond parameters for **TMA·C_{12}Py**:

O1 C1 1.282(2)
O2 C1 1.226(2)
O3 C8 1.314(2)
O4 C8 1.193(2)
O5 C9 1.289(2)
O6 C9 1.227(2)
O7 C12 1.338(2)
O7 C15 1.453(2)
N1 C14 1.337(3)
N1 C10 1.339(3)
C1 C2 1.514(2)
C2 C3 1.389(2)
C2 C7 1.389(2)
C3 C4 1.396(2)
C4 C5 1.395(2)
C4 C8 1.491(2)
C5 C6 1.384(2)
C6 C7 1.394(2)
C6 C9 1.500(2)
C10 C11 1.383(3)
C11 C12 1.380(3)
C12 C13 1.396(3)
C13 C14 1.358(3)
C15 C16 1.503(3)
C16 C17 1.516(3)
C17 C18 1.519(3)
C18 C19 1.520(3)
C19 C20 1.515(3)
C20 C21 1.526(3)
C21 C22 1.515(3)
C22 C23 1.521(3)
C23 C24 1.513(3)
C24 C25 1.515(3)
C25 C26 1.507(4)

C12 O7 C15 121.11(15)
C14 N1 C10 121.06(18)
O2 C1 O1 122.51(16)
O2 C1 C2 119.07(16)
O1 C1 C2 118.42(15)
C3 C2 C7 119.05(17)
C3 C2 C1 119.72(16)
C7 C2 C1 121.21(16)
C2 C3 C4 120.20(17)
C5 C4 C3 120.23(17)
C5 C4 C8 119.92(16)
C3 C4 C8 119.86(16)
C6 C5 C4 119.71(17)
C5 C6 C7 119.69(16)
C5 C6 C9 121.32(15)
C7 C6 C9 118.99(15)
C2 C7 C6 121.11(16)
O4 C8 O3 123.28(17)
O4 C8 C4 125.21(17)
O3 C8 C4 111.51(16)
O6 C9 O5 123.30(16)
O6 C9 C6 123.97(15)
O5 C9 C6 112.72(15)
N1 C10 C11 120.9(2)
C12 C11 C10 118.24(19)
O7 C12 C11 125.16(18)
O7 C12 C13 114.95(17)
C11 C12 C13 119.88(18)
C14 C13 C12 118.80(19)
N1 C14 C13 121.15(19)
O7 C15 C16 104.62(17)
C15 C16 C17 115.34(19)
C16 C17 C18 110.61(18)
C17 C18 C19 116.30(19)
C20 C19 C18 112.35(19)
C19 C20 C21 114.98(19)
C22 C21 C20 113.47(19)
C21 C22 C23 114.54(19)
C24 C23 C22 114.09(18)
C23 C24 C25 113.68(18)
C26 C25 C24 113.9(2)

Bond parameters for **11**:

Cu1 O2 1.9426(14)
Cu1 N1 1.9987(16)
Cu1 N2 2.0679(16)
Cu1 O3 2.1682(16)
Cu1 Cl1 2.3758(6)
Cu1A O2A 1.9792(14)
Cu1A O3A 1.9824(16)
Cu1A N1A 2.0113(17)
Cu1A N2A 2.0217(17)
Cu1A Cl1A 2.5633(6)
N1 C6 1.339(3)
N1 C10 1.352(2)
N2 C15 1.343(3)
N2 C11 1.348(2)
N1A C6A 1.341(3)
N1A C10A 1.356(2)
N2A C15A 1.338(3)
N2A C11A 1.355(3)
O1 C5 1.240(2)
O2 C5 1.277(2)
O1A C5A 1.252(2)
O2A C5A 1.273(2)
C1 C2 1.393(3)
C1 C2A 1.402(3)
C2 C3 1.392(3)
C2 C5 1.516(3)
C3 C4 1.391(3)
C4 C3A 1.387(3)
C6 C7 1.389(3)
C7 C8 1.383(3)
C8 C9 1.384(3)
C9 C10 1.388(3)
C10 C11 1.483(3)
C11 C12 1.393(3)
C12 C13 1.382(3)
C13 C14 1.383(3)
C14 C15 1.385(3)
C2A C3A 1.389(3)
C2A C5A 1.506(3)
C6A C7A 1.380(3)
C7A C8A 1.376(3)
C8A C9A 1.379(3)
C9A C10A 1.388(3)
C10A C11A 1.475(3)

O2 Cu1 N1 166.89(7)
O2 Cu1 N2 88.98(6)
N1 Cu1 N2 79.94(7)
O2 Cu1 O3 91.95(6)
N1 Cu1 O3 90.71(7)
N2 Cu1 O3 133.76(7)
O2 Cu1 Cl1 98.88(5)
N1 Cu1 Cl1 93.07(5)
N2 Cu1 Cl1 123.09(5)
O3 Cu1 Cl1 102.41(5)
O2A Cu1A O3A 92.52(6)
O2A Cu1A N1A 90.31(6)
O3A Cu1A N1A 159.34(7)
O2A Cu1A N2A 166.78(6)
O3A Cu1A N2A 92.64(7)
N1A Cu1A N2A 80.67(7)
O2A Cu1A Cl1A 92.26(5)
O3A Cu1A Cl1A 98.38(5)
N1A Cu1A Cl1A 101.95(5)
N2A Cu1A Cl1A 99.02(5)
C6 N1 C10 119.21(18)
C6 N1 Cu1 124.41(14)
C10 N1 Cu1 116.38(13)
C15 N2 C11 119.06(18)
C15 N2 Cu1 126.73(14)
C11 N2 Cu1 114.19(13)
C6A N1A C10A 119.12(18)
C6A N1A Cu1A 125.61(14)
C10A N1A Cu1A 115.09(14)
C15A N2A C11A 118.56(18)
C15A N2A Cu1A 126.74(15)
C11A N2A Cu1A 114.68(14)
C5 O2 Cu1 129.34(14)
C5A O2A Cu1A 128.37(13)
C2 C1 C2A 120.88(18)
C3 C2 C1 119.15(18)
C3 C2 C5 121.12(18)
C1 C2 C5 119.73(18)
C4 C3 C2 120.17(19)
C3A C4 C3 120.44(19)
O1 C5 O2 125.41(19)
O1 C5 C2 119.31(18)
O2 C5 C2 115.28(18)
N1 C6 C7 122.4(2)

Bond parameters for **11**: (continued)

C11A C12A 1.396(3)
C12A C13A 1.385(3)
C13A C14A 1.382(3)
C14A C15A 1.384(3)
Cu2 O6 1.9727(16)
Cu2 O5 1.9735(14)
Cu2 N4 1.9983(17)
Cu2 N3 2.0257(17)
Cu2 O7 2.196(2)
Cu3 O9 1.9437(14)
Cu3 N6 1.9971(17)
Cu3 N5 2.0635(17)
Cu3 O10 2.1722(16)
Cu3 Cl2 2.3738(6)
N3 C23 1.339(3)
N3 C27 1.350(3)
N4 C32 1.343(3)
N4 C28 1.359(3)
N5 C34 1.341(3)
N5 C38 1.350(3)
N6 C43 1.341(3)
N6 C39 1.355(2)
O4 C22 1.252(2)
O5 C22 1.277(2)
O8 C33 1.241(2)
O9 C33 1.274(2)
C16 C21 1.395(3)
C16 C17 1.404(3)
C17 C18 1.389(3)
C17 C22 1.504(3)
C18 C19 1.382(3)
C19 C20 1.395(3)
C20 C21 1.391(3)
C21 C33 1.518(3)
C23 C24 1.379(3)
C24 C25 1.382(4)
C25 C26 1.380(3)
C26 C27 1.394(3)
C27 C28 1.480(3)
C28 C29 1.387(3)
C29 C30 1.383(3)
C30 C31 1.383(3)
C31 C32 1.380(3)
C34 C35 1.387(3)

C8 C7 C6 118.4(2)
C7 C8 C9 119.5(2)
C8 C9 C10 119.24(19)
N1 C10 C9 121.23(18)
N1 C10 C11 114.72(17)
C9 C10 C11 124.05(18)
N2 C11 C12 121.62(19)
N2 C11 C10 114.74(17)
C12 C11 C10 123.64(19)
C13 C12 C11 118.6(2)
C12 C13 C14 120.0(2)
C13 C14 C15 118.3(2)
N2 C15 C14 122.4(2)
C3A C2A C1 119.13(18)
C3A C2A C5A 121.29(18)
C1 C2A C5A 119.59(18)
C4 C3A C2A 120.22(19)
O1A C5A O2A 125.21(19)
O1A C5A C2A 118.23(18)
O2A C5A C2A 116.56(18)
N1A C6A C7A 121.9(2)
C8A C7A C6A 119.3(2)
C7A C8A C9A 119.4(2)
C8A C9A C10A 119.1(2)
N1A C10A C9A 121.2(2)
N1A C10A C11A 114.62(17)
C9A C10A C11A 124.14(19)
N2A C11A C12A 121.5(2)
N2A C11A C10A 114.87(17)
C12A C11A C10A 123.60(19)
C13A C12A C11A 119.1(2)
C14A C13A C12A 119.1(2)
C13A C14A C15A 118.9(2)
N2A C15A C14A 122.8(2)
O6 Cu2 O5 93.02(6)
O6 Cu2 N4 164.63(7)
O5 Cu2 N4 90.94(6)
O6 Cu2 N3 92.97(7)
O5 Cu2 N3 168.53(7)
N4 Cu2 N3 80.82(7)
O6 Cu2 O7 97.48(7)
O5 Cu2 O7 92.42(8)
N4 Cu2 O7 97.18(7)
N3 Cu2 O7 96.49(8)

Bond parameters for **11**: (continued)

C35 C36 1.380(3)
C36 C37 1.387(3)
C37 C38 1.395(3)
C38 C39 1.485(3)
C39 C40 1.382(3)
C40 C41 1.382(3)
C41 C42 1.380(3)
C42 C43 1.385(3)

O9 Cu3 N6 167.17(7)
O9 Cu3 N5 88.92(6)
N6 Cu3 N5 80.13(7)
O9 Cu3 O10 91.65(6)
N6 Cu3 O10 90.84(7)
N5 Cu3 O10 132.35(7)
O9 Cu3 Cl2 98.68(5)
N6 Cu3 Cl2 92.96(5)
N5 Cu3 Cl2 123.44(5)
O10 Cu3 Cl2 103.55(5)
C23 N3 C27 118.51(19)
C23 N3 Cu2 126.96(15)
C27 N3 Cu2 114.53(14)
C32 N4 C28 118.80(18)
C32 N4 Cu2 125.71(14)
C28 N4 Cu2 115.39(14)
C34 N5 C38 119.38(18)
C34 N5 Cu3 126.57(15)
C38 N5 Cu3 113.97(14)
C43 N6 C39 119.09(18)
C43 N6 Cu3 124.36(14)
C39 N6 Cu3 116.54(14)
C22 O5 Cu2 128.85(13)
C33 O9 Cu3 129.22(14)
C21 C16 C17 120.41(18)
C18 C17 C16 119.25(18)
C18 C17 C22 121.15(18)
C16 C17 C22 119.60(18)
C19 C18 C17 120.51(19)
C18 C19 C20 120.22(19)
C21 C20 C19 120.18(19)
C20 C21 C16 119.43(19)
C20 C21 C33 121.09(18)
C16 C21 C33 119.48(18)
O4 C22 O5 125.07(19)
O4 C22 C17 118.48(18)
O5 C22 C17 116.45(18)
N3 C23 C24 122.9(2)
C23 C24 C25 118.8(2)
C26 C25 C24 119.3(2)
C25 C26 C27 119.0(2)
N3 C27 C26 121.6(2)
N3 C27 C28 114.86(18)
C26 C27 C28 123.5(2)
N4 C28 C29 121.7(2)
N4 C28 C27 114.35(17)
C29 C28 C27 123.96(19)
C30 C29 C28 118.6(2)
C29 C30 C31 119.9(2)
C32 C31 C30 118.7(2)
N4 C32 C31 122.4(2)
O8 C33 O9 125.29(19)
O8 C33 C21 119.35(18)
O9 C33 C21 115.34(18)
N5 C34 C35 122.2(2)
C36 C35 C34 118.5(2)
C35 C36 C37 120.0(2)
C36 C37 C38 118.5(2)
N5 C38 C37 121.4(2)
N5 C38 C39 115.10(17)
C37 C38 C39 123.45(19)
N6 C39 C40 121.08(19)
N6 C39 C38 114.20(18)
C40 C39 C38 124.71(19)
C39 C40 C41 119.6(2)
C42 C41 C40 119.4(2)
C41 C42 C43 118.5(2)
N6 C43 C42 122.4(2)